Quality Testing of Wisconsin Aggregates

Hani H. Titi, Ph.D., P.E., M. ASCE
Rani ElHajjar, Ph.D., P.E.
Habib Tabatabai, Ph.D., P.E., S.E.
Benjamin M. Stark, M.S., P.E.

Department of Civil and Environmental Engineering
University of Wisconsin-Milwaukee
3200 N. Cramer St.
Milwaukee, WI 53211

Issam Qamhia, Ph.D.

Illinois Center for Transportation
Department of Civil and Environmental Engineering
University of Illinois at Urbana-Champaign
205 N. Mathews, Urbana, IL 61801

WisDOT ID no. 0092-20-05
October 2022

RESEARCH & LIBRARY UNIT

WISCONSIN HIGHWAY RESEARCH PROGRAM

WISCONSIN DOT
PUTTING RESEARCH TO WORK

TECHNICAL REPORT DOCUMENTATION PAGE

1. Report No. 0092-20-05	**2. Government Accession No.**	**3. Recipient's Catalog No.**
4. Title and Subtitle Quality Testing of Wisconsin Aggregates		**5. Report Date** October 2022 **6. Performing Organization Code**
7. Author(s) Hani H. Titi, Rani ElHajjar, Habib Tabatabai, Benjamin M. Stark, and Issam Qamhia		**8. Performing Organization Report No.**
9. Performing Organization Name and Address Department of Civil and Environmental Engineering University of Wisconsin-Milwaukee 3200 N. Cramer St. Milwaukee, WI 53211		**10. Work Unit No.** **11. Contract or Grant No.** 0092-20-05
12. Sponsoring Agency Name and Address Wisconsin Department of Transportation Research & Library Unit 4822 Madison Yards Way Room 911 Madison, WI 53705		**13. Type of Report and Period Covered** Final Report November 2019 – October 2022 **14. Sponsoring Agency Code** 0092-20-05
15. Supplementary Notes		

16. Abstract

The main objective of this research project was to investigate the feasibility of implementing coarse aggregates (CA) soundness testing based on AASHTO T 103 or WisDOT Modified AASHTO T103 test procedures. To accomplish this goal, a better understanding of the current soundness testing procedures is needed with respect to Wisconsin CA performance and use. Coarse aggregates samples were collected for laboratory testing and evaluation from 34 sources consisting of different rock formations and various classifications. The laboratory testing included measurements of specific gravity, absorption, and vacuum absorption, sodium sulfate soundness (SSS) , and freeze-thaw tests (F-T). Additionally, the influence of the following on the test results was investigated: test type, F-T test equipment, test laboratory, test repeatability, number of wetting/drying cycles, number of F-T cycles, absorption, aggregate source, aggregate size fraction, and aggregate classification. To investigate the influence of the CA quality on F-T durability of PCC in pavements, PCC test cylinders were made and exposed to rapid freeze-thaw test as well as evaluations of the static and dynamic moduli up to 300 F-T cycles. PCC testing included ASTM C666, ASTM C215, C597, C39, and C856. Additionally, field investigation including coring was conducted to quantify the effect of CA on PCC pavement durability and performance. Professional petrographic analysis was performed on the PCC cylinders and pavement surface cores.

Test results showed there is no typical SSS vs F-T relationship. CA absorption is an influencing factor of F-T durability, but mixed results were also observed when considering carbonates (calcareous vs dolomitic limestone). Results also showed that different CA classifications exhibited different F-T results due to the variability in the CA size fractions. PCC F-T performance evaluation showed that PCC exposed to F-T at younger age will exhibit larger deterioration and loss of elastic moduli. Field investigation showed that low and medium severity D-cracking, PCC pavement surface pitting/popouts exist on PCC pavement in Wisconsin, but not to a great extent.

17. Key Words Coarse aggregate durability, freeze-thaw, sodium sulfate soundness, PCC freeze-thaw, PCC pavement durability, D-cracking, PCC dynamic modulus, UPV of PCC.	**18. Distribution Statement** No restrictions. This document is available through the National Technical Information Service. 5285 Port Royal Road Springfield, VA 22161

19. Security Classif. (of this report) Unclassified	**20. Security Classif. (of this page)** Unclassified	**21. No. of Pages** 53	**22. Price**

Form DOT F 1700.7 (8-72) Reproduction of completed page authorized

DISCLAIMER

This research was funded through the Wisconsin Highway Research Program by the Wisconsin Department of Transportation and the Federal Highway Administration under Project 0092-20-05. The contents of this report reflect the views of the authors who are responsible for the facts and accuracy of the data presented herein. The contents do not necessarily reflect the official views of the Wisconsin Department of Transportation or the Federal Highway Administration at the time of publication.

This document is disseminated under the sponsorship of the Department of Transportation in the interest of information exchange. The United States Government assumes no liability for its contents or use thereof. This report does not constitute a standard, specification or regulation.

The United States Government does not endorse products or manufacturers. Trade and manufacturers' names appear in this report only because they are considered essential to the object of the document.

Acknowledgements

This research project is financially supported by Wisconsin Highway Research Program (WHRP)–Wisconsin Department of Transportation (WisDOT).

The research team would like to acknowledge and thank WisDOT POC chair Erik Lyngdal, and POC members Dan Reid and Russell Frank as well as Bob Downing and Josh Seaman for their help, support, input, guidance, and effort provided to the research team.

The input and feedback from WHRP Geotechnical TOC chair David Staab and members Andrew Zimmer and Jeffrey Horsfall are greatly appreciated.

The research team would like to thank Andrew Schilling, John Thompson, and Michael Wolf of WisDOT Pavement Data Unit for providing the needed data.

The research team would like to thank Prof. Dante Fratta for his great help in providing the UPV device and training.

The help and support of the Erik Olson (Mathy Construction Co.), Michael Hammitt (Trierweiler Construction and Supply Co. Inc), Stacy Glidden and Cheng Thao (Walbec Group), and Kevin McMullen (WCPA) are greatly appreciated.

The research team also acknowledges the help of UW-Milwaukee graduate and undergraduate students for their help in various phases of this project.

Table of Contents

List of Figures

List of Tables

Executive Summary

The main objective of this research project was to investigate the feasibility of implementing coarse aggregates soundness testing based on AASHTO T 103 or WisDOT Modified AASHTO T103 test procedures. To accomplish this goal, a better understanding of the current soundness testing procedures (AASHTO T 103/ WisDOT Modified AASTHO T 103, and AASHTO T 104) is needed with respect to Wisconsin coarse aggregates' performance and use.

Coarse aggregates (CA) samples were collected for laboratory testing and evaluation by WisDOT certified technicians from 34 sources (pits and quarries) consisting of different rock formations (limestone, igneous, and metamorphic) and various classifications (base course, concrete #1, concrete #2, 1 in. clear stone, and 1½ in. bituminous).

The laboratory testing included measurements of specific gravity, absorption, and vacuum absorption as well as mass loss due to sodium sulfate soundness (SSS) and freeze-thaw (F-T) tests, in accordance with the standard testing procedures described in Chapter 3 of this report. Additionally, the influence of the following variables on the test results was investigated: test type, F-T test equipment, test laboratory, test repeatability, number of wetting/drying cycles, number of F-T cycles, absorption, aggregate source, aggregate size fraction, and aggregate classification. In total, 106 SSS and 170 F-T tests were conducted on the collected CA samples. The SSS tests included the standard five wetting/drying cycles as well as additional five cycles (i.e., total of 10 cycles) performed on two limestone sources. The F-T test included the standard 16 F-T cycles in addition to 16, 32, and 48 cycles (from 32 to 64) on 12 CA sources. The F-T tests were conducted in three different laboratories with the majority of those tests performed at UW-Milwaukee using both automated/programmable F-T machines and chest freezer-manual thaw systems.

In order to investigate the influence of the F-T soundness aggregate quality on PCC in pavements, eight CA sources were used to make PCC test cylinders following WisDOT mixture design requirement for PCC pavements. Fifteen PCC cylinders of each of the eight CA sources were cast, placed in curing tank for 28 days, then three PCC cylinders of each group were immediately subjected to freeze-thaw cycles according to ASTM C666 (this is labeled as the short-term study). In addition, another three PCC cylinders of each group were taken from the curing tank after 28 days and placed on the shelf in the lab for five more months, then subjected to freeze-thaw cycles according to ASTM C666 (after a total of 6 months from mixing and casting, which is labeled as the long-term study). The short-term and long-term PCC cylinders were subjected to 300 F-T cycles in accordance with ASTM C666 and were also subjected to standard tests to evaluate their static and dynamic moduli using ASTM C215, ASTM C597, and ASTM C39. The laboratory testing was conducted on the PCC cylinders at ages of 28 days and 6 months to account for the effect of the age of PCC when first exposed to freezing and thawing. In addition, professional petrographic analysis (per ASTM C856) was conducted on the PCC cylinders after the completion of the 300 F-T cycles to investigate the degradation, deterioration, and disintegration of both the CA and PCC/paste materials.

Field work was also conducted at twelve PCC pavement sites that exhibited durability related distress consisting of D-cracking and/or coarse aggregates pitting/popouts. The field work consisted of pavement distress surveys and evaluation, analysis of WisDOT's PIF database, coring of concrete at three pavement sites, and professional petrographic analysis of the PCC cores.

Finally, the research team conducted detailed analyses on a database of historical Wisconsin coarse aggregate test results, including various CA sources. This included analyzing differences in test results on calcareous limestone (CLS) and dolomitic limestone (DLS) coarse aggregates.

Based on the results of the laboratory and field investigations as well as analyses of the database information, the following conclusions are drawn:

- Absorption of CLS coarse aggregates is greater than that of DLS aggregates.
- CA from igneous and metamorphic formations exhibited the lowest absorption.
- The base materials have the highest absorption when compared with the CA from concrete # 1 and #2.
- The SSS mass loss of quarried CA is greater than the SSS mass loss of pit gravel.
- The F-T mass loss of quarried CA is greater than the F-T mass loss of pit gravel.
- The SSS mass loss of CLS is nearly equal to the SSS mass loss of DLS, noting that the absorption of CLS is higher than the absorption of DLS.
- The F-T mass loss of CLS is less than the F-T mass loss of DLS, noting that the absorption of CLS is higher than the absorption of DLS.
- SSS and F-T mass losses are the lowest for CA from igneous and metamorphic rock formation.

The SSS and F-T data averages for CLS and DLS indicate the following based on CA classification:

- SSS mass loss of base CLS CA is greater than SSS mass loss of concrete #1 and #2 CLS.
- SSS mass loss of base DLS CA is greater than SSS mass loss of concrete #1 and #2 DLS.
- F-T mass loss of base CLS CA is nearly equal to F-T mass loss of concrete #1 CLS and is greater than F-T mass loss of concrete #2 CLS.
- F-T mass loss of base DLS CA is greater than F-T mass loss of concrete #1 and #2 DLS.
- The larger CA particles (larger size fractions) exhibited more SSS weighted mass loss, on average, when compared with the smaller size particles for CLS.
- The smaller CA particles exhibited more F-T weighted mass loss by both CLS and DLS.
- The middle size fractions exhibit the highest SSS mass loss by DLS.
- The detailed size fraction study showed that greater F-T mass loss was observed for the smaller size fraction.

When considering the influence of F-T test systems and the choice of testing laboratory on CA performance, the following was observed:

- Temperature-time graphs recorded by the automated freeze-thaw test system was consistent and repeatable while the corresponding graphs recorded by the chest freezer was inconsistent and required more cycle time.
- F-T test results did not indicate a clear relationship between the chest freezer and automated freeze-thaw mass loss.
- Round robin F-T test results showed higher variability of the mass loss when using the chest freezers compared with the automated F-T systems.
- Repeatability of F-T test results was obtained from three different laboratories (using automated F-T systems) was considered good even with a higher number of F-T cycles and the inherent variability of CA materials.

The results of the ASTM C666 test on the PCC cylinders placed in the F-T chamber at 28 days of age (short-term study) indicated the following:

- The PCC with limestone gravel from pits deteriorated the most at 300 F-T cycles.
- PCC with CLS and DLS aggregates had mixed F-T performance, but the PCC cylinders with CLS aggregates exhibited significant deterioration.
- PCC with igneous and metamorphic quarried coarse aggregates and pit gravel did not show significant deterioration.

The results of the ASTM C666 tests on the PCC cylinders placed in the F-T chamber at 6 months of age (long-term study) indicated:

- PCC with DLS deteriorated the most due to 300 F-T cycles.
- PCC with igneous and metamorphic quarried coarse aggregates and pit gravel did not show deterioration.
- Performance of PCC with late-age F-T exposure did not show significant deterioration when compared with the PCC with early-age F-T exposure.
- Examination of the PCC cylinders indicated that the age at first exposure of PCC to freeze-thaw cycles influenced its durability. PCC cylinders subjected to F-T exposure at a younger age (28 days) exhibited more cracking, deterioration, and loss of static and dynamic moduli when compared with PCC cylinders exposed to the F-T cycles at 6 months of age.
- Petrographic analyses showed that the CA and the PCC both exhibited cracking/breakage and deterioration as well as scaling and pitting of the PCC surface.

Field surveys and subsequent evaluation of PCC pavement sites showed durability related distress consisting of D-cracking and coarse aggregate pitting/popouts. Several projects were identified with PCC pavement pitting/popouts as well as low severity and medium severity D-cracking that was confirmed by coring and inspecting PCC material. Evaluation of cores by a professional petrographer and field surveys indicated presence of CA durability related problems.

A comprehensive analysis of the test data and other subsets indicated that approximately 7% of CA tested in Wisconsin failed the 12% total mass loss threshold in the SSS test currently specified by WisDOT for CA acceptance. Based on statistical analyses, keeping the same sample failure percentage will require approximately the same mass loss percentage of 12.

Chapter 1

Introduction

1.1 Problem Statement

At a minimum, Wisconsin Department of Transportation (WisDOT) requires sodium sulfate soundness testing (AASHTO T 104) and Los Angeles wear (AASHTO T 96) aggregate quality testing be completed once every three years for quarried aggregate sources and once every five years for pit aggregate sources. Aggregate sources located in the Sinnippee geological group, generally in the southwest part of Wisconsin, require an additional freeze-thaw test (AASHTO T103) on a three-year or five-year testing cycle.

An internal audit of WisDOT specifications concluded that the frequency of testing for quality is lacking relative to surrounding states. Reduced testing frequencies is due, in part, to the higher level of aggregate quality available to paving contractors in Wisconsin. Despite the inventory of high-quality construction aggregates, localized pavement performance issues have raised concerns about the effectiveness of the current quality testing program. Recent changes to the standard specifications have partially addressed concerns regarding the minimal quality testing frequencies, but there is a need to revisit quality thresholds and accuracy of current testing methods to represent aggregate durability.

Wisconsin Department of Transportation engineers have been tasked with improving specifications for aggregate quality. Based on internal research, WisDOT representatives have concluded that AASHTO T 103 may be a more accurate representation of aggregate soundness and could potentially replace AASHTO T 104 entirely.

1.2 Background

Various types of aggregates are used annually in Wisconsin for road- and bridge-related construction projects. Aggregates are important parts of base course and pavement surface layers in asphalt and Portland cement concrete roadways. As such, the long-term durability of roadways can be directly impacted by the quality of aggregates. Aggregates selected for transportation projects in Wisconsin and other northern states must be durable to withstand particularly harsh exposure conditions.

Several quality control aggregate tests have long been conducted on Wisconsin aggregates during construction projects. The Wisconsin Department of Transportation (WisDOT) has collected the test results in a database. The tests involved measured absorption (Abs) and specific gravity (SG) for coarse (AASHTO T 85) and fine (AASHTO T 84) aggregates, Los Angeles abrasion (LAA) (AASHTO T 96), sodium sulfate soundness (SSS) (AASHTO T 104) and unconfined freeze-thaw (UFT) (AASHTO T 103). The newer micro-Deval (MD) test (AASHTO T 327) has not been routinely performed (only from 2000 to 2003). Tabatabai et al. (2013, 2018) presented results of comprehensive statistical analyses on three sets of aggregate test data (two from Wisconsin and one nationally), which included a database containing 2,052 sets of quality control aggregate tests

from various construction projects in Wisconsin, an earlier Wisconsin aggregate research study (69 data sets), and a set of test results of aggregates from different parts of the United States and Canada (111 data sets). In addition, Tabatabai et al. (2013, 2018) conducted durability tests on 12 types of marginal or poor Wisconsin aggregates. The objectives were to evaluate relevant statistical parameters for various aggregate test results and identify correlations among them. The possibility of predicting the outcomes of the unconfined freeze-thaw from other more common test results was studied. Multiparameter logistic regression analyses indicated that the outcome of freeze-thaw tests could not be forecast using the results of other tests.

The recent NCHRP Synthesis 524 (Tutumluer et al. 2018) reported about 10 state agencies that are conducting their modified versions of the freeze-thaw durability tests adopted by the agency. The report also identified nine transportation agencies that reported a link between an aggregate quality issue and poor performance of a given pavement layer in which five agencies have aggregate freeze-thaw problems with aggregates affecting the performance of PCC pavement layer and two agencies with performance problems of HMA pavement layers.

Durability tests can also be used to evaluate HMA and PCC pavement materials such as the AASHTO T 161 (ASTM C666): Resistance of Concrete to Rapid Freezing and Thawing. However, there are issues associated with some tests in general. For example, AASHTO T 161 test protocol was criticized in Europe because of its high rate of freezing that does not represent the natural freeze-thaw exposure of concrete. Accordingly, the RILEM TC 117-FDC work group has decided not to accept ASTM C666 as a CEN-testing method (Kuosa et al. 2013). Moreover, the Iowa DOT experienced problems with AASHTO T 161 test method, which will fail durable coarse aggregates that contain a minor amount (less than 3%) of expansive material such as tripolic chert or iron spall. In addition, this test method tends to pass all dolomite coarse aggregates, regardless of their PCC pavement service records (Dubberke 1999).

1.3 Research Objectives

Before statewide implementation of AASHTO T 103, new limitations need to be selected for each aggregate application: base course, Hot Mix Asphalt (HMA) pavement and Portland Cement Concrete (PCC) pavement. The objective of this research is to:

- Investigate the feasibility of implementing statewide freeze-thaw testing.
- Understand the accuracy of the existing soundness procedures (AASHTO T 103/T 104).
- Recommend thresholds for Wisconsin aggregates used in base course, HMA pavement and PCC pavement regarding freeze-thaw durability.

1.4 Organization of the Report

This report is organized in seven chapters. Chapter One introduces the problem statement and objective of the research. The literature review is presented in Chapter Two, and the research methodology is discussed in Chapter Three. Chapters Four and Five present a detailed analysis for laboratory testing on coarse aggregates and PCC, respectively. Field investigation of coarse aggregates in PCC pavements is presented in Chapter Six. The conclusions and recommendations are provided in Chapter Seven.

Chapter 2

Background

This chapter presents a review of relevant literature regarding the performance of coarse aggregates in terms of resistance to breakage and disintegration due to exposure to freeze-thaw (F-T) cycles. Standard laboratory characterization tests performed on coarse aggregates and Portland cement concrete, including explanations and the significance of each test, are discussed. Additional literature review materials, including the geologic history of Wisconsin, are presented in Appendix A due to the report page limits.

2.1 Specific Gravity and Absorption of Coarse Aggregates

Specific gravity and absorption are physical properties of coarse aggregates that can be a measure of aggregate quality. Relatively high absorption values can indicate that an aggregate is not durable (AASHTO, 2021). Pigeon and Pleau (1995) suggested that a limit of 2% absorption be used to avoid freeze-thaw damage in coarse aggregates. The Minnesota Department of Transportation (MnDOT) Standard Specifications for Construction (MnDOT, 2020) requires that a Class B aggregate (quarried carbonates, rhyolites, schist) have a maximum absorption of 1.75% when used in concrete pavements (Koubaa et al., 1997).

The Michigan Department of Transportation (MDOT) procedures for preparing coarse aggregate samples for freeze-thaw durability testing, as outlined in MTM-113 (MDOT, 2020), utilize a vacuum saturation technique to maximize water absorption. The procedure requires samples to be oven-dried, placed under vacuum (28.5 in. mercury) for one hour, immersed in a chamber with water while maintaining the vacuum, and then soaked for 23 hours under normal atmospheric pressure. The samples are drained, and absorption testing is performed. Stanton and Anderson (2009) evaluated the MTM-113 vacuum saturation procedures. In their study, five coarse aggregates were sampled, dried and partitioned for various soaking periods up to three years. Additionally, five aggregate specimens from each source were vacuum-saturated for comparison purposes. Test results indicated that 30 days of conventional soaking time was necessary to attain approximately 90% of the absorption achieved with the MTM-113 vacuum saturation procedures. These aggregates reached vacuum saturation levels of absorption after one year of soaking. The comparison of absorption values using MTM-113 vacuum absorption procedures and the standard 24-hour saturation per AASHTO T 85 indicated that the 24-hour saturation achieved 33 to 78% of the absorption achieved using MTM 113. Thus, soaking time influences the absorption of coarse aggregates.

Weyers et al. (2005) investigated testing methods for Wisconsin coarse aggregates. As part of their study, coarse aggregate samples representing the full range of aggregates available

in Wisconsin were tested for vacuum saturated specific gravity and absorption with a modified ASTM C127 test method. The aggregates were placed under a vacuum of 635 mm (25 in.) of mercury for 5 minutes and then saturated for 24 hours. Weyers et al. (2005) recommended the use of vacuum saturation over standard saturation for evaluating absorption in coarse aggregates.

Another comparison between the standard absorption and vacuum saturation absorption was performed by Richardson (2009) for the Missouri Department of Transportation (MoDOT). Coarse aggregate samples were subjected to a vacuum of 27.5±2.5 mm (1.08±0.10 in.) absolute mercury pressure for 5 minutes. The vacuum chamber was then flooded, and the aggregates were submerged while maintaining the vacuum for an additional 25 minutes. The material was then submerged at atmospheric pressure for 24 hours. Following saturation, AASHTO T 85 standard test procedure was followed. Richardson (2009) reported that the change in absorption using vacuum saturation condition ranged from -0.2% to +0.9% with an average increase of 0.3%.

2.2 Laboratory Tests used as Aggregate Durability Indicators

The sodium sulfate soundness (SSS) test is conducted to evaluate freeze-thaw resistance of aggregates through a mechanism involving sodium sulfate or magnesium sulfate salt rehydration and expansion (i.e., via wetting and drying cycles). The AASHTO T 104 standard test procedure consists of five cycles. Each cycle consists of two phases: 1) immersing the aggregate specimen in the sodium sulfate or magnesium sulfate solution for 16 to 18 hours; and 2) oven-drying the specimen to a constant mass. Rehydration and growth of salt crystals within aggregate pores during immersion generate an internal expansive force that is intended to simulate the expansion of water during freezing conditions. Sieve analysis of the aggregate to determine mass loss is performed after completion of the five wetting/drying cycles.

Sodium sulfate soundness is used by WisDOT as a main quality indicator of coarse aggregates for durable long-term performance. WisDOT requires that the coarse aggregate mass loss using the SSS test be less than 12% (WisDOT, 2022). The SSS test is imprecise and has been shown to have relatively variable single operator coefficients of variation (Weyers et al., 2005). Williams and Cunningham (2012) evaluated the SSS test method and found that the results variability decreased the reliability of the test.

Another direct freeze-thaw laboratory test is the AASHTO T 103 *Standard Method of Test for Soundness of Aggregates by Freezing and Thawing*. This procedure utilizes the mass loss of an unconfined aggregate sample after cyclic freezing and thawing. In this test, the aggregate is fractioned and placed in containers. Samples are conditioned via either procedures A, B, or C. Procedure B consist of placing aggregates in a vacuum chamber under air pressure not exceeding 3.4 kPa (1″ of mercury) and then immersing the aggregates in 0.5% ethyl alcohol-water solution for 15 minutes while maintaining the vacuum. The purpose of the alcohol-water solution is to increase the penetration of water into aggregate pores during the soaking period

(Qiao et. al, 2012). The aggregates are then placed (as a single layer) into a container with an ethyl alcohol-water solution. The freeze-thaw cycles consist of cooling the samples to -23±3ºC, holding for a minimum of 2 hours, thawing to 21±3ºC and holding for a minimum of 30 minutes.

The AASHTO T 103 test procedures specify 25 freeze-thaw cycles. However, authorities can require 50, 16, and 25 cycles for procedures A, B, and C, respectively (AASHTO, 2021). WisDOT (2022) uses a modified version of the standard AASHTO T 103 in which 0.5% methyl alcohol-water solution is used to prepare samples following procedure B and requires that 16 freeze-thaw cycles be applied for durability evaluation. After the cycles are complete, samples are dried, sieved, and weighed to determine the mass loss.

The AASHTO T 103 test was evaluated by Williams and Cunningham (2012). As part of the study, triplicate samples of eight Arkansas limestone aggregate sources were prepared and tested using procedure A of AASHTO T 103. A coefficient of variability of 36% was reported, and over half of the variability in the results was attributed to errors related to the testing procedures. Pure error represents the variability of the test method and was quantified by removing the percentage of variability that could be attributed to differences between aggregate sources (Williams et al., 2012). Results of the variability analysis of the freeze-thaw test indicated that the test method was as variable as the tested aggregate sources.

2.3 WisDOT Coarse Aggregate Durability Testing

Tabatabai et al. (2013) investigated the performance of Wisconsin coarse aggregate for durability evaluation. Aggregate test results from WisDOT test database as well as data from tests performed on 69 aggregates by Weyers et al. (2005) were analyzed. A multi-parameter regression analysis was performed on the data from the WisDOT database. Results of the multi-parameter regression analysis indicated that little correlation existed between the unconfined freeze-thaw test and the other durability tests . Tabatabai et al. (2013) noted that the sodium sulfate soundness and unconfined freeze-thaw had very low correlation (R^2=0.13), even though the sodium sulfate soundness test has long been regarded as a test to rapidly measure freeze-thaw resistance. Tabatabai et al. (2013) concluded that the unconfined freeze-thaw test was measuring an aggregate characteristic that was different from the other test methods and recommended the test to be a standalone requirement for any aggregate test protocol.

2.4 Iowa Pore Index Test (AASHTO TP 120)

Porosity, pore size, and pore size distribution are important factors affecting the coarse aggregate durability and freeze-thaw performance. The Iowa Pore Index (IPI) Test (Iowa DOT, 1980), which is also designated as AASHTO TP 120 *Standard Method of Test for Pore Index for Carbonate Coarse Aggregate*, was developed to identify the potential for D-cracking within

carbonate aggregates. For this test, samples of ½ in. and ¾ in. aggregates are placed in water under a pressure of 35 psi for 15 minutes. The volume of water entering the aggregate pores in the first minute is termed the 'primary load', while the volume entering the aggregate pores for the remaining 14 minutes is termed the 'pore index' (secondary load). The primary load represents macropores and the secondary load represents micropores in the aggregate. The basis of the test is the assumption that micropores are directly related to the freeze-thaw durability of an aggregate (Bektas et al., 2016).

Bektas et al. (2016) conducted a study in which the IPI was compared to aggregate mass loss by unconfined freeze-thaw testing using ASTM C666 conditioning procedure, soundness by sulfate solution (ASTM C88), and Canadian unconfined freezing-thawing test (CSA A23.2-24A). Analysis of test results indicated that the mass loss of aggregates generally increases with an increase in the IPI.

2.5 Aggregate Breakage/Disintegration Mechanisms in Freezing Conditions

The pore structure of an aggregate plays an important role for long-term resistance of an aggregate to freeze-thaw conditions. Aggregate pore systems consist of pore space accessible from the surface and pore space isolated from the surrounding. The latter forms most of the pores in an aggregate (Alexander and Mindess, 2005). The distribution of pores within aggregates affect saturation, and subsequently freeze-thaw durability. Coarse aggregates have a critical saturation point, which is typically about 91% for most aggregates. This is due to the fact that water increases in volume by approximately 9% when it freezes and turns into ice. If the capillaries are saturated with more than 91%, the expansion resulting from ice formation will not be accommodated, and internal stresses would be generated due to freezing (Alexander and Mindess, 2005).

Alexander and Mindess (2005) suggested that the main mechanism of freeze-thaw damage in an aggregate's pore structure is either because of the increase in volume of water during freezing or because of the pressure increase due to the growth of ice. Alexander and Mindess (2005) stated that aggregates can be classified into three groups with respect to freeze-thaw behavior: (1) aggregates with a small pore volume (generally less than about 0.5%) in which the expansion due to freezing results in strains that are too small to cause cracking; (2) aggregates in which the hydraulic pressure generated by the flow of water ahead of a freezing front in a critically saturated pore system is able to crack the aggregate itself. Such aggregates must have a sufficiently low permeability and long enough flow path to generate high pressures; and (3) aggregates with a sufficiently high permeability to prevent hydraulic pressures becoming large enough to crack the aggregate. Smaller aggregates are considered less likely to suffer distress based on the suggested mechanism.

2.6 Resistance of Concrete to Rapid Freezing and Thawing (ASTM C666)

The ASTM C666 standard test evaluates the resistance of Portland cement concrete (PCC) specimens to rapid cycles of freezing and thawing using either procedure A (rapid freezing and thawing of samples in water), or procedure B (rapid freezing of samples in air and thawing in water). A freeze-thaw cycle consists of lowering the temperature in the middle of the specimen from 4ºC to -18ºC (39.2ºF to -0.4ºF) and then raising it from -18ºC to 4ºC (-0.4ºF to 39.2ºF). A freeze-thaw cycle is specified to last between 2 and 5 hours. ASTM specifies that the concrete test specimens shall be prism or cylinders made in accordance with ASTM C192/192M *Standard Practice for Making and Curing Concrete Test Specimens in the Laboratory* and Specification ASTM C490 *Standard Practice for Use of Apparatus for the Determination of Length Change of Hardened Cement Paste, Mortar, and Concrete*. During the test, samples are removed periodically (intervals not exceeding 36 cycles) to test for resonant frequency and estimate the relative dynamic modulus. The test is continued to 300 cycles or until a specimens' relative dynamic modulus of elasticity reaches 60% of the initial modulus, whichever occurs first (ASTM C666, 2021).

Crovetti and Kevern (2018) performed freeze-thaw durability tests in accordance with ASTM C666, Procedure A. The freeze-thaw testing was performed on concrete prisms that were 3″×4″×12″. The prisms were saw-cut from pavement test strips with two mix designs: one using southern Wisconsin limestone aggregates, and the other using northern Wisconsin igneous aggregates. During testing, the dynamic modulus and mass of the concrete prisms were measured at every 30 freeze-thaw cycles. Testing of the specimens from each concrete mix was performed to 300 cycles, and to 600 cycles for the select specimens. The measured dynamic modulus normalized with respect to the initial dynamic modulus for the specimens made with limestone (i.e., the relative dynamic modulus) are shown in Figures 2.1.

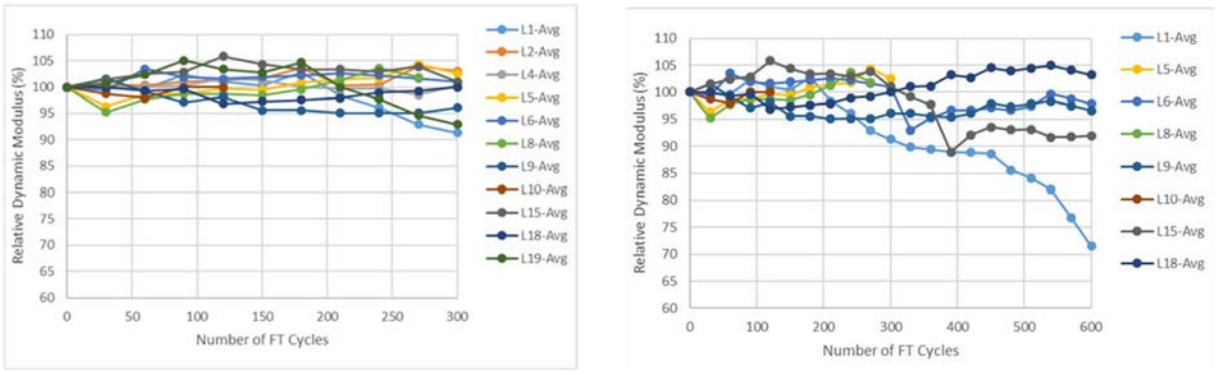

Figure 2.1: Limestone freeze-thaw results after 300 and 600 cycles (Crovetti and Kevern, 2018).

Crovetti and Kevern (2018) reported that concrete specimens made with limestone and granite gravel maintained high durability levels after 600 cycles. Only one concrete specimen made with limestone exhibited a low relative dynamic modulus, which decreased below 90% after about 330 cycles, and decreased below 75% at cycle 600.

Hamoush et al. (2011) studied the freeze-thaw durability of high strength concrete prisms (3″×4″×16″). For their study, the ASTM C666 procedures were followed for freeze-thaw conditioning and the dynamic modulus values were measured at 0, 40 , 70 , and 100 cycles. Hamoush et al. (2011) reported that the measured dynamic modulus increased from 0 to 40 cycles and then decreased from 40 to 100 cycles (Hamoush et al., 2011). Results of the longitudinal and transverse modulus measurements are depicted in Figures 2.2.

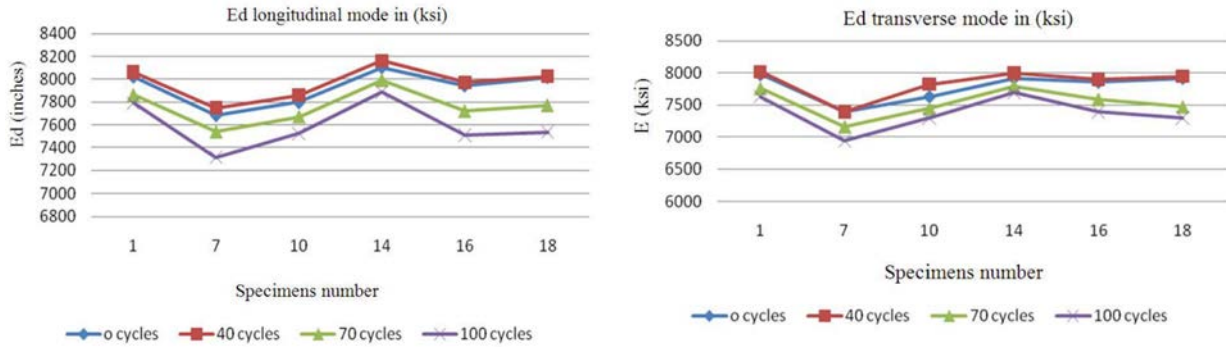

Figure 2.2: Longitudinal and transverse dynamic modulus of concrete samples with respect to freeze-thaw cycles (Hamoush et al. 2011).

A study conducted by Chen and Qiao (2014) measured the dynamic modulus of concrete prisms (3″×4″×16″). Samples were freeze-thaw conditioned in accordance with ASTM C666, Procedure A. The mix design was unchanged for all the concrete specimens, and the dynamic modulus of the prims was measured. Chen and Qiao (2014) reported that a larger variance of dynamic modulus between specimens was apparent after 600 freeze-thaw cycles. Additionally, all the relative dynamic modulus values (for all samples) dropped below 60% after 1,200 freeze-thaw cycles, which was considered to be the failure threshold (Chen and Qiao, 2014). The results of the study are shown in Figures 2.3.

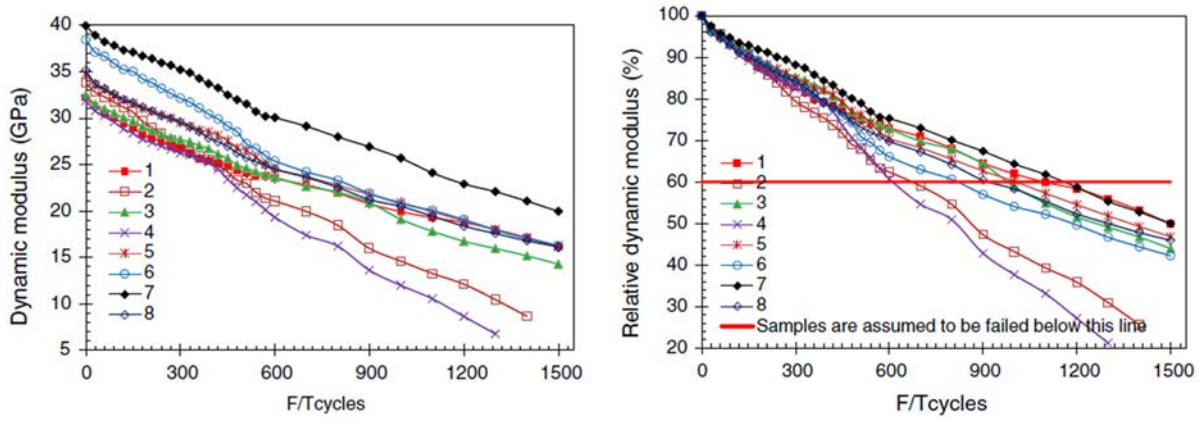

Figure 2.3: Dynamic modulus of concrete samples with respect to freeze-thaw cycles (Chen and Qiao, 2014).

The effect of rapid freeze-thaw cycles on concrete durability, beyond 300 cycles, was studied by Olba et al. (2016) using ASTM C666, Procedure A. In the study, Olba et al. (2016) measured the mass loss and dynamic modulus of concrete beams (3″×4″×15.5″) after up to 3,200 freeze-thaw cycles. After 3,200 freeze-thaw cycles, most of the tested samples showed excellent freeze-thaw performance and possessed relative dynamic modulus values above 80%. Additionally, the relationship between freeze-thaw cycles and degree of saturation was studied using sealed concrete samples with various degrees of saturation. Olba et al. (2016) concluded that there is a critical degree of saturation that the concrete must possess for the freeze-thaw failure to occur. Results of the freeze-thaw testing on the investigated concrete specimens indicated that the critical degree of saturation was around 88% (Olba et al., 2016).

2.7 Fundamental Resonant Frequencies of Concrete (ASTM C215)

The fundamental resonant frequency test procedure is provided in ASTM C215 *Standard Test Method for Fundamental Transverse, Longitudinal, and Torsional Resonant Frequencies of Concrete Specimens* (ASTM, 2021). ASTM C215 provides two methods for measurement: (1) the use of a driving circuit with a variable frequency oscillator and a pickup circuit ; and (2) impacting the specimen with a 110-gram steel ball peen hammer and measuring the frequency with an accelerometer connected to a frequency analyzer. The dynamic modulus of elasticity can be calculated using the measured fundamental frequencies (ASTM, 2021). The dynamic modulus for the transverse frequency can be calculated using Equation 2.1 (ASTM C215, 2020):

$$Dynamic\ E = CMn^2 \qquad \textbf{(Equation 2.1)}$$

where:

M = mass of specimen, kg
n = fundamental transverse frequency, Hz
C = 1.6067 (L^3T/d^4) m^{-1} for a cylinder
L = length of specimen, m
d = diameter of cylinder, m
T = correction factor depending on the radius of gyration K ($d/4$ for a cylinder) to the length of the specimen, L, and on the Poisson's ratio

The dynamic modulus for the longitudinal frequency is calculated using Equation 2.2 in ASTM C 215 (2020):

$$Dynamic\ E = DM(n')^2 \quad \textbf{(Equation 2.2)}$$

where:

n' = fundamental longitudinal frequency, Hz
D = 5.093 (L/d^2) m^{-1} for a cylinder

2.8 Pulse Velocity Through Concrete (ASTM C597)

The pulse velocity test procedure is provided in ASTM C597 *Standard Test Method for Pulse Velocity Through Concrete* (ASTM, 2021). The standard test procedure measures the propagation velocity of longitudinal stress wave pulses (P-waves) through a concrete specimen. Longitudinal stress waves must have a resonant frequency in the range of 20 to 100 kHz and are generated from an ultrasonic pulse generator. A receiving circuit measures the travel time through the concrete specimen, which is used to calculate the dynamic modulus of elasticity of the concrete specimen (ASTM, 2021).

The propagated P-wave velocity is a property of the transport medium and is affected by the Young's modulus, Poisson's ratio, and material density. In general, materials with higher densities have relatively higher P-wave velocities (Dashti, 2016). Typical P-wave velocities through concrete are reported to be between 3000 m/s and 5000 m/s (Trifone, 2017).

The dynamic modulus of elasticity for a concrete cylinder is calculated using the cylinder dimensions and weight using Equation 2.3 in ASTM C597 (2016):

$$V = \sqrt{\frac{E(1-\mu)}{\rho(1+\mu)(1-2\mu)}} \quad \textbf{(Equation 2.3)}$$

where:

V = ultrasonic pulse velocity
E = dynamic modulus of elasticity
μ = dynamic Poisson's ratio
ρ = specimen density

Several factors may affect the measurement of the ultrasonic pulse velocity through concrete. Temperature and the moisture content of the sample can both affect the measured pulse velocity. However, variations in the concrete temperature between 10ºC and 30ºC have been shown not to cause any significant change in pulse velocity (IAEA, 2002). Additionally, free water in the voids of concrete can also affect the measured pulse velocity. Candelaria et al. (2020) demonstrated a positive correlation between P-wave velocities and concrete saturation. Higher concrete saturation values result in higher measured pulse velocities.

2.9 Relationship Between the Resonant Frequency and UPV Testing

Both the pulse velocity test (ASTM C597) and the impact resonant frequency test (ASTM C215) allow for the evaluation of the dynamic elastic modulus of a concrete specimen. Trifone (2017) determined the dynamic elastic modulus using both the ultrasonic pulse method and the resonant frequency method on 4″×8″ concrete cylinders, 6″×12″ concrete cylinders, and 3″×4″×16″ concrete prisms. Test results indicated that the dynamic elastic modulus calculated from an ultrasonic pulse test is 10% higher than the dynamic modulus determined through resonant frequency impact testing. Further, a coefficient of determination, R^2=0.97, was reported between the ultrasonic pulse velocity dynamic modulus and the resonance impact dynamic modulus (Trifone, 2017).

Chapter 3

Research Methodology

In this chapter, the laboratory test procedures performed herein to investigate the durability of coarse aggregates are described. This includes methods of durability testing for seven types of coarse aggregates, in Portland cement concrete (PCC) samples, prepared with these coarse aggregates, according to WisDOT PCC pavement mixture design requirements. In addition, field investigations were conducted at several highway pavement sites with apparent aggregate durability related distress such as D-cracking and pitting.

3.1 Coarse Aggregate Sources

The Project Oversight Committee (POC) identified and selected the coarse aggregate (CA) sources for this research project. These sources included calcareous/calcite limestone (CLS), dolomitic limestone (DLS), granite or other igneous rock aggregates (I), and quartzite and other metamorphic rock aggregates (M). The coarse aggregate sources consisted of quarries (Q) and pits (P) with no recycled materials (i.e., all virgin coarse aggregates). A total of 34 coarse aggregate sources (pits and quarries) were identified for this study. The coarse aggregate samples were obtained from these quarries and pits while representatives from WisDOT/POC, the research team, and the quarry/pit managers/staff were present. In a few cases, these representatives were present during sampling. The CA sampling was conducted by WisDOT certified technicians to ensure that coarse aggregate samples were properly collected and processed for the laboratory testing program. The collected CA were classified as 1¼″ dense graded base, ¾″ dense graded base, concrete #1, concrete #2, 1″ clear stone, and 1½″ bituminous aggregate as described by WisDOT Standard Specifications for Highway and Structure Construction (WisDOT 2022). Two to three five-gallon buckets of each coarse aggregate type were collected and transported to the UWM Geotechnical and Pavement Research Laboratory for processing and testing. Figure 3.1 depicts some of the collected aggregates.

The coarse aggregates collected were subjected to standard test procedures, as presented in Table 3.1, to evaluate their specific gravity (G_s), absorption (Abs.), sodium sulfate soundness (SSS), and unconfined freeze-thaw soundness (F-T). In this study, a total of 106 SSS and 170 F-T tests were conducted. The SSS test included the standard five wetting/drying cycles as well as an additional five cycles (i.e., ten total cycles) performed on two limestone sources in order to investigate the number of wetting/drying cycles on the performance of limestone coarse aggregates. The F-T test included the standard 16 F-T cycles in addition to either 16, 32, or 48 cycles (total cycles from 32 to 64) on 12 CA sources. The F-T tests were conducted in three

different laboratories with the majority of these tests performed at UW-Milwaukee using both automated/programmable F-T setups and chest freezer-manual thaw systems.

Figure 3.1: Pictures of typical calcareous (CLS) and dolomitic limestone (DLS) coarse aggregates used for this study.

To differentiate between CLS and DLS, chemical reaction test using hydrochloric acid (HCl) was conducted on all limestone samples. In addition, visual observation and source information provided additional information on the aggregate type.

Table 3.1: Laboratory tests conducted on coarse aggregate samples and PCC specimens.

Standard Test Procedure	Standard Designation	
	ASTM	AASHTO
Standard Test Method for Relative Density (Specific Gravity) and Absorption of Coarse Aggregate (ASTM); Standard Method of Test for Specific Gravity and Absorption of Coarse Aggregate (AASHTO)	C127	T 85
Standard Test Method for Soundness of Aggregates by Use of Sodium Sulfate or Magnesium Sulfate	C88	T 104
Standard Test Method for Soundness of Aggregates by Freezing and Thawing	-	T 103
Vacuum Absorption Test (Modified)	MDOT MTM 113	
WisDOT Test Method for Soundness of Aggregates by Freezing and Thawing		
Standard Test Method for Air Content of Freshly Mixed Concrete by the Pressure Method	C231	T 152
Standard Test Method for Resistance of Concrete to Rapid Freezing and Thawing (Modified)	C666/C666M	T 161
Standard Test Method for Fundamental Transverse, Longitudinal, and Torsional Resonant Frequencies of Concrete Specimens	C215	-
Standard Test Method for Pulse Velocity Through Concrete	C597	-
Standard Test Method for Compressive Strength of Cylindrical Concrete Specimens	ASTM C39/C39M	T 22M/T
Standard Test Method for Static Modulus of Elasticity and Poisson's Ratio of Concrete in Compression	C469/C469M	-
Standard Practice for Petrographic Examination of Hardened Concrete	ASTM C856	

3.1.1 Specific Gravity and Absorption

The coarse aggregate samples collected were processed in accordance with AASHTO T 85 standard test procedure in which the bulk specific gravity G_s (oven dry), saturated surface dry specific gravity G_s (SSD) and apparent specific gravity G_s (Apparent) were calculated from test measurements. Moreover, the absorption was calculated from the AASHTO T 85 test

measurements. The test equipment used in this study conform to the standard test procedure requirements and are periodically calibrated.

3.1.2 Vacuum Absorption Test

Vacuum absorption tests were performed in accordance with the test procedure described in Michigan DOT standard MTM-113 (MDOT, 2020). This procedure utilizes vacuum saturation to maximize coarse aggregate water absorption. The procedure required samples to be oven-dried, placed under a vacuum equivalent to 28.5 inches of mercury for one hour, immersed in the chamber with water while maintaining the vacuum, released from the vacuum, and then soaked for 23 hours. After the 24-hour period, the samples are drained, and the absorption testing was performed. Pictures of the test setup used in this research project are shown in Figure 3.2.

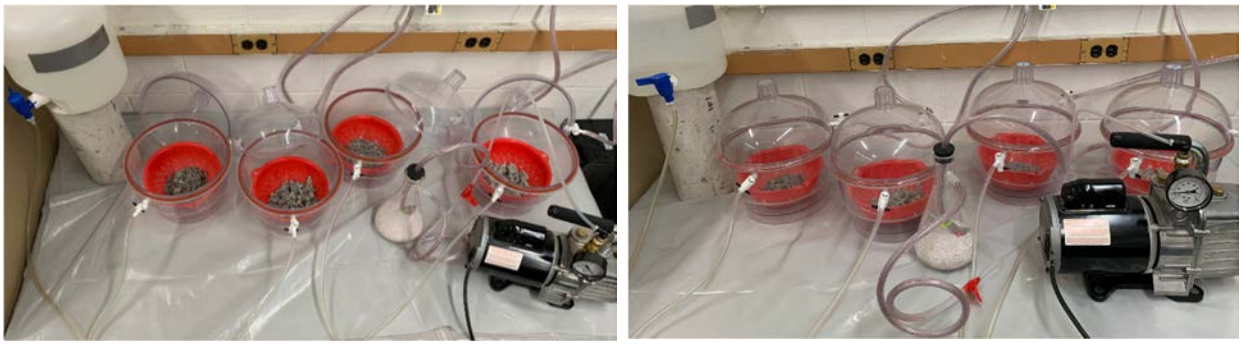

Figure 3.2: Vacuum desiccator and immersion system setup.

3.1.3 Sodium Sulfate Soundness Test

The sodium sulfate soundness test was performed on the coarse aggregate samples in accordance with AASHTO T 104 standard test procedures. A sodium sulfate solution was prepared conforming to the required concentration range as verified by the required specific gravity range. Sieve analysis was used to separate samples into five size fractions per AASHTO T 104 requirements (i.e., passing 1½″ and retained on 1″, passing 1″ and retained on ¾″, passing ¾″ and retained on ½″, passing ½″ and retained on $^{3}/_{8}$ ″, and passing $^{3}/_{8}$ ″ and retained on #4 sieve). The coarse aggregates within each size fraction were washed, dried, weighed to the required weight (specimens), placed in a stainless-steel colander, and then immersed in sodium sulfate container inside a temperature-controlled water tank for 18 hours (wetting cycle), as depicted in Figure 3.3. The coarse aggregate specimens were then removed from the sodium sulfate (SS) solution, drained, and then placed in the oven for the drying cycle. The specimens were kept in the same stainless-steel colander during both the wetting and drying cycles to minimize particle disturbance during the test. At the end of the fifth wet/dry cycle, the coarse

aggregate specimens (still in the colander) were stacked. Plastic colanders were used to separate the colanders containing the aggregate samples. Then, the aggregate in the colanders were washed until sodium sulfate was completely removed, which was verified by testing the water with a Barium Chloride solution. Finally, the aggregate fractions were dried, sieved using the appropriate sieve size for each fraction, and then weighed to determine the mass loss.

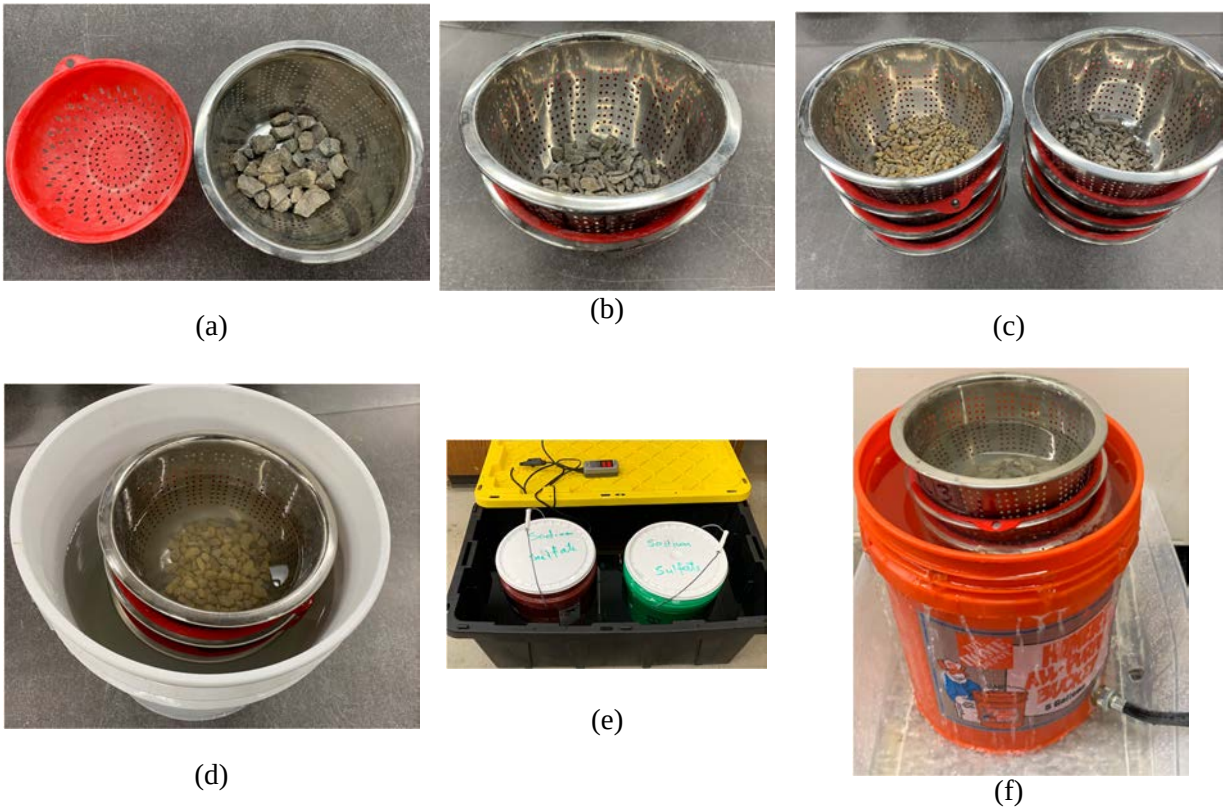

(a) (b) (c) (d) (e) (f)

Figure 3.3: (a) Colanders used to hold coarse aggregates; (b) Typical colander stacking practice; (c) Example of colander stacks for SSS test containing CLS (left) and DLS (right) aggregate specimens; (d) Colander stack in SS solution bucket; (e) SS solution buckets in temperature regulated water bath; (f) Setup for flooding colander stacks to wash specimens.

3.1.4 Soundness of Aggregates by Freezing and Thawing

The coarse aggregates were subjected to both: (a) the freeze-thaw (F-T) soundness testing by WisDOT-Modified AASHTO T103 test procedure, and (b) the AASHTO T 103 standard test procedure. Coarse aggregate samples in different size fractions were prepared per AASTHO T 103 requirements (the same procedure used to prepare specimens for AASHTO T 104). In this study, AASHTO T 103 procedure B was used to prepare the coarse aggregate specimens and condition them for F-T testing. These specimens, with measured dry masses, were placed in vacuum desiccators to achieve 1 in. air pressure (~ 28.5 in. Hg of vacuum). The samples were

then inundated with a water-ethanol solution (with a concentration of 0.5% ethanol for AASHTO T 103 and methanol for WisDOT-Modified AASHTO T 103) while maintaining the vacuum for 15 minutes. Each aggregate sample was then placed in a plastic container under a ¼ in. deep water-ethanol or water-methanol solution, covered, and placed in an automated F-T testing machine conforming to AASHTO T 103 F-T cycle requirements, as shown in Figure 3.4.

To compare the automated and manual freezing-thawing, the samples were divided into two sets of duplicate aggregate samples. Each set had nine coarse aggregate types and four size fractions, resulting in a total of 36 specimens in each set. One set was placed in the automated/programmable F-T test machine and the other set was placed in a commercial grade chest freezer (manual freeze-thaw cycles with air circulating fans). Sample preparation and conditioning was the same in both the automated system and the chest freezer. The freezing and thawing temperature requirements of the AASHTO T 103 standard procedure were satisfied during the F-T cycles.

The coarse aggregate samples in the automated system were kept for eight continuous days to complete sixteen F-T cycles (six hours of freezing and six hours of thawing were enough to satisfy the temperature requirements). On the other hand, the coarse aggregate samples placed in the chest freezer needed 16 days of continuous testing to complete the sixteen F-T cycles. It should be noted that the chest freezer experiment was difficult to perform. Observation of the freezer temperatures indicated that freezing times were inconsistent. A data acquisition system with thermocouples connected to a coarse aggregate particle was used to monitor and verify the test temperature when the chest freezer was used. The freezing cycle time ranged between eight and twelve hours to achieve the temperature requirement, and the thawing cycle time varied between four and six hours when the chest freezer was used.

After the completion of the 16th cycle, each specimen was washed, oven-dried, and sieved on the appropriate sieve size. The retained mass of each sample was measured and recorded, and the mass loss was calculated. To investigate the effect of the number of F-T cycles on the durability performance of coarse aggregate (primarily CLS and DLS), 12 aggregate sources were subjected to 16, 32, 48, and 64 F-T cycles.

Figure 3.4: Freeze-thaw test systems used to process the investigated coarse aggregates.

3.2 Coarse Aggregates in Portland Cement Concrete

Eight coarse aggregate sources were used to design Portland cement concrete mixes following WisDOT mixture design requirement for PCC pavements. These included two CLS, two DLS, one limestone-Pit (LS-P), one igneous-metamorphic-pit (I+M-P), one igneous (I-Q), and one metamorphic (M-Q) aggregate sources. Seven CA sources were used in the PCC samples from the lab mixing and one CA source from a PCC obtained from paving project. The other concrete mix ingredients (i.e., the fine aggregates, Portland cement, fly ash, air entraining admixtures, etc.) were all kept the same for all seven PCC mixes. The mixing of PCC, quality control testing, preparation/casting of 4 in. and 6 in. diameter cylinders, and the curing were conducted by the research team and the Trierweiler Construction & Supply Co., Inc. at the latter's PCC laboratory in Marshfield, WI. Figure 3.5 depicts the PCC mixing, test cylinders preparation, and curing. The eighth CLS coarse aggregate was used in a WisDOT approved PCC mix by a paving contractor, who provided the 4 in. PCC cylinders. PCC mixture constituents and properties used to make the test cylinders in this study are presented in the Appendix B.

Figure 3.5: Picture of the various steps taken to prepare PCC test cylinders.

The laboratory testing program for this study was conducted on concrete cylinders at ages of 28 days and 6 months. This was done to account for the effect of the age of PCC when first exposed to freezing and thawing. The testing performed on the concrete cylinders consisted of the following: ASTM C666 *Standard Test Method for Resistance of Concrete to Rapid Freezing and Thawing,* ASTM C215 *Standard Test Method for Fundamental Transverse, Longitudinal, and Torsional Resonant Frequencies of Concrete Specimens*, ASTM C597 *Standard Test Method for Pulse Velocity Through Concrete,* and ASTM C39 *Standard Test Method for Compressive Strength of Cylindrical Concrete Specimens and* ASTM C856 *Standard Practice for Petrographic Examination of Hardened Concrete.*

3.2.1 Resistance of Concrete to Rapid Freezing and Thawing

The PCC cylinders (4 in. diameter by 8 in. long) prepared using the investigated coarse aggregates were used to evaluate the F-T durability of the PCC used in pavement surface layers. A group of these cylinders were prepared using the same mix design and mixture constituents, while only varying the coarse aggregate type/source. The other group was obtained from a pavement construction site during paving operation and was cast by a WisDOT certified technician. These concrete cylinders were cured for 28 days and then separated into two groups, one group was immediately processed using ASTM C666 test procedure (early age exposure) and the other kept in a dry state on a shelf in the laboratory for six months (late age exposure). At the age of six months, the second group of cylinders were subjected to ASTM C666 test procedure. It should be noted that both groups were subjected to the rapid freeze-thaw cycles in accordance with the ASTM C666 standard test procedure B, but with a modified freeze-thaw cycle time and sample size. It was not possible to reach the temperature ranges required in ASTM C666 standard procedure in the middle of the 4″×8″ concrete cylinders within the specified time limits. On average, seven hours were needed to achieve the temperature ranges.

The research objective was to evaluate the effect of coarse aggregate type on the performance of the PCC considering first exposure to freeze-thaw cycles at a young age (concrete pours in October-November timeline) or more mature age (concrete pours in May-June timeline). Since all samples in each group were subjected to the same test conditions, the relative performance of the PCC (and the coarse aggregate used to produce it) can still be evaluated even with the modified ASTM C666 test procedures. All PCC cylinders were subjected to 300 F-T cycles. However, a limited number of specimens were subjected to 450 freeze-thaw cycles. Pictures of the concrete samples in the freeze-thaw chamber are shown in Figure 3.6.

(a) (b)

Figure 3.6: (a) PCC cylinders in frozen state inside the rapid freeze-thaw chamber; (b) The temperature-time freeze-thaw cycles applied to these cylinders.

3.2.2 Evaluation of PCC Properties due to Rapid Freeze-Thaw Cycles

In order to investigate the influence of coarse aggregate quality on PCC performance, the dynamic modulus of elasticity was evaluated for the PCC cylinders after the completion of a certain number of freeze-thaw cycles. The number of cycles between dynamic modulus tests was generally about 30 freeze-thaw cycles.

The dynamic modulus of elasticity (E_d) of the PCC cylinders was determined using the impact resonance frequency method in accordance with ASTM C215 *Standard Test Method for Fundamental Transverse, Longitudinal, and Torsional Resonant Frequencies of Concrete Specimens*. In this method, the fundamental resonant frequencies (longitudinal and transverse) were measured, as depicted in Figure 3.7. The 4 in. diameter PCC cylinders were tested using a commercially available system that included software for signal processing.

Prior to placing the PCC cylinders in the ASTM C666 rapid freeze-thaw chamber, the resonant frequency testing was performed on three cylinders to establish the initial values of the dynamic elastic modulus (E_{d0}) before any freeze-thaw cycles are applied. The PCC cylinders were removed from the freeze-thaw chamber at roughly 30 cycle intervals to perform the resonant frequency testing. The cylinders were then placed back in the freeze-thaw chamber.

In addition, the dynamic elastic modulus of the PCC cylinders was determined through ultrasonic pulse velocity (UPV) testing in accordance with ASTM C597 *Standard Test Method for Pulse Velocity Through Concrete*. The UPV method measures the travel time of ultrasonic waves that travel through the PCC cylinders. The dynamic modulus of elasticity was then calculated using the measured UPV and the dimensions/weight of the cylinder.

The ultrasonic pulse was propagated through the concrete cylinders with a pulse generator and measured with a receiving circuit. The pulse wave was additionally monitored using an oscilloscope to increase the measurement accuracy. Figure 3.7 depicts a set of images for the stiffness and strength tests conducted on the investigated PCC cylinders.

Twelve PCC cylinders, which were subjected to 300 F-T cycles, were taken to the American Engineering Testing, Inc. laboratory in St. Paul, MN for petrographic analysis following ASTM C856. The purpose was to evaluate the PCC degradation due to F-T conditioning and to determine the influence of the coarse aggregate type on PCC durability (distress/deterioration).

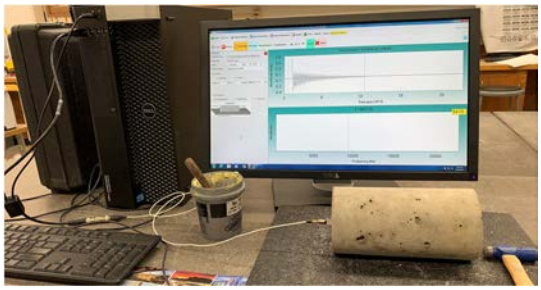

(a) Longitudinal resonant frequency test of PCC cylinder

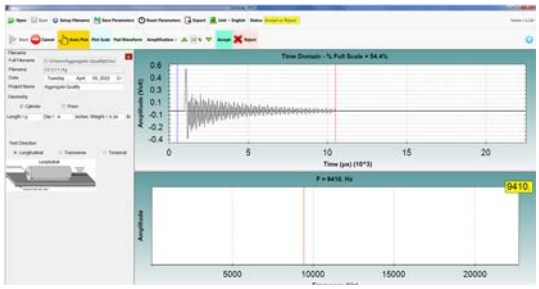

(b) Software for signal perocessing

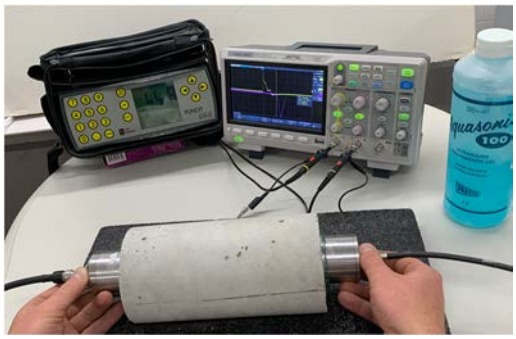

(c) Ultrasonic pulse velocity test of PCC cylinder

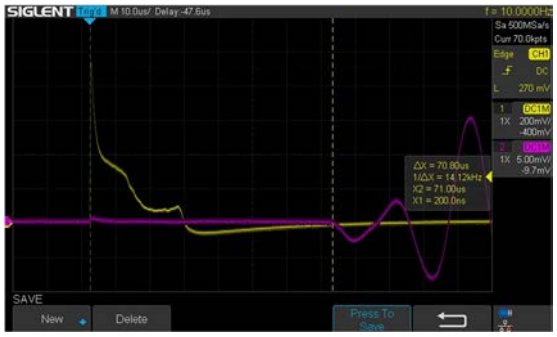

(d) Oscilloscope for signal processing

Figure 3.7: Laboratory tests to evaluate the PCC stiffness and strength properties due to freeze-thaw cycles.

3.3 Coarse Aggregate Durability Performance – Field Investigation

The Project Oversight Committee (POC) identified a few PCC pavement sites that were exhibiting distress attributed to aggregate quality, which were selected for field evaluation. The research team also contacted WisDOT pavement engineers and Wisconsin Concrete Pavement Association (WCPA) for help in identifying additional distressed PCC pavement sites. Furthermore, the research team performed analyses using WisDOT's PIF database and identified a few projects with such distress issues. A total of 16 PCC pavement sites were identified based on this combined effort; however, field survey and subsequent evaluation conducted by the research indicated that only 12 PCC pavement sites showed a durability related distress consisting of D-cracking and coarse aggregate pitting/popouts.

The field work conducted at the 12 sites consisted of pavement distress surveys and evaluation, analysis of WisDOT's PIF database, coring of concrete at three pavement sites, and petrographic analysis of the PCC cores. Historical coarse aggregate data from these pavement sites were obtained (when possible) and analyzed to help evaluate the possible cause(s) of the observed distress and its relationship to the CA source. Figure 3.8 depicts coring at one of the field sites.

(a) (b) (c) (d)

Figure 3.8: Field investigation coring: (a) and (b) coring at D-cracking location, (c) retrieved PCC core with significant CA and PCC paste cracking, and (d) inside the cored hole with visible cracking in CA and PCC paste.

3.4 Analysis of Wisconsin Aggregate Durability Tests

In order to help achieve the project objectives, the research team conducted detailed analyses on historical Wisconsin coarse aggregate test results, including various CA sources in addition to analysis of test results subset of CLS and DLS coarse aggregates.

Chapter 4

Laboratory Test Results and Analysis – CA Durability Performance

This chapter presents the results of the various laboratory tests conducted on the acquired unbound coarse aggregates. The results include specific gravity, absorption, vacuum absorption, and mass loss due to sodium sulfate soundness (SSS) and freeze-thaw (F-T) tests. Additionally, the influence of the following variables on the results was investigated: test type, test equipment, test laboratory, number of wetting/drying cycles, F-T cycles, absorption, aggregate source, aggregate size fraction, and aggregate classification. A critical analysis and evaluation of the test results is also included in this chapter.

4.1 Coarse Aggregate – Laboratory Test Results

In this study, a total of 106 SSS and 170 F-T tests were conducted on 34 coarse aggregate (CA) sources, from pits and quarries. The various CA classifications are: 1¼″ dense graded base, concrete #1, concrete #2, 1″ clear stone, and 1½″ bituminous. The SSS test included the standard five wetting/drying cycles as well as additional five cycles (i.e., total of 10 cycles) on two limestone sources. The F-T test included the standard 16 F-T cycles in addition to 16, 32, and 48 cycles (from 32 to 64) on 12 CA sources. The F-T tests were conducted in three different laboratories with the majority done at UW-Milwaukee using both automated/programmable F-T and chest freezer-manual thaw systems.

4.1.1 Specific Gravity, Absorption, and Vacuum Absorption

The results of AASHTO T 85 test conducted to determine the specific gravity of the investigated CA are depicted in Appendix C. The bulk specific gravity of the calcareous limestone aggregates (CLS) ranges from 2.40 to 2.64 with an average of 2.55 and the bulk specific gravity of the dolomitic limestone (DLS) varies between 2.60 and 2.77 with an average of 2.73. The results show that the CLS aggregates possessed lower bulk specific gravity values, on average, compared to the DLS aggregates. In addition, the difference between the bulk specific gravity and the apparent specific gravity for the CLS coarse aggregates is larger than that of the DLS, demonstrating that the CLS aggregates are more porous than the DLS aggregates. The bulk specific gravity, the saturated-surface dry (SSD) specific gravity, and the apparent specific gravity values are generally within the typical ranges of coarse-grained aggregates, with sedimentary rock origin.

The results of the AASHTO T 85 and MDOT MTM 113 tests to determine the absorption and vacuum absorption values of the investigated coarse aggregates are shown in Figure 4.1. The results shown are for the size fractions retained on $^{3}/_{8}$ ″ and ½″ sieves. Inspection of Figure 4.1

shows that the vacuum absorption (VAbs.) values of the investigated coarse aggregates, with an average of VAbs.=2.50%, are greater that the absorption (Abs.) values, with an average of Abs.=2.04%. In addition, the test results indicate that the DLS coarse aggregate had lower absorption values (average of 1.07%) compared with CLS values (average of 2.71%). It should be noted that the vacuum absorption test presented herein was conducted on all CLS and DLS CA sources using only the $^{3}/_{8}$ ″ and ½ ″ size fractions. Figure 4.2 presents the variation of CA absorption based on source and classification, which show that CA absorption of CLS > DLS > Igneous and Metamorphic. Also, this figure shows that the base materials have the highest absorption when compared with the CA of concrete # 1 and #2.

The research team conducted statistical analyses on a large dataset of absorption test results of coarse aggregates from various Wisconsin rock formations as depicted in Figure 4.3. The dataset absorption values vary between 0.21% and 5.90%, with an average of 1.92% and standard deviation of 0.89%. The coarse aggregates, from all sources, investigated in this study possessed an average absorption of 1.78% with standard deviation of 1.02%, while the CLS and DLS coarse aggregates possessed an average absorption of 2.19% with a standard deviation of 1.02%.

Examination of Figure 4.3a shows that the distribution of the absorption data is bimodal, which is attributed to the presence of two groups of coarse aggregates. Group No.1 coarse aggregates have relatively low absorption values that are typically obtained from igneous and metamorphic rocks such as granite and quartzite formation, in addition to some low-porosity dolomitic limestones (a sedimentary rock). Group No.2 consists of coarse aggregates collected from rock formations with relatively high absorption values (such as calcareous limestone with high porosity and some dolomitic limestone formations that possess relatively high porosity). Therefore, the absorption data is split into two groups with two separate distributions, as shown on Figure 4.3b. The absorption data for thirteen CLS coarse aggregates fell within the second group with an average absorption of 3.01%. Also, eight DLS aggregates fell within the first group with an average absorption value of 1.33%. This shows that the absorption of the investigated aggregates, on average, is relatively high.

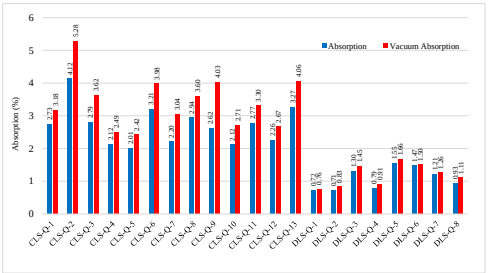

(a) weighted average for 3/8 and ½ ″ size fractions

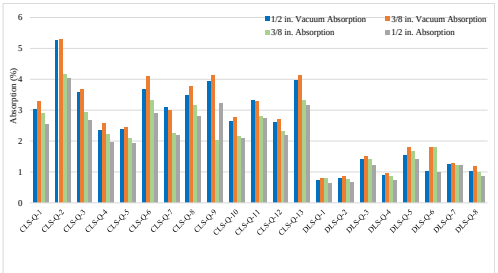

(b) 3/8 and ½ ″ size fractions (CLS and DLS)

Figure 4.1: Absorption and vacuum absorption test results of the investigated coarse aggregates.

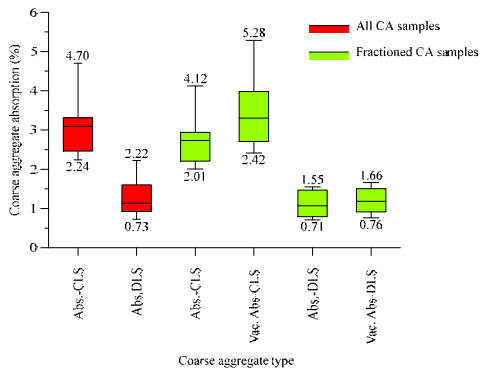

(a) Whole (non-fractioned) CLS and DLS vs. fractioned CLS and DLS(Abs. & VAbs.)

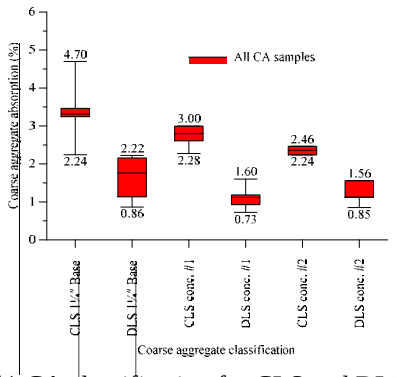

(b) CA classification for CLS and DLS

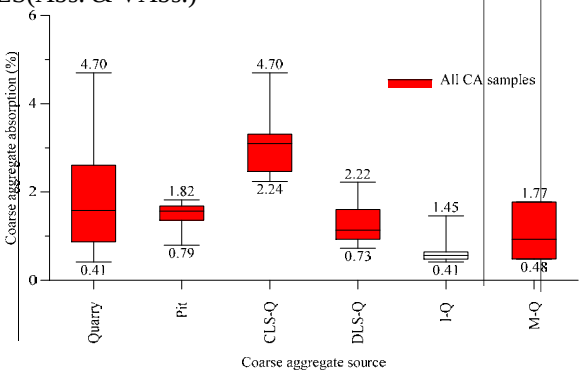

(c) CA source/origin type

Figure 4.2: Absorption and vacuum absorption test results of the investigated coarse aggregates.

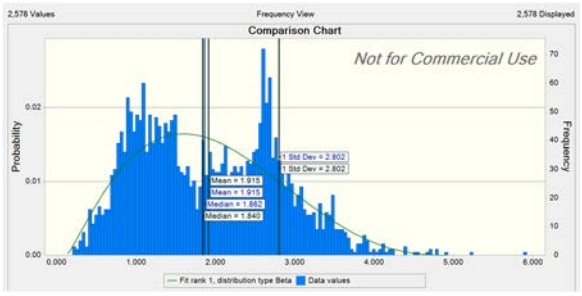

(a) Bimodal distribution

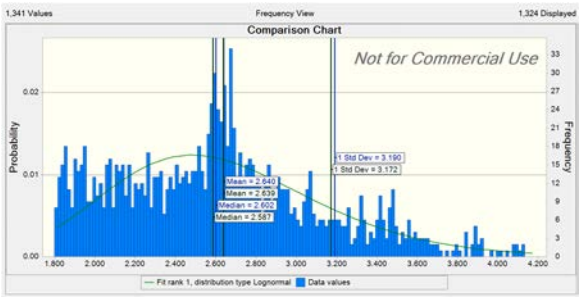

(b) High absorption data

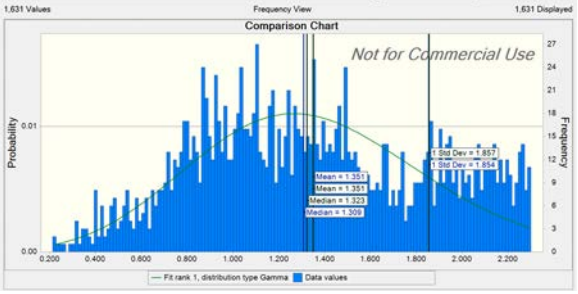

(c) low absorption data

Figure 4.3: Results of statistical analysis on a large dataset of absorption tests conducted on Wisconsin aggregates of various rock formations.

4.1.2 Sodium Sulfate and Freeze-Thaw Durability Testing

The results of the SSS and F-T test for the investigated coarse aggregate samples are summarized in Tables 4.1 and 4.2 and are shown in Figure 4.4. The variation of the mass loss (in percent) for the investigated coarse aggregates is also presented in the figure in the form of box-whisker plots. An inspection of the SSS and F-T average values from the tables and figures indicate the following based on CA source:

- SSS mass loss of quarried CA > SSS mass loss of pit gravel.
- F-T mass loss of quarried CA > F-T mass loss of pit gravel.
- SSS mass loss of CLS ≅ SSS mass loss of DLS *note: Abs.(CLS)>Abs.(DLS).*
- F-T mass loss of CLS < F-T mass loss of DLS *note: Abs.(CLS)>Abs.(DLS).*
- SSS and F-T are lowest for CA of igneous and metamorphic rock origins.

Moreover, the SSS and F-T data averages from the tables and figures for CLS and DLS indicate the following based on CA classification:

- SSS mass loss of base CLS CA > SSS mass loss of concrete #1 and #2 CLS.
- SSS mass loss of base DLS CA > SSS mass loss of concrete #1 and #2 DLS.
- F-T mass loss of base CLS CA ≅ F-T mass loss of concrete #1 CLS and > F-T mass loss of concrete #2 CLS.
- F-T mass loss of base DLS CA > F-T mass loss of concrete #1 and #2 DLS.

Table 4.1: SSS and F-T test results based on the CA source.

CA Source	Total Mass Loss (%)				Absorption (%)	
	SSS Test		F-T Test			
	Average	COV	Average	COV	Average	COV
All Quarry	12.0	76.9	11.6	98.3	1.82	60.2
All Pit	5.8	48.7	7.1	64.9	1.47	22.1
CLS – Quarry	14.6	44.1	10.5	85.2	3.01	21.0
DLS – Quarry	15.0	75.1	19.1	66.9	1.33	37.1
Igneous – Quarry	3.4	129.1	1.1	163.0	0.72	56.9
Metamorphic – Quarry	9.8	56.6	12.5	89.2	1.02	63.6

Table 4.2: SSS and F-T test results based on the CA classification.

CA Classification	CLS Total Mass Loss (%)				DLS Total Mass Loss (%)				Absorption (%)			
	SSS Test		F-T Test		SSS Test		F-T Test		DLS		CLS	
	Ave.	COV	Ave.	COV	Ave.	COV	Ave.	COV	Ave.	COV	Ave.	COV
1¼″ Base	16.7	40.5	11.1	81.7	22.3	38.6	21.8	52.9	3.39	18.8	1.63	32.6
Concrete #1	13.4	46.3	11.8	74.4	14.5	79.3	16.1	92.5	2.72	12.7	1.14	25.7
Concrete #2	14.1	52.2	8.7	103.4	3.1	83.1	13.5	126.9	2.35	4.8	1.17	25.1

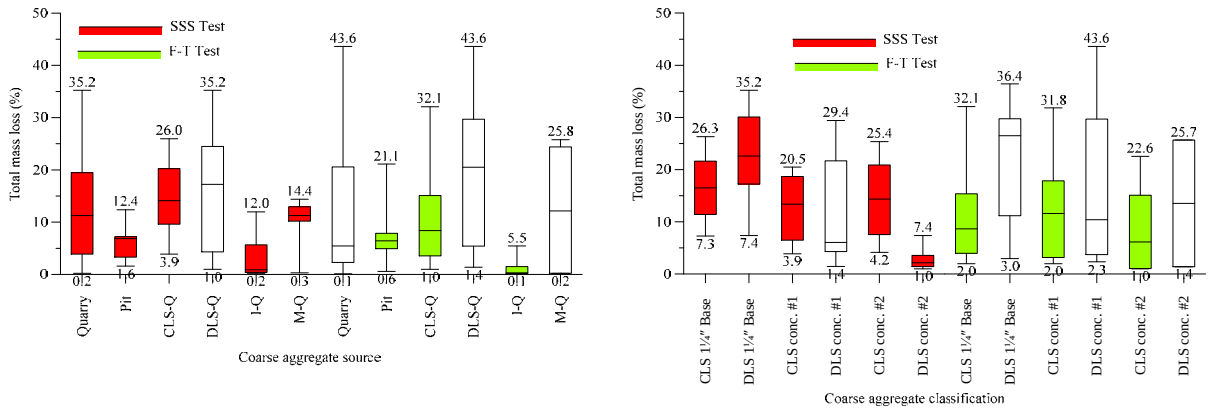

(a) based on CA source (b) based on CA classification

Figure 4.4: SSS and F-T test results based on the CA source.

When comparing CLS and DLS mass loss for individual samples, there is no specific trend, with both CLS and DLS aggregates exhibiting relatively low and high values of mass loss. Attempts to find a relationship between SSS mass loss and absorption (as well as vacuum absorption) of the CLS and DLS coarse aggregates did not yield any promising trends. The same outcome was reached when considering F-T mass loss vs. absorption and vacuum absorption. There are coarse aggregates with high absorption (porosity) that exhibited low SSS and F-T mass loss and vice versa.

In addition, the CLS and DLS coarse aggregate samples contained non-formation particles such as shale, chalk, chert, and other materials that influence the mass loss results if present in the tested specimen. Figure 4.5 depicts particles that are considered non-formation within the coarse aggregate tested specimens showing significant degradation/breakage and disintegration due to sodium sulfate wetting/drying and F-T cycles.

The research team conducted comprehensive statistical analyses on SSS and F-T tests conducted on Wisconsin aggregates as presented in Figures 4.6 and 4.7. Inspection of Figure 4.6 shows that 7.35% of Wisconsin CA would fail the SSS test when the corresponding cut-off mass loss percentage is 12% (measured using the SSS test). When comparing the investigated coarse aggregate SSS mass loss to the large data set analyzed herein, eight out of the thirteen CLS CA samples possessed a mass loss > 12% and five out of the eight DLS CA samples exhibited SSS mass loss larger than 12%. The relatively large population of higher mass loss indicates that the investigated coarse aggregates possessed physical properties related to porosity, pore size, and pore size distribution, which resulted in high absorption values and subsequently influenced the durability of the aggregates. In addition, several aggregate sources exhibited poor to marginal quality with non-formation materials.

When comparing the test results with the Wisconsin aggregate test database, as shown in Figure 4.7, three out of the thirteen CLS samples exhibited a mass loss greater than 12.4% due to F-T testing, which corresponds to 92.6% passing specimens out of the large test population (remaining consistent with the previous 7.35% failure rate used for the SSS dataset analysis). For

the dolomitic limestone sources, five out of eight samples possessed a freeze-thaw mass loss greater than 12.44%. It should be noted that the five dolomitic limestone specimens that failed the large set threshold limit of 12% for the SSS test are the same coarse aggregate samples that failed the freeze-thaw threshold limit of 12.44%, based on the analysis of the large dataset.

(a) Shale within DLS CAsample

(b) Chalk within CLS CA sample

(c) Chert within pit gravel CA sample

(d) Shale was “common” on DLS samples investigated

(e) Heterogenous composition of pit gravel leads to unpredictable out come

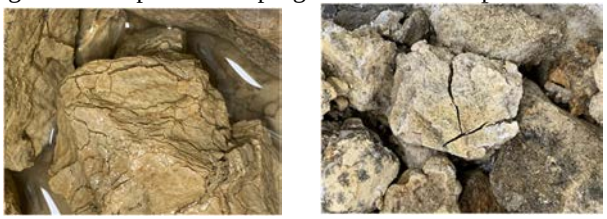

(f) CA CLS disintegration/breakage

Figure 4.5: Non-formation particles within tested coarse aggregate specimens.

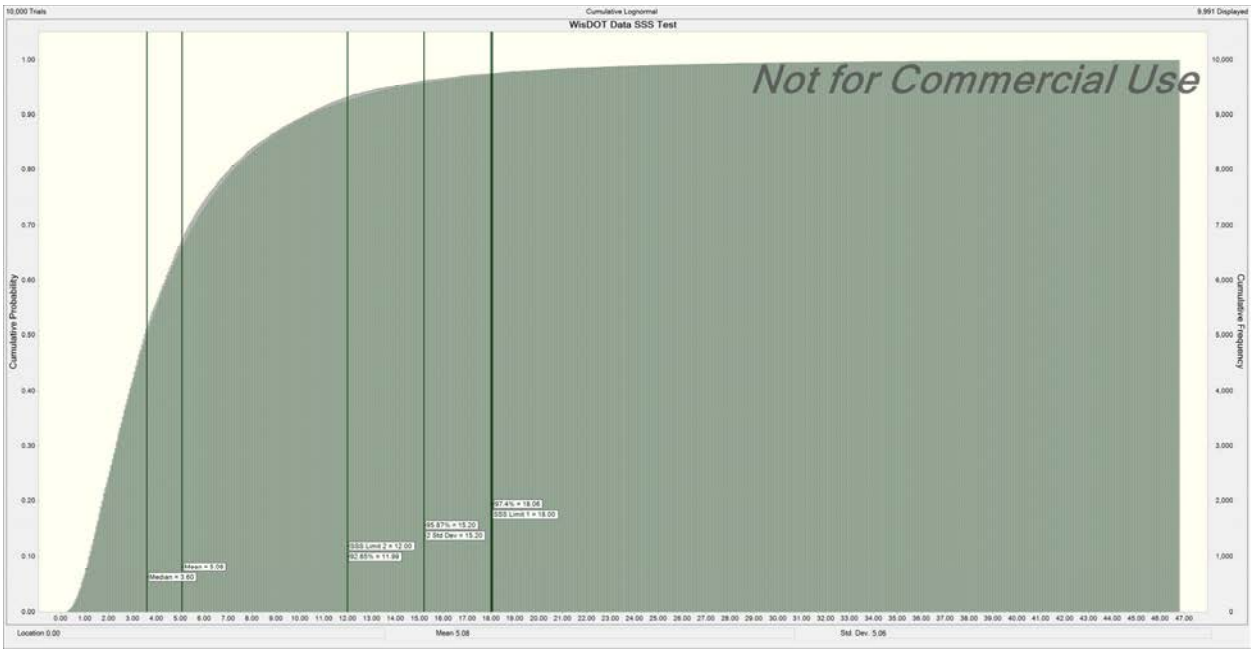

(a) Cumulative distribution

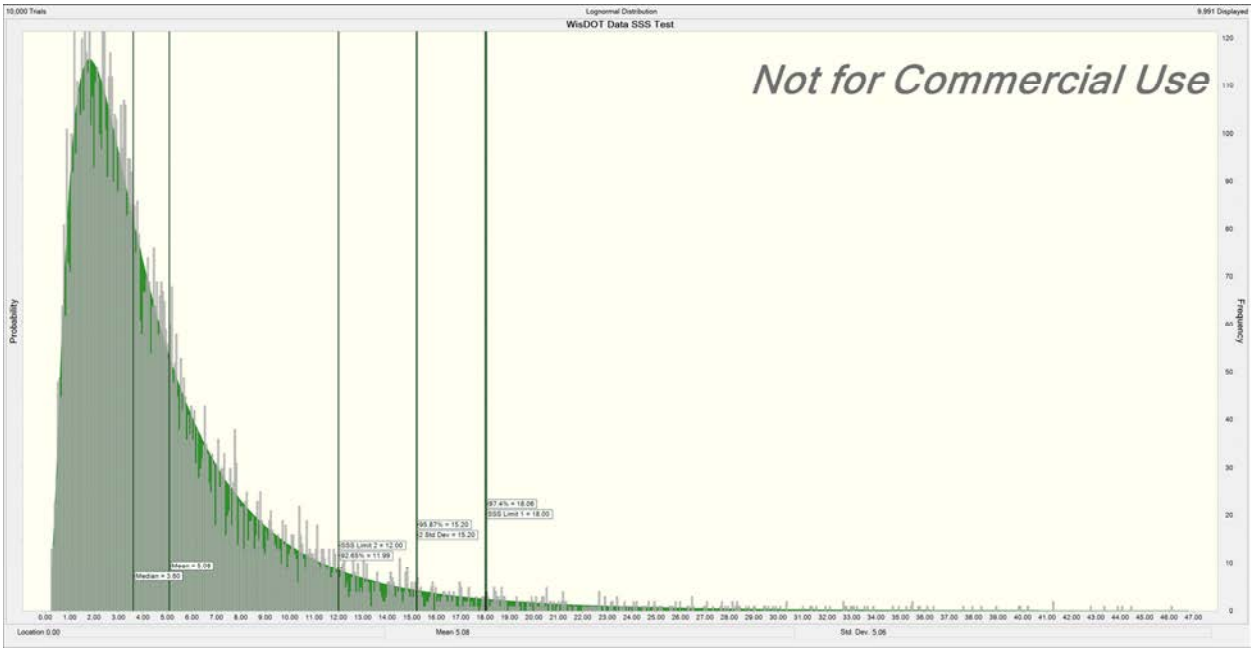

(b) Lognormal distribution

Figure 4.6: Results of statistical analysis on a large dataset of SSS tests conducted on Wisconsin aggregates of various rock formations.

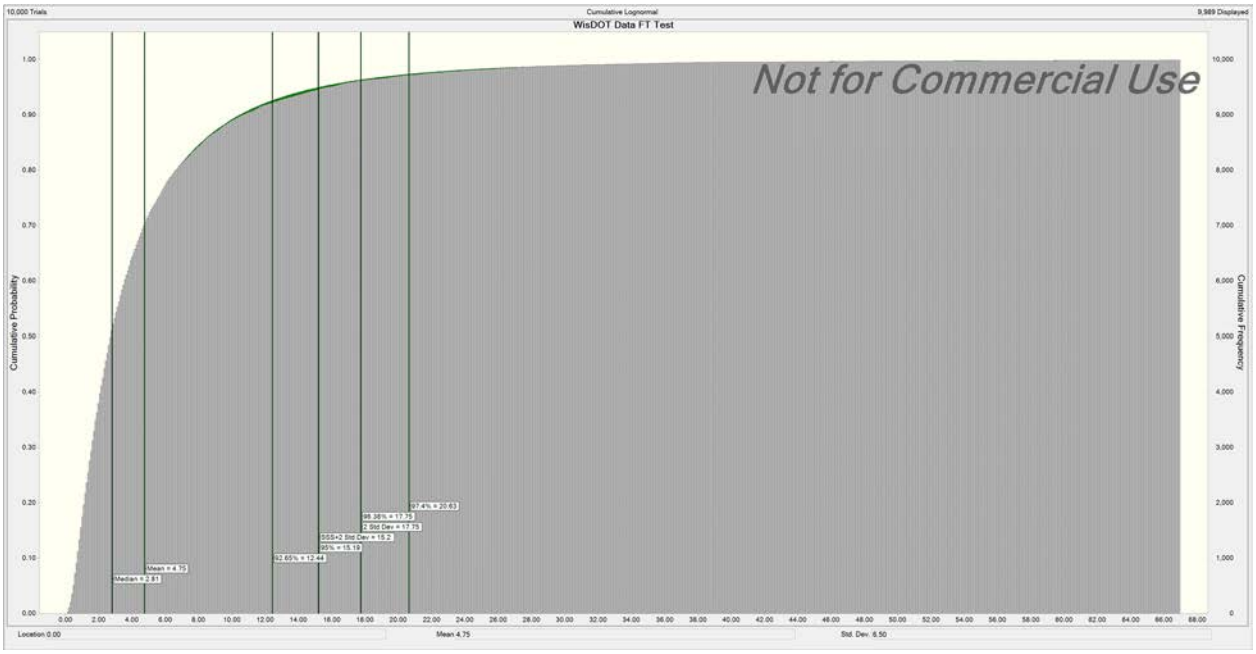

(a) Cumulative distribution

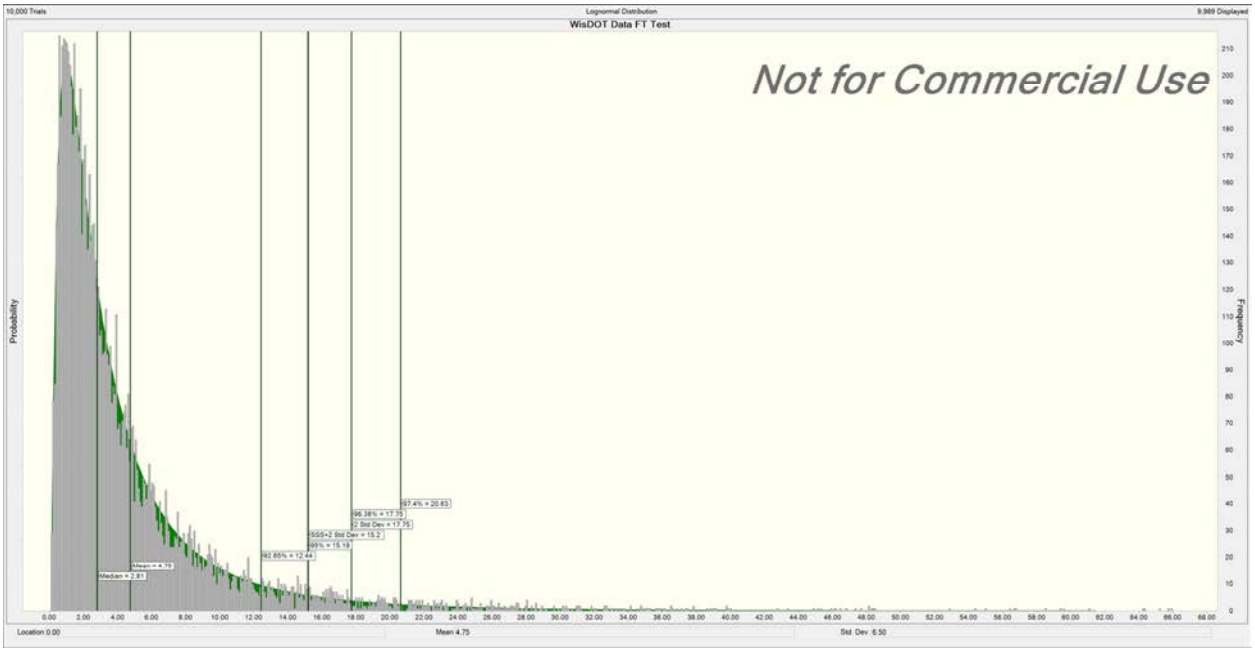

(b) Lognormal distribution

Figure 4.7: Results of statistical analysis on a large dataset of F-T tests conducted on Wisconsin aggregates of various rock formations.

4.1.3 F-T and SSS Performance of CA Size Fractions

Analysis of SSS and F-T test results presented earlier were performed using WisDOT weighted multipliers. The WisDOT method is based on combining two size fractions when calculating the total mass loss in which the size fractions of 1½″→1″ and 1″→¾″ are combined,

and size fractions of ¾″→½″ and ½″→⅜″ are also combined, while the size fraction of ⅜″→#4 is not combined.

Total mass loss due to SSS and FT presented earlier focused on the coarse aggregate source and classification. To study the mass loss based on the size fractions, a separate weighted average needs to be used for each size fraction based on its initial weight. The current WisDOT method cannot be used since it is based on combining two size fractions when calculating the total mass loss and will not produce data for all size fractions. Figure 4.8 presents the results of SSS and F-T tests with the mass loss calculated based on WisDOT's method and the weighted average approach. This shows that both methods are "similar;" therefore, the CA size fractions mass loss comparison can be used herein.

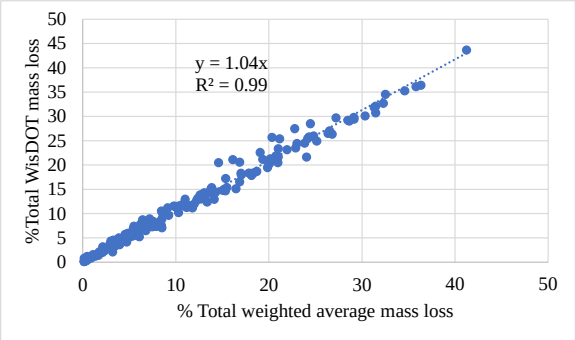

Figure 4.8: comparison of total SSS and FT mass loss using the weighted average and WisDOT weighted multiplier.

The research team conducted analyses of the SSS and F-T mass loss based on the size fractions and the results are presented in Table 4.3 and Figure 4.9. Considering the SSS test results, the larger CA particles (larger size fractions) exhibited more weighted mass loss, on average, when compared with the smaller size particles for CLS. The opposite trend is exhibited by both CLS and DLS when considering the results of the F-T test. On the other hand, there is no clear trend for DLS with the middle size fractions exhibiting the highest SSS mass loss. The authors speculate that the test procedure has an influence on the size fractions mass loss. In SSS test, all CA particles are fully immersed in the sodium sulfate solution, while in the F-T test, the smaller size fractions particles of less or equal ¼″ are fully immersed in the alcohol-water solution and the larger particles are partially immersed.

To further investigate the effect of F-T test on size fraction mass loss, freeze-thaw tests were performed on CLS and DLS aggregates of 3/8″ and ½″ size fractions. Test results, presented Figure 4.10, showed greater mass loss exhibited by the smaller size fraction of 3/8″ compared with ½″ size fraction. The average mass loss for the 3/8″ and ½″ aggregate fractions aggregate fractions were 19.1% and 10%, respectively.

Table 4.3: SSS and F-T test results based on the CLD and DLS size fractions.

Test	Size Fraction	CLS Weighted Mass Loss (%)		DLS Weighted Mass Loss (%)	
		Average	COV	Average	COV
Sodium Sulfate Soundness	1½″→1″	4.8	55.0	3.7	85.9
	1″→¾″	4.6	48.9	4.1	73.6
	¾″→½″	4.1	48.5	4.7	83.0
	½″→⅜″	2.8	47.7	3.1	81.3
	⅜″→#4	2.4	52.9	2.5	77.6
Freeze-Thaw	1½″→1″	1.4	112.0	2.8	70.2
	1″→¾″	2.4	106.2	3.4	84.7
	¾″→½″	2.9	89.8	5.4	80.3
	½″→⅜″	2.5	89.2	4.5	68.6
	⅜″→#4	2.9	81.2	5.1	65.1

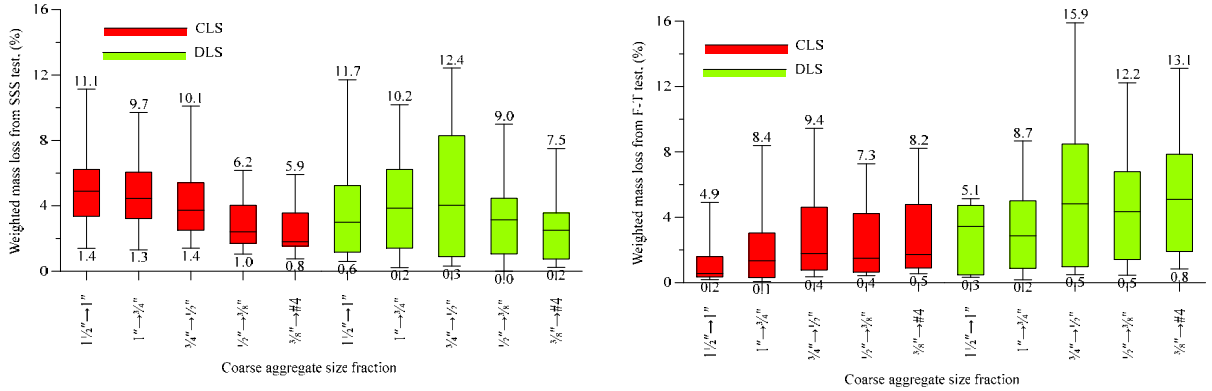

(a) SSS test (b) F-T test

Figure 4.9: Weighted mass loss per size fractions of CLS and DLS CA.

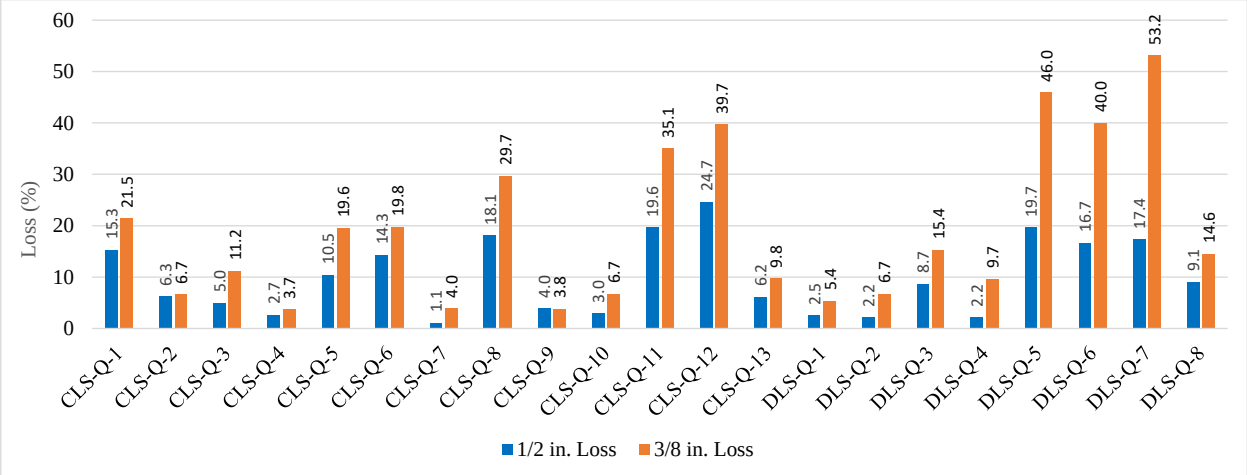

Figure 4.10: Comparison of 3/8 ″and ½″ coarse aggregate fraction loss from freeze-thaw testing.

4.1.4 Influence of Freeze-Thaw System on CA Performance

AASHTO T 103 standard test procedures describe the "freeze apparatus" requirements solely based on temperature range and minimum time for both freezing and thawing states. In Wisconsin, chest freezers and automated/programmable freeze-thaw system are used by commercial testing laboratories, the WisDOT materials testing laboratory, and research laboratories at academic institutions. Chest freezers are commonly used by commercial testing laboratories due to low initial investment. However, operation of chest freezers is usually labor intensive. They are very difficult to control and achieve uniform freezing temperatures among the different test specimens. The freezing rates are also not consistent across the different cycles as they depend on the number of containers in the freezer and require manually removing specimens from the freezer. This is done to allow thawing outside in which samples are usually disturbed/shaken when placed in the freezer again after the thaw cycle ends. On the other hand, automated freeze-thaw systems are available and gaining popularity due to their systematic and consistent freeze-thaw cycles, automation, uninterrupted processing time, and convenience.

Freeze-thaw testing in accordance with AASHTO T 103 was performed on select coarse aggregate samples with a commercially available chest freezer and with an automated freeze-thaw system. The measured temperature-time graphs for the chest freezer method and automated F-T system methods are shown in Figure 4.11. Figure 4.11 indicates that one freeze-thaw cycle for chest freezer #1 was approximately 16 hours (which varied throughout testing depending on the measured freezing rate) whereas, one freeze-thaw cycle for the automated system was approximately 12 hours. It should be noted that the automated system provided a greater ease of use. The test protocol was programmed and automatically run, compared with the chest freezer, where inconvenient times were required to place and remove samples from the chest freezer.

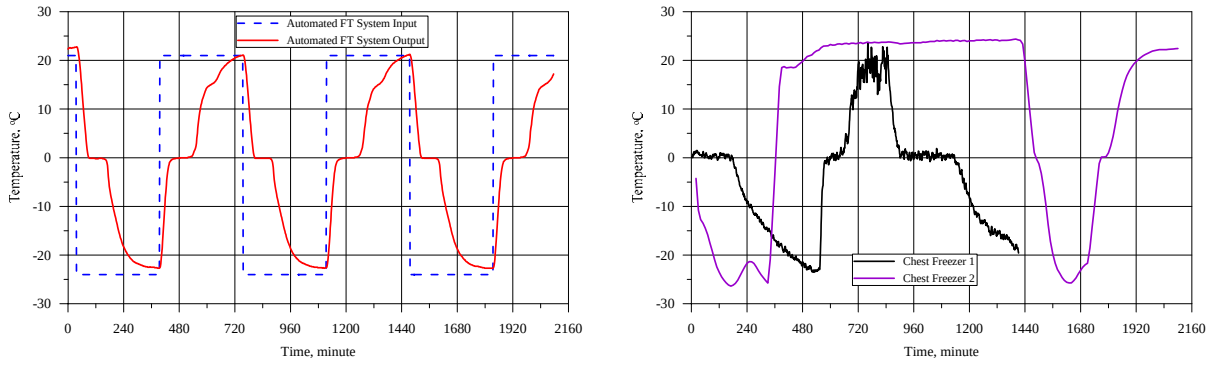

(a) Automated/programmable F-T System (b) Chest freezer

Figure 4.11: Temperature-time graph recorded by an automated freeze-thaw system freeze-thaw and by a thermocouple inside the CA specimen container.

Weighted average mass loss of CA using both the automated F-T system and chest freezer methods is presented in Figure 4.12. Test results indicates no clear relationship between the chest freezer and automated freeze-thaw machine methods.

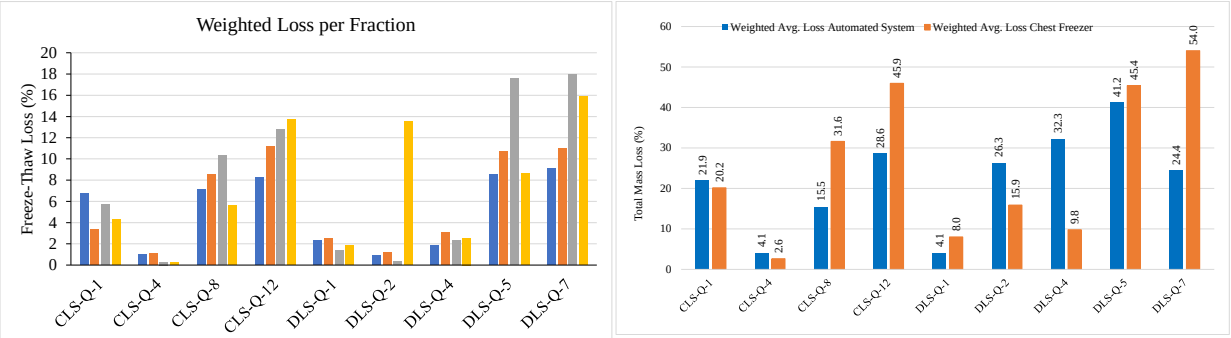

(a) Weighted loss per fractions (chest freezer) (b) Total mass loss

Figure 4.12: Comparison of F-T mass loss of CA using chest freezer-manual thawing and automated freeze-thaw system.

Furthermore, the research team conducted analyses of WisDOT round robin CA testing which was performed by several commercial labs, WisDOT, and UW-Milwaukee. The F-T test of the CLS aggregate samples was conducted in accordance with WisDOT modified AASHTO T 103 and using F-T automated systems as well as chest freezers. Comparison of F-T test results are depicted in Figure 4.13. While test results showed variability, the average mass loss from 10 different labs using the automated F-T system was 8.1% with COV of 29.4%. This was lower than the 9.9% average mass loss and COV of 47.8% that was obtained from nine different labs using the chest freezer-manual thawing. The COV when using the chest freezer was higher demonstrating the superiority of the automated F-T system. In addition, higher variability of the F-T test results is evident when using the chest freezers as shown in the box-whisker plot of Figure 4.13b.

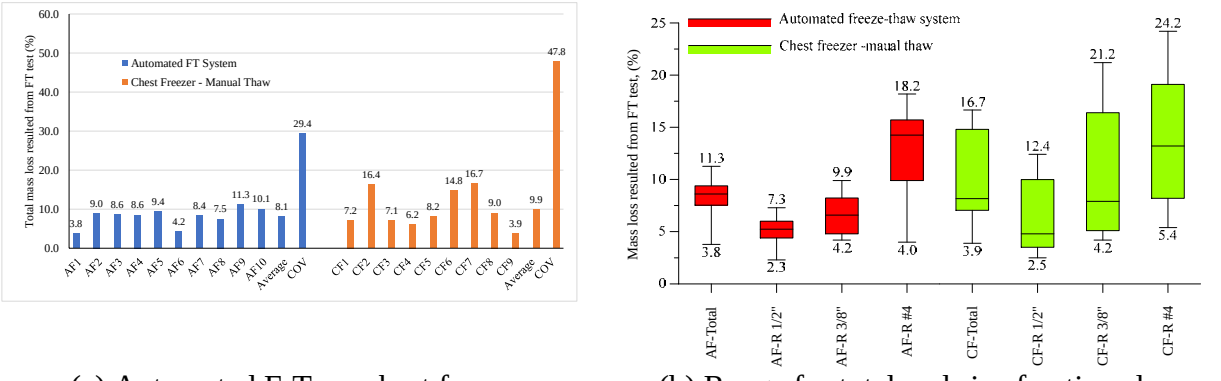

(a) Automated F-T vs. chest freezer (b) Range for total and size fractions loss

Figure 4.13: Performance of WisDOT round robin CLS CA based on F-T test system used (AF: automated F-T system; CF: chest freezer).

4.1.5 Influence of Laboratory on F-T Test Results

The previous section demonstrated the superiority of the automated F-T system over the chest freezer with manual thawing when testing CA is performed in accordance with the standard or modified AASHTO T 103 test. To further evaluate the automated F-T systems and the repeatability of their results, coarse aggregate samples were processed by three different labs with automated/programmable system from two different manufacturers. The test results are depicted in Figure 4.14. Inspection of the test results demonstrated the repeatability of the F-T test results obtained from three different laboratories (using automated F-T systems) even when considering the higher number of F-T cycles involved and the inherent variability of materials.

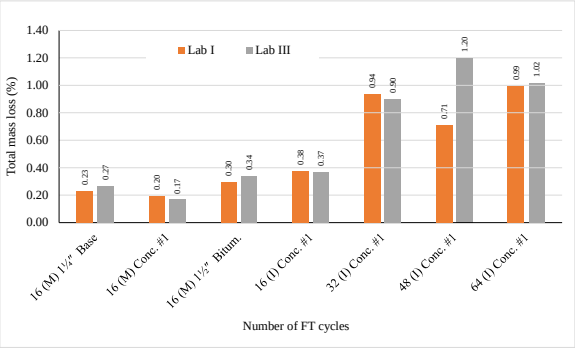

(a) F-T test results from Labs I and III

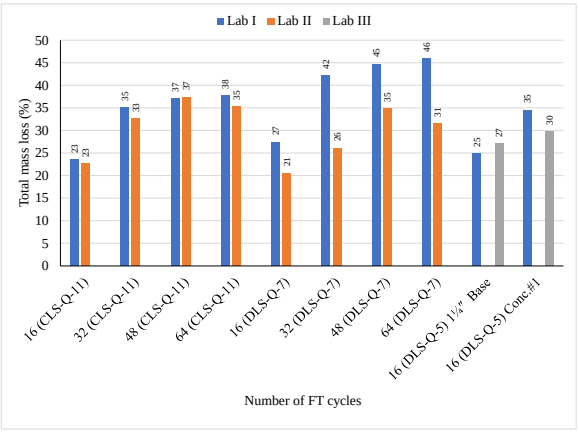

(a) F-T test results from Labs, I, II and III

Figure 4.14: Comparison of F-T test results obtained by three different labs using automated F-T systems.

Chapter 5

Laboratory Test Results and Analysis – CA Durability Performance in PCC

The results of the rapid freeze-thaw testing on the PCC cylinders made with coarse aggregates are presented in this chapter. The study includes both PCC cylinders that were tested starting at a young concrete age (short-term) and PCC cylinders that began freeze-thaw exposure at older concrete age (long-term). This was meant to assess concrete that is cast in the October-November time frame versus the concrete cast in the May-June time frame.

5.1 Resistance of Concrete to Rapid Freezing and Thawing

The results of the ASTM C666 test on the PCC cylinders placed in the F-T chamber at 28 days of age (short-term study) are presented in Figures 5.1 to 5.3. Figure 5.1 depicts the variation of the relative dynamic modulus with the number of freeze-thaw cycles for both the relative longitudinal and transverse dynamic moduli of the tested PCC cylinders. The relative dynamic modulus value (E_d/E_{d0}) is defined as the ratio of the measured dynamic modulus tested at a particular F-T cycle to the dynamic modulus measured just before the start of the freeze-thaw exposure. An examination of Figure 5.1 indicates:

- PCC with limestone gravel from pits deteriorated the most at 300-FT cycles.
- PCC with CLS and DLS aggregates had mixed performance, but the PCC cylinders with CLS aggregate exhibited significant deterioration.
- PCC with I and M quarried coarse aggregate and I and M pit gravel did not show significant deterioration.

The average values as well as the variation of the dynamic and static moduli for the short-term cylinders are depicted in Figure 5.3. In addition, the percentage of dynamic and elastic moduli reductions due to the 300 F-T cycles are presented in Figure 5.3.

Figures 5.4 and 5.5 depict the cracking of coarse aggregate within PCC cylinders due to F-T cycles and the impact of such cracking on PCC deterioration. Figure 5.5 shows that cracking within the limestone LS-P-1 pit gravel particles caused the observed PCC cracking as a result of 300 F-T cycles . It should be noted that cracking is not limited to the lightweight particles or chert/shale/chalk etc. Fracture and disintegration of the coarse aggregate particles near the concrete surface led to concrete surface pitting/popouts.

The results of the ASTM C666 tests on the PCC cylinders placed in the F-T chamber at 6 months of age (long-term study) are presented in Figures 5.6 to 5.7. Figure 5.6 depicts the variation of the relative dynamic modulus with the number of freeze-thaw cycles for both the longitudinal and transverse dynamic moduli of the PCC cylinders.

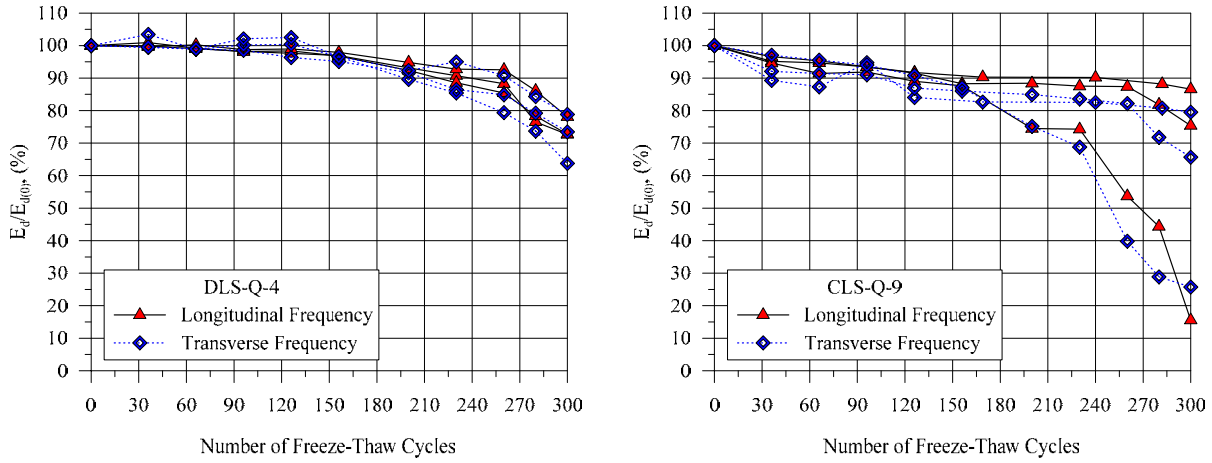

a) Dolomitic limestone CA from quarry (MQ)

b) Calcareous limestone CA from quarry (EC)

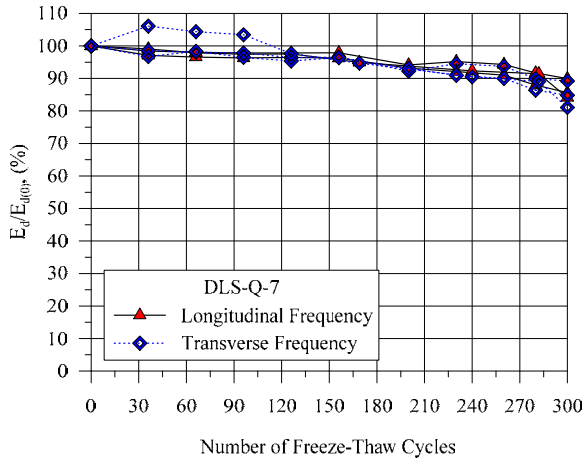

c) Dolomitic limestone CA from quarry (AQ)

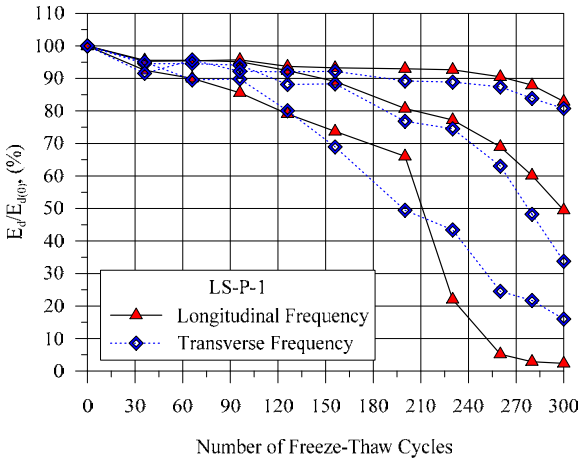

d) Limestone CA from pit (AP)

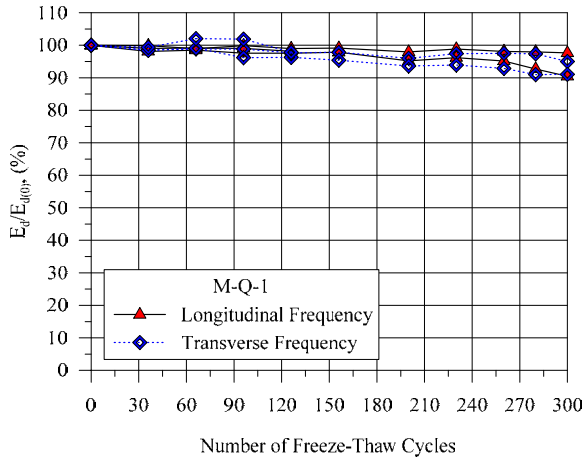

e) Quartzite CA from quarry (WQ)

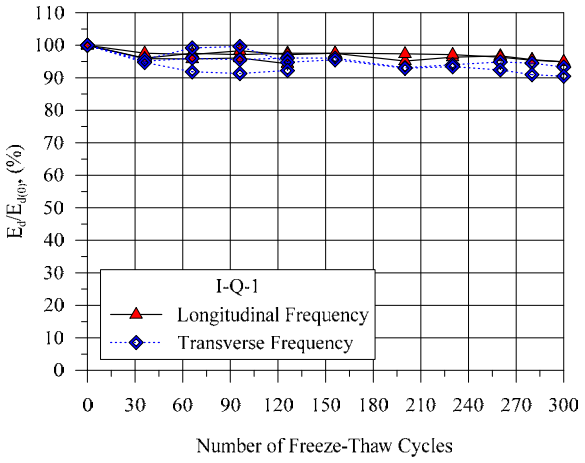

f) Granite CA from quarry (GQ)

Figure 5.1: Reduction of dynamic modulus of elasticity, E_d, in percent calculated from measuring the fundamental longitudinal and transverse frequency (ASTM C215).

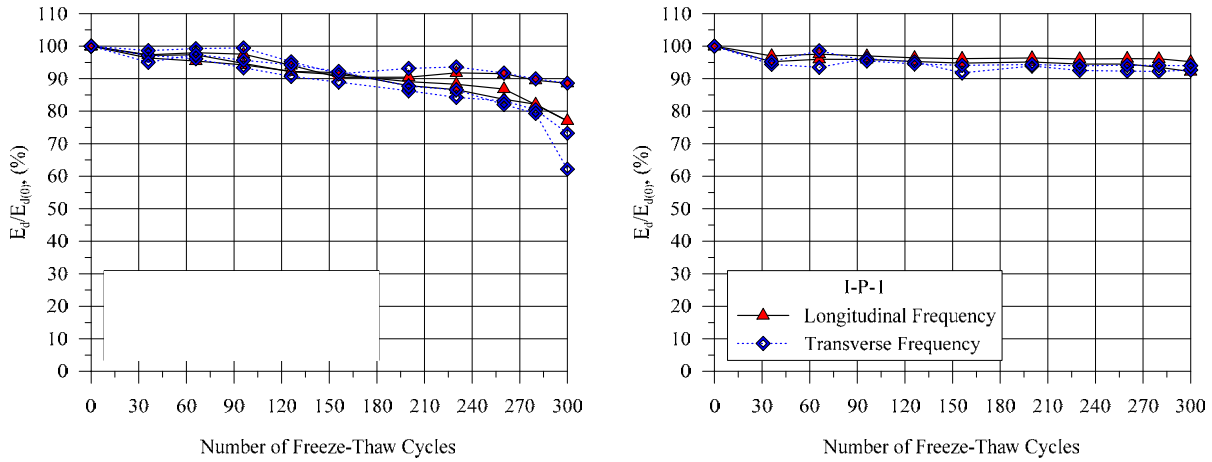

Calcareous limestone CA from quarry (LQQ) Igneous CA from pit (WP)

Figure 5.1 (Cont.): Reduction of dynamic Young's modulus of elasticity, E_d, in percent calculated from measuring the fundamental longitudinal and transverse frequency (ASTM C215).

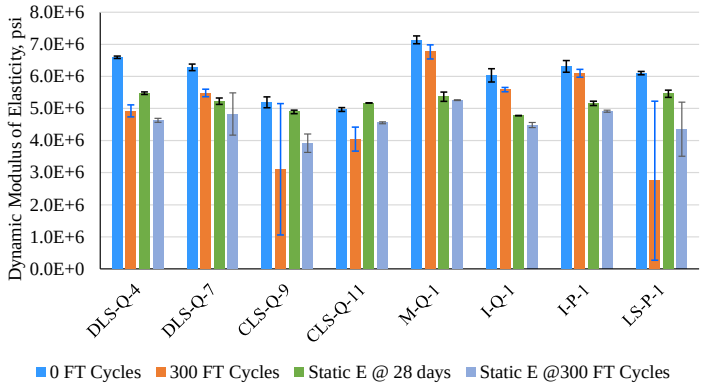

(a) Fundamental longitudinal frequency (ASTM C215)

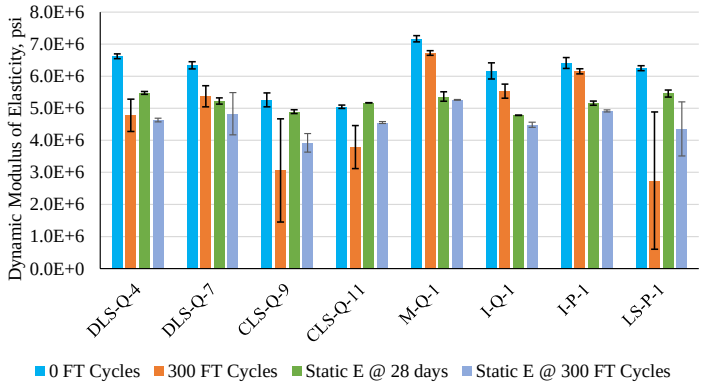

(b) Fundamental transverse frequency (ASTM C215)

Figure 5.2: Average static and dynamic modulus of elasticity for the PPC cylinders made with various CA and subjected to 300 F-T cycles.

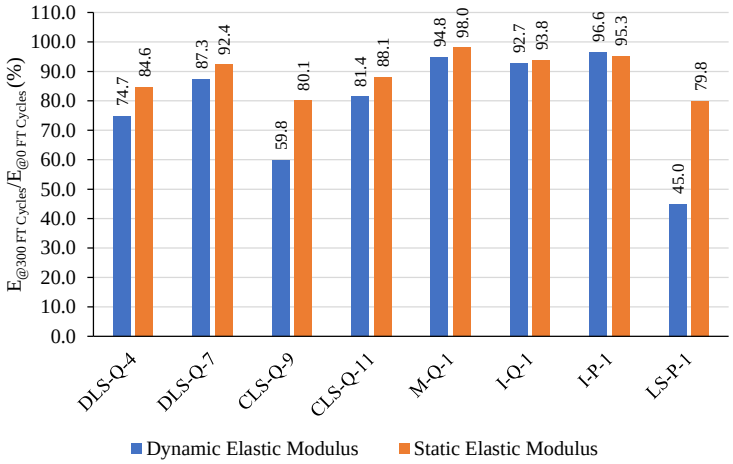

Figure 5.3: Effect of F-T cycles on the elastic moduli of concrete (longitudinal ASTM C215, E based on average values).

(a) Coarse aggregate fracture (b) PCC surface scaling

(c) Coarse aggregate initiate cracking in PCC cylinder surface

Figure 5.4: Picture of PCC cylinders during F-T cycles showing the effect of coarse aggregate quality on the PCC they form.

Inspection of Figure 5.6 indicates:

- PCC with DLS deteriorated the most due to 300-FT cycles.
- PCC with I and M quarried coarse aggregate and I and M pit gravel did not show deterioration.
- Performance of PCC with long-term F-T exposure did not show significant deterioration when compared with the PCC with short-term F-T exposure.

The average values as well as the variation of the dynamic and static moduli for the long-term cylinders are depicted in Figure 5.7. In addition, the percent reduction in dynamic and elastic moduli (due to the 300 F-T cycles) are presented in Figure 5.8.

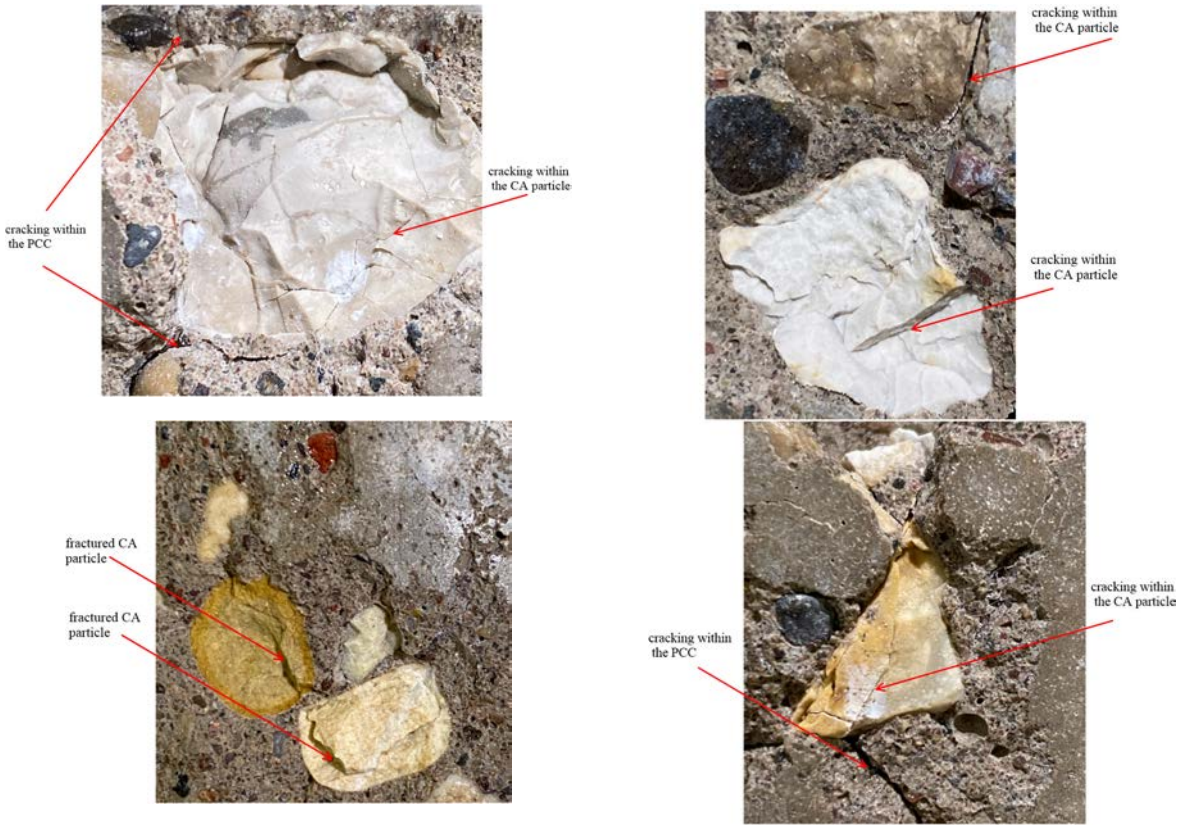

Figure 5.5: Picture of PCC cylinders during F-T cycles showing the coarse aggregate cracking and the impact on PCC quality.

The results of the short- and long-term studies of the effect of F-T cycles on PCC cylinders are summarized in Table 5.1 and compared in Figure 5.9. Examination of the test results indicate that the age at first exposure of PCC to freeze-thaw cycles influenced its durability. PCC cylinders subjected to F-T exposure at younger age (28 days) exhibited more cracking, deterioration, and loss of static and dynamic moduli compared with PCC cylinders exposed to the F-T cycles at 6 months of age.

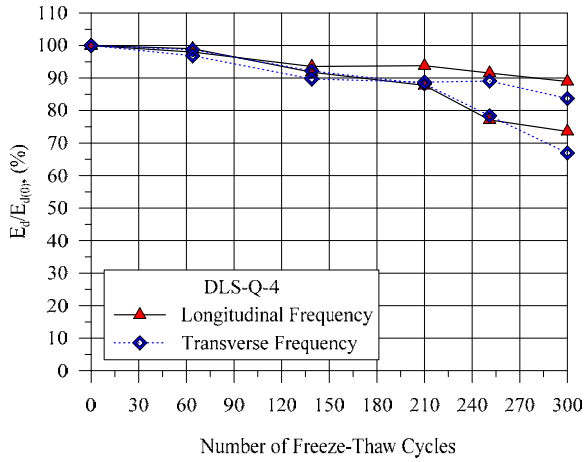

a) Dolomitic limestone CA from quarry (MQ)

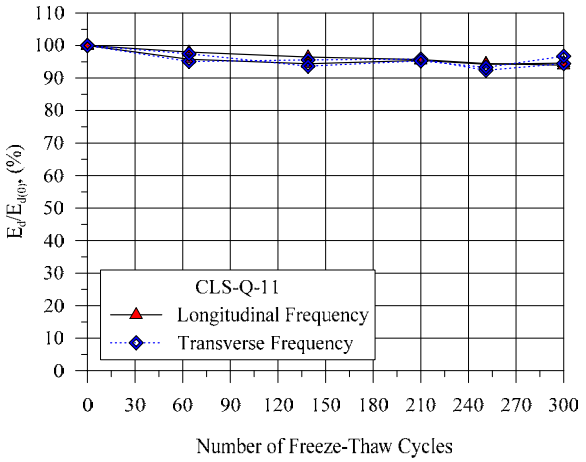

b) Calcareous limestone CA from quarry (LQQ)

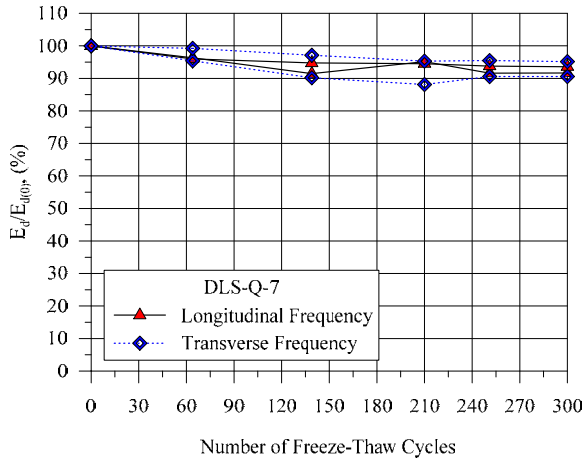

c) Dolomitic limestone CA from quarry (AQ)

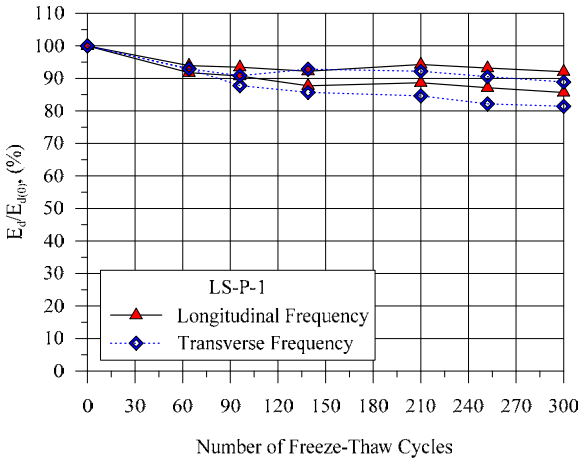

d) Limestone CA from pit (AP)

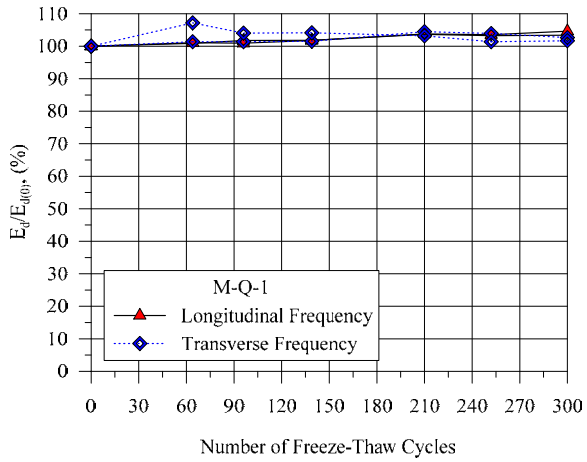

e) Quartzite CA from quarry (WQ)

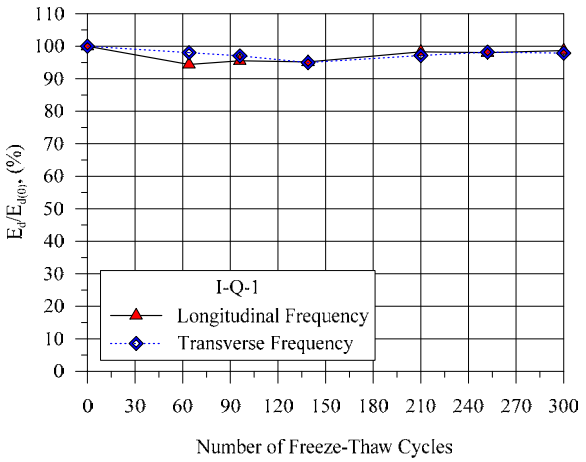

f) Granite CA from quarry (GQ)

Figure 5.6: Reduction of dynamic modulus of elasticity, E_d, in percent calculated from measuring the fundamental longitudinal and transverse frequency (ASTM C215).

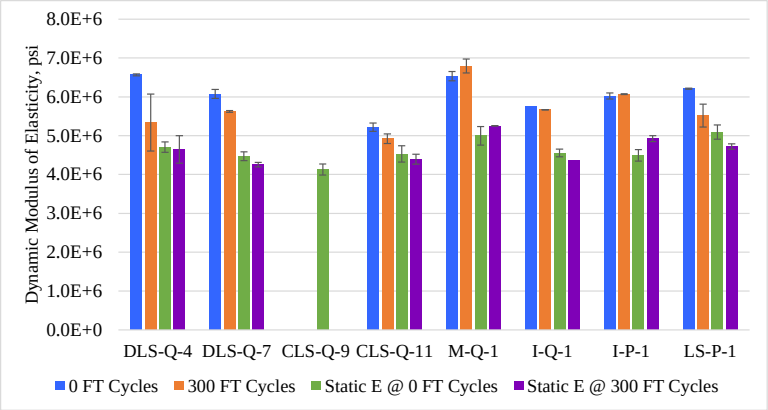

(a) Fundamental longitudinal frequency (ASTM C215)

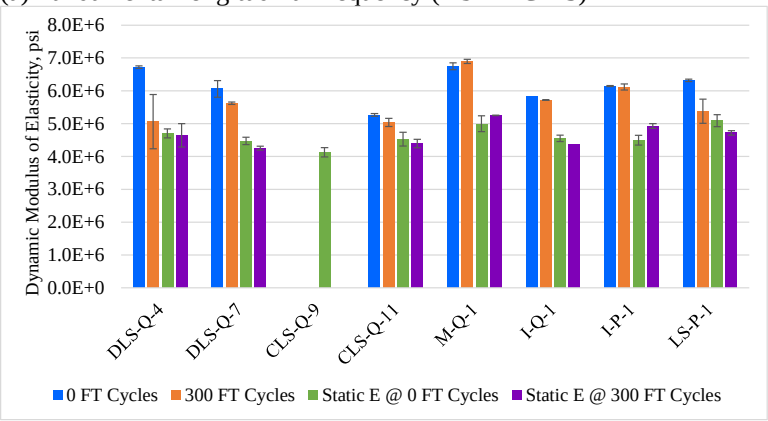

(b) Fundamental transverse frequency (ASTM C215)

Figure 5.7: Average static and dynamic modulus of elasticity for the PCC cylinders made with various CA and subjected to 300 F-T cycles.

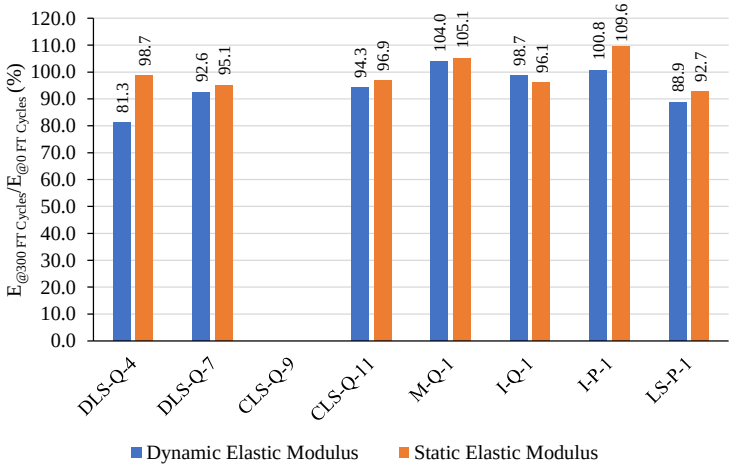

Figure 5.8: Effect of F-T cycles on elastic moduli of concrete (longitudinal ASTM C215, E based on average values).

Table 5.1: Dynamic modulus C215, elastic modulus from compression test (average values, longitudinal)

F-T Conditioning	CA Source	0 FT Cycles		300 FT Cycles		0 FT Cycles		300 FT Cycles	
		E_d (ksi)	COV (%)	E_d (ksi)	COV (%)	$E_{Elastic}$ (ksi)	COV (%)	$E_{Elastic}$ (ksi)	COV (%)
Short-term	DLS-Q-4	6,595	0.6	4.927	3.8	5.479	0.8	4.633	1.3
	DLS-Q-7	6,282	1.6	5.482	2.1	5.227	1.9	4.828	13.6
	CLS-Q-9	5,192	3.2	3.105	65.9	4.894	1.1	3.920	7.3
	CLS-Q-11	4,970	1.2	4.044	9.2	5.171	0.0	4.554	0.7
	M-Q-1	7,137	1.7	6,765	3.2	5,367	2.7	5,261	0.3
	I-Q-1	6,031	3.4	5,590	1.2	4,781	0.1	4,484	1.8
	I-P-1	6,311	2.9	6,099	2.0	5,160	1.3	4,917	0.6
	LS-P-1	6,106	0.9	2,749	90.1	5,458	2.0	4,356	19.3
Long-term	DLS-Q-4	6,567	0.4	5,339	13.7	4,704	2.9	4,646	7.7
	DLS-Q-7	6,074	1.9	5,624	0.4	4,471	2.5	4,254	1.4
	CLS-Q-9					4,129	3.4		
	CLS-Q-11	5,219	2.0	4,920	2.5	4,531	4.6	4,391	2.9
	M-Q-1	6,533	1.8	6,794	2.6	4,997	4.8	5,252	0.2
	I-Q-1	5,744	0.0	5,668	0.0	4,553	2.2	4,374	0.0
	I-P-1	6,023	1.3	6,068	0.2	4,494	3.3	4,924	1.5
	LS-P-1	6,207	0.2	5,516	5.4	5,090	3.6	4,719	1.5

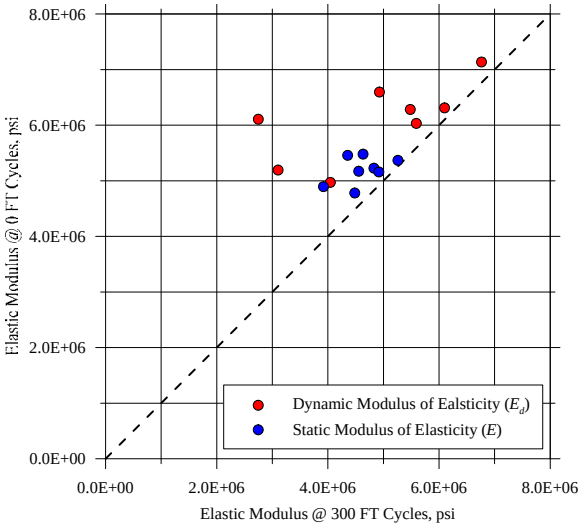

(a) PCC cylinders of young age (short-term study).

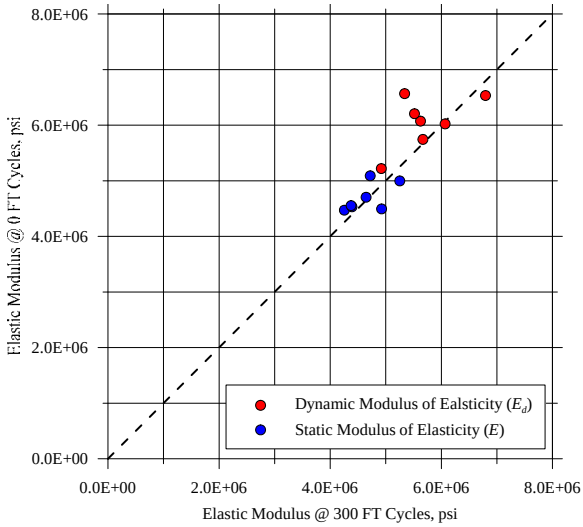

(b) PCC cylinders of old age (long-term study).

Figure 5.9: Effect of F-T cycles on the dynamic (E_d) and static (E) modulus of elasticity (E_d obtained from longitudinal frequency using ASMT C215).

5.2 Ultrasonic Pulse Velocity Testing of PCC Cylinders

Ultrasonic pulse velocity (UPV) testing was performed in accordance with ASTM C597 on concrete cylinders to determine the dynamic modulus of elasticity. Test results are presented in Figures 5.10 to 5.113. The values of dynamic modulus, measured through UPV testing, are also compared with the static modulus of elasticity, and the dynamic modulus of elasticity from the ASTM C215 tests. Samples were tested (UPV) at the conclusion of the 300 freeze –thaw cycles. Additionally, dynamic moduli of the control samples for each cylinder was tested in both a saturated and oven-dry state at the same time as the freeze-thaw tested samples. Inspection of the figures indicate that for each PCC cylinder type, the E_d (saturated) was greater than the E_d (dry) for the control samples. Also, the saturated and dry control sample E_d values were greater than the respective E_d values at the conclusion of 300 cycles of freeze thaw testing.

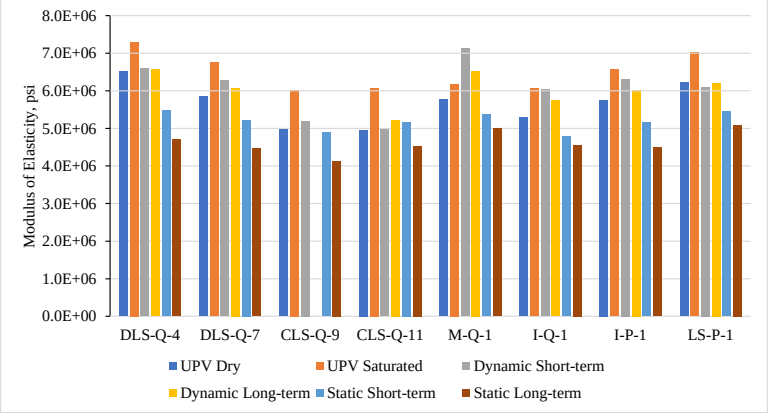

Figure 5.10: Elastic modulus using UPV (sat and dry), C215, and static at 0F-T cycles.

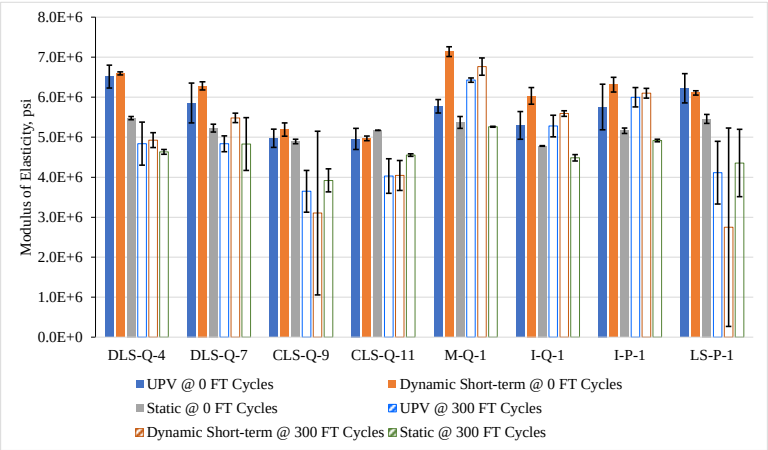

Figure 5.11: UPV PCC modulus vs. all moduli for short-term study (0 FT to 300 FT cycles).

Examination of the test results using UPV test on PCC cylinders subjected to F-T confirm that the age of the PCC influenced its durability performance. PCC cylinders placed in the F-T test machine at younger age (28 days) exhibited a higher loss of moduli compared with PCC cylinders exposed to the F-T cycles at 6 months of age (Figure 5.13).

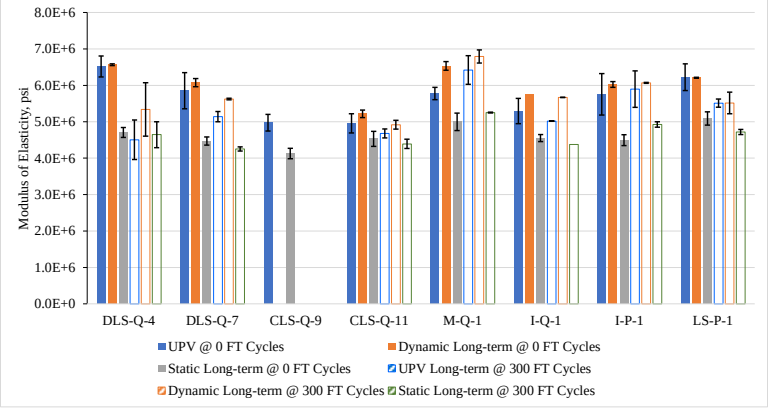

Figure 5.12: UPV PCC modulus vs. all moduli for long-term study (0 FT to 300 FT cycles).

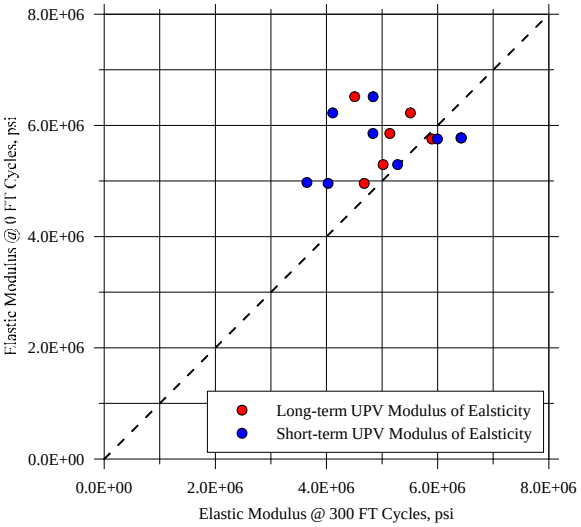

Figure 5.13: Effect of F-T cycles on the dynamic modulus elasticity (*E* obtained using ASMT C597).

5.3 Petrographic Analysis

A detailed petrographic analysis was performed on PCC cylinders subjected to 300 F-T cycles by AET, Inc. (in Minneapolis, MN), in accordance with ASTM C856 “Petrographic Examination of Hardened Concrete.” The summary of the findings regarding aggregate condition is presented in Table 5.2. The following is a summary of the findings from the petrographic analysis of cylinders.:

LS-P-1: 38 mm (1-1/2") natural gravel consisting of limestone, dolostone, chert, gabbro, granite, and basalt. A few microcracks were observed propagating from the top surface to a maximum depth of 25 mm (1"). One microcrack oriented sub-parallel to the top surface was observed propagating through the diameter of the cylinder between 95 mm (3-3/4") and 108 mm (4-1/4") depth. A few microcracks up to 15 mm (9/16") in length were observed propagating in from the formed outer surface of the cylinder at various depths within the cylinder. A few chert coarse aggregate particles were intersected by the microcracks.

DLS-Q-7: 19 mm (3/4") nominal sized quarried and crushed carbonate consisting of dolostone. A few microcracks propagated from the top surface to a maximum depth of 16 mm (5/8"). A few microcracks oriented sub-parallel to the top surface of the cylinder and up to 42 mm (1-5/8") in length were observed propagating from the outer surface of the cylinder between 5 mm (3/16") and 80 mm (3-1/8") depth. The microcracks were observed propagating through a few dolostone coarse aggregate particles.

CLS-Q-9: 38 mm (1-1/2") nominal sized quarried and crushed carbonate consisting of micritic to sparitic fossiliferous limestone, and dolomitic limestone. No observed microcracking.

CLS-Q-9: 38 mm (1-1/2") nominal sized quarried and crushed carbonate consisting of micritic to sparitic fossiliferous limestone, and dolomitic limestone. Two sub-vertical macrocracks propagated from the top surface to a maximum depth of 51 mm (2") before merging into a single macrocrack that propagated further to a depth of 93 mm (3-11/16"). Several variously oriented microcracks up to 25 mm (1") in length were observed splaying off from the macrocracks. A few randomly oriented microcracks up to 32 mm (1-1/4") in length were observed in the top up to 51 mm (2") of the cylinder. The microcracks were observed propagating through several limestone coarse aggregate particles.

I-Q-1: 19 mm (3/4") nominal sized quarried and crushed gravel consisting of granite. No observed microcracking.

CLS-Q-11: 38 mm (1-1/2") nominal sized quarried and crushed carbonate consisting of micritic to sparitic fossiliferous limestone, and dolomitic limestone. A few carbonate coarse aggregate particles within up to 10 mm (3/8") of the outer surface of the cylinder exhibited macrocracking and microcracking oriented sub-parallel to the length of the cylinder. A few of the microcracks were observed propagating a few millimeters into the surrounding paste.

CLS-Q-11: 25 mm (1") nominal sized quarried and crushed carbonate consisting of micritic to sparitic fossiliferous limestone, and dolomitic limestone. One macrocrack propagated diagonally from the top surface to a maximum depth of 42 mm (1-5/8") before intersecting the outer cylinder surface; the macrocrack propagated through four limestone coarse aggregate particles.

DLS-Q-4: 19 mm (3/4") nominal sized quarried and crushed carbonate consisting of dolostone. Several microcracks were observed propagating 6 mm (1/4") up to 30 mm (1-3/16") from the top, bottom, and outer surfaces of the cylinder, at various depths throughout the cylinder; the microcracks were observed propagating through several dolostone coarse aggregate particles.

I-P-1: 25 mm (1") nominal sized natural gravel consisting of limestone, dolostone, gabbro, granite, felsite and basalt. A few sub-parallel microcracks, oriented sub-parallel to the length of the cylinder, were observed between 7 mm (1/4") and 33 mm (1-5/16") depth; the microcracks were observed propagating through one limestone coarse aggregate particle.

M-Q-1: 25 mm (1") nominal sized quarried and crushed gravel consisting of quartzite and meta-granite. No microcracking was observed.

Table 5.2: Coarse aggregate characteristics.

Sample ID	Aggrege Type	Condition	Degree of ASR	Reactive Aggregates
LS-P-1	Natural Gravel	Few microcracks through a few chert and carbonate particles	None	None
DLS-Q-7	Crushed Carbonate	Several microcracks proceeded through several carbonate particles	None	None
CLS-Q-9	Crushed Carbonate	No cracking observed	None	None
CLS-Q-9	Crushed Carbonate	Several microcracks, a few proceed through a few carbonate particles	None	None
I-Q-1	Crushed Granite	No cracking observed	None	None
CLS-Q-11	Crushed Carbonate	Few microcracks proceed through a few carbonate particles	None	None
CLS-Q-11	Crushed Carbonate	One microcrack proceeded through a few carbonate particles	None	None
DLS-Q-4	Crushed Carbonate	A few microcracks proceeded through several carbonate particles	None	None
I-P-1	Natural gravel	Several parallel microcracks proceeded through one carbonate particle	None	None
M-Q-1	Crushed Quartzite	No cracking observed	None	None

Chapter 6

Field Investigation of CA Durability Performance in PCC Pavements

This chapter presents the results of the field work conducted to evaluate the presence of aggregate durability issue in PCC pavements in Wisconsin.

6.1 Field Investigation

Field work conducted on a total of 16 PCC pavement sites; however, field survey and subsequent evaluation conducted by the research indicated that only 12 PCC pavement sites showed a durability related distress consisting of D-cracking and coarse aggregate pitting/popouts. Table 6.1 presents a summary for the projects.

Table 6.1: Summary of PCC pavements investigated across Wisconsin.

PCC Investigated Pavement	Construction Year	Visual Observation
STH 81 – Beloit	1991	Apparent D-cracking of low to medium severity.
Cranston Road – Beloit	NA	Apparent D-cracking of medium to high severity.
US 51 – Janesville	1994	Apparent D-cracking of medium to high severity.
US 14 – La Crosse	1982	Apparent cracking of medium to high severity.
US 45 – Larsen	2008	Significant pavement surface popouts/pitting due to deterioration/broken/fractured coarse aggregate particles. A number of joints are also affected.
I-41 – De Pere	2015	Significant pavement surface popouts/pitting due to deterioration/broken/fractured coarse aggregate particles.
STH 26 – Watertown	2012	Significant pavement surface popouts/pitting due to deterioration/broken/fractured coarse aggregate particles. A number of joints are also affected.
US 151 – Sun Prairie	2006	Significant pavement surface popouts/pitting due to deterioration/broken/fractured coarse aggregate particles.
STH 20 – East Troy	1972	Apparent D-cracking of medium to high severity.
STH 13 – Wisconsin Rapids	1979	Apparent D-cracking of medium to high severity.
STH 31 – Kenosha	1988	Apparent D-cracking of medium to high severity.
STH 50 – Paddock Lake	1989	Apparent D-cracking of medium to high severity.

6.2 Petrographic Analysis

A petrographic analysis was performed on core obtained from PCC pavements by AET, Inc., in accordance with ASTM C856 “Petrographic Examination of Hardened Concrete.” The summary of the aggregate condition is presented in Table 6.1 and the following is a summary of the analysis of the PCC cores:

STH 81-Beloit: The sample was bisected sub-vertically by a fracture proceeding through the length of the sample. Two sub-vertical microcracks proceeded from the top surface to 13 mm (1/2") depth. A sub-horizontal microcrack propagated from the cored surface to intersect the fracture at depth within the core. The microcrack propagated through one carbonate coarse aggregate particle. Minimal/negligible alkali silica reactivity (ASR) was observed. The offending aggregates, when present, were chert fine aggregate particles.

Cranston-Beloit: Poor. The sample had broken into three sections along sub-horizontal fractures; the top-most section had further broken into two irregular pieces. Many sub-horizontal microcracks were observed throughout the depth of the core. The cracking proceeded through many carbonate and several chert coarse aggregate particles. ASR was observed as alkali silica gel lining / filling many air voids and a few microcracks at various depths in the core. The degree of alkali-silica reactivity was considered minor to moderate. The reactive aggregates observed where chert coarse and fine aggregate particles and one sandstone fine aggregate.

US 51 Janesville: Poor. Approximately 50% of the top surface had broken away to a depth of up to 51 mm (2") due to sub-vertical fracturing. Few sub-vertical microcracks, ranging from 20 mm (13/16") to 27 mm (1-1/16") long, were observed within the top 51 mm (2"). many sub-horizontal microcracks were observed beneath 45 mm (1-7/8″) depth. The microcracks propagated through several carbonate coarse and fine aggregate particles, several chert coarse and fine aggregate particles and one quartzite coarse aggregate. ASR was observed as alkali silica gel lining to filling several air voids and a few microcracks at various depths throughout the core. The degree of alkali-silica reactivity was considered minor to moderate.

US 51-Janesville: Poor. The sample had fractured into several irregular-shaped pieces; several smaller fragments were received which could not be re-attached to the core. Many randomly oriented microcracks were observed at various depths throughout the core; the microcracks were mostly concentrated between 43 mm (1-11/16") and 112 mm (4-7/16") depth. Several of the fractures and many of the microcracks were observed propagating through carbonate and chert coarse aggregate particles, and one quartzite coarse aggregate. ASR was observed as alkali silica gel lining to filling several air voids and microcracks at various depths in the core. Gel “plugs” were observed at the outer surface of a few cracked chert aggregate

particles. The degree of alkali-silica reactivity was considered minor to moderate. The reactive aggregate particles observed with chert coarse and fine aggregate particles.

Table 6.2: Coarse aggregate condition.

Sample ID	Aggregate Type	Condition	Degree of ASR	Reactive Aggregates
STH 81	Natural Gravel	Few microcracks through several carbonates and a few cherts	Minor	Chert CA and FA
STH 81	Natural Gravel	Sub-vertical fracture proceeded through several carbonates	Minimal/ Negligible	Chert FA
Cranston	Natural Gravel	Fractures and many microcracks through many carbonates and several cherts	Minor to Moderate	Chert CA and FA, one sandstone FA
US 51 Janesville	Natural Gravel	Many microcracks through several carbonates, few cherts and one quartzite	Minor to Moderate	Chert CA and FA
US 51 Janesville	Natural Gravel	Fractures and many microcracks through many carbonates, several cherts, one quartzite and one gabbro	Minor to Moderate	Chert CA and FA

Chapter 7

Summary, Conclusions and Recommendations

The main objective of this research project was to investigate the feasibility of implementing coarse aggregates soundness testing based on AASHTO T 103 or WisDOT Modified AASHTO T103 test procedures. To accomplish this goal, a better understanding of the current soundness testing procedures (AASHTO T 103/ WisDOT Modified AASTHO T 103, and AASHTO T 104) is needed with respect to Wisconsin coarse aggregates' performance and use.

Coarse aggregates samples were collected for laboratory testing and evaluation by WisDOT certified technicians from 34 sources (pits and quarries) consisting of different rock formations (limestone, igneous, and metamorphic) and various classifications (dense graded base, concrete #1, concrete #2, 1″ clear stone, and 1½ ″ bituminous).

The laboratory testing included measurements of specific gravity, absorption, and vacuum absorption as well as mass loss due to sodium sulfate soundness (SSS) and freeze-thaw (F-T) tests, in accordance with standard testing procedures described in Chapter 3 of this report. Additionally, the influence of the following variables on the test results was investigated: test type, F-T test equipment, test laboratory, test repeatability, number of wetting/drying cycles, number of F-T cycles, absorption, aggregate source, aggregate size fraction, and aggregate classification. In total, 106 SSS and 170 F-T tests were conducted on the collected CA samples. The SSS tests included the standard five wetting/drying cycles as well as additional five cycles (i.e., total of 10 cycles) performed on two limestone sources. The F-T test included the standard 16 F-T cycles in addition to 16, 32, and 48 cycles (from 32 to 64) on 12 CA sources. The F-T tests were conducted in three different laboratories with the majority of those tests performed at UW-Milwaukee using both automated/programmable F-T machines and chest freezer-manual thaw systems.

In order to investigate the influence of the F-T soundness aggregate quality on PCC in pavements, eight CA sources were used to make PCC test cylinders following WisDOT mixture design requirement for PCC pavements. The PCC cylinders were subjected to 300 F-T cycles in accordance with ASTM C666 and were subjected to standard tests to evaluate their static and dynamic moduli using ASTM C215, ASTM C597, and ASTM C39. The laboratory testing was conducted on concrete cylinders at ages of 28 days and 6 months to account for the effect of the age of PCC when first exposed to freezing and thawing. In addition, professional petrographic analysis (per ASTM C856) was conducted on the PCC cylinders after the completion of the 300 F-T cycles to investigate the degradation, deterioration, and disintegration of both the CA and PCC materials.

Field work was also conducted at twelve PCC pavement sites that exhibited durability related distress consisting of D-cracking and/or coarse aggregates pitting/popouts. The field work consisted of pavement distress surveys and evaluation, analysis of WisDOT's PIF database, coring of concrete at three pavement sites, and professional petrographic analysis of the PCC cores.

Finally, the research team conducted detailed analyses on a database of historical Wisconsin coarse aggregate test results, including various CA sources. This included analyzing differences in test results on CLS and DLS coarse aggregates.

Based on the results of the laboratory and field investigations as well as analyses of the database information, the following conclusions are drawn:

- Absorption of CLS coarse aggregates is greater than that of DLS aggregates.
- CA from igneous and metamorphic formations exhibited the lowest absorption.
- The base materials have the highest absorption when compared with the CA from concrete # 1 and #2.
- The SSS mass loss of quarried CA is greater than the SSS mass loss of pit gravel.
- The F-T mass loss of quarried CA is greater than the F-T mass loss of pit gravel.
- The SSS mass loss of CLS is nearly equal to the SSS mass loss of DLS, noting that the absorption of CLS is higher than the absorption of DLS.
- The F-T mass loss of CLS is less than the F-T mass loss of DLS, noting that the absorption of CLS is higher than the absorption of DLS.
- SSS and F-T mass losses are the lowest for CA from igneous and metamorphic rock formation.

The SSS and F-T data averages for CLS and DLS indicate the following based on CA classification:

- SSS mass loss of base CLS CA > SSS mass loss of concrete #1 and #2 CLS.
- SSS mass loss of base DLS CA > SSS mass loss of concrete #1 and #2 DLS.
- F-T mass loss of base CLS CA ≅ F-T mass loss of concrete #1 CLS and > F-T mass loss of concrete #2 CLS.
- F-T mass loss of base DLS CA > F-T mass loss of concrete #1 and #2 DLS.
- The larger CA particles (larger size fractions) exhibited more SSS weighted mass loss, on average, when compared with the smaller size particles for CLS.
- The smaller CA particles exhibited more F-T weighted mass loss by both CLS and DLS.
- The middle size fractions exhibit the highest SSS mass loss by DLS.
- The detailed size fraction study showed that greater F-T mass loss was observed for the smaller size fraction.

When considering the influence of F-T test systems and the choice of testing laboratory on CA performance, the following was observed:

- Temperature-time graphs recorded by the automated freeze-thaw test system was consistent and repeatable while the corresponding graphs recorded by the chest freezer was inconsistent and required more cycle time.
- F-T test results did not indicate a clear relationship between the chest freezer and automated freeze-thaw mass loss .
- Round robin F-T test results showed higher variability of the mass loss when using the chest freezers compared with the automated F-T systems.
- Repeatability of F-T test results was obtained from three different laboratories (using automated F-T systems) was considered good even with a higher number of F-T cycles and the inherent variability of CA materials.

The results of the ASTM C666 test on the PCC cylinders placed in the F-T chamber at 28 days of age (short-term study) indicated the following:

- The PCC with limestone gravel from pits deteriorated the most at 300 F-T cycles.
- PCC with CLS and DLS aggregates had mixed F-T performance, but the PCC cylinders with CLS aggregates exhibited significant deterioration.
- PCC with igneous and metamorphic quarried coarse aggregates and pit gravel did not show significant deterioration.

The results of the ASTM C666 tests on the PCC cylinders placed in the F-T chamber at 6 months of age (long-term study) indicated:

- PCC with DLS deteriorated the most due to 300 F-T cycles.
- PCC with igneous and metamorphic quarried coarse aggregates and pit gravel did not show deterioration.
- Performance of PCC with late-age F-T exposure did not show significant deterioration when compared with the PCC with early-age F-T exposure.
- Examination of the PCC cylinders indicated that the age at first exposure of PCC to freeze-thaw cycles influenced its durability. PCC cylinders subjected to F-T exposure at a younger age (28 days) exhibited more cracking, deterioration, and loss of static and dynamic moduli when compared with PCC cylinders exposed to the F-T cycles at 6 months of age.
- Petrographic analyses showed that the CA and the PCC both exhibited cracking/breakage and deterioration as well as scaling and pitting of the PCC surface.

Field surveys and subsequent evaluation of PCC pavement sites showed durability related distress consisting of D-cracking and coarse aggregate pitting/popouts. Several projects were identified with PCC pavement pitting/popouts as well as low severity and medium severity D-cracking that was confirmed by coring and inspecting PCC material. Evaluation of cores by a

professional petrographer and field surveys indicated presence of CA durability related problems.

A comprehensive analysis of the test data and other subsets indicated that approximately 7% of CA tested in Wisconsin failed the 12% total mass loss threshold in the SSS test currently specified by WisDOT for CA acceptance. Based on statistical analyses, keeping the same sample failure percentage will require approximately the same mass loss percentage of 12.

The research team recommends the following:

- Implement the WisDOT Modified AASHTO T 103 for CA durability evaluation.
- Require more frequent F-T testing for rock formations with CLS and DLS CA.
- When the rock formation changes in a quarry, WisDOT should be notified, and a sample should be evaluated.
- Different specifications for coarse aggregate acceptance can be implemented based on the source type, aggregate classification, and use in high-value projects.

References

AASHTO T 103 (2008). Standard Method of Test for Soundness of Aggregates by Freezing and Thawing. American Association of State Highway and Transportation Officials (AASHTO) Provisional Standards. Washington, D.C.

AASHTO T 104 (2021). Standard Method of Test for Soundness of Aggregate by Use of Sodium Sulfate or Magnesium Sulfate. AASHTO Provisional Standards. Washington, D.C.

AASHTO T 113 (2019). Standard Method of Test for Lightweight Particles in Aggregate. AASHTO Provisional Standards. Washington, D.C.

AASHTO T 161 (2017). Standard Method of Test for Resistance of Concrete to Rapid Freezing and Thawing. AASHTO Provisional Standards. Washington, D.C.

Alexander, M., & Mindess, S. (2005). Aggregates in concrete. Book by Taylor and Francis. First Edition. CRC Press.

ASTM C88 (2018). Standard Test Method for Soundness of Aggregates by Use of Sodium Sulfate or Magnesium Sulfate. ASTM International. West Conshohocken, PA.

ASTM C123 (2011). Standard Test Method for Lightweight Particles in Aggregate. ASTM International. West Conshohocken, PA.

ASTM C127 (2016). Standard Test Method for Relative Density (Specific Gravity) and Absorption of Coarse Aggregate. ASTM International. West Conshohocken, PA.

ASTM C131 (2010). Standard Test Method for Resistance to Degradation of Small-Size Coarse Aggregate by Abrasion and Impact in the Los Angeles Machine. ASTM International. West Conshohocken, PA.

ASTM C192/C192M (2015). Standard Practice for Making and Curing Concrete Test Specimens in the Laboratory. ASTM International. West Conshohocken, PA.

ASTM C233 (2010). Standard Test Method for Air-Entraining Admixtures for Concrete. ASTM International. West Conshohocken, PA.

ASTM C490 (2010). Standard Practice for Use of Apparatus for the Determination of Length Change of Hardened Cement Paste, Mortar, and Concrete. ASTM International. West Conshohocken, PA.

ASTM C494/C494M (2017). Standard Specification for Chemical Admixtures for Concrete. ASTM International. West Conshohocken, PA.

ASTM C666 (2017). Standard Test Method for Resistance of Concrete to Rapid Freezing and Thawing. ASTM International. West Conshohocken, PA.

ASTM C671 (1994). Standard Test Method for Critical Dilation of Concrete Specimens Subjected to Freezing (Withdrawn 2003). ASTM International. West Conshohocken, PA.

ASTM C682 (1994). Standard Practice for Evaluation of Frost Resistance of Coarse Aggregates in Air-Entrained Concrete by Critical Dilation Procedures (Withdrawn 2003). ASTM International. West Conshohocken, PA.

ASTM C688 (2021). Standard Specification for Functional Additions for Use in Hydraulic Cements. ASTM International. West Conshohocken, PA.

ASTM C1260 (2021). Standard Test Method for Potential Alkali Reactivity of Aggregates (Mortar-Bar Method). ASTM International. West Conshohocken, PA.

ASTM C1293 (2020). Standard Test Method for Determination of Length Change of Concrete Due to Alkali-Silica Reaction. ASTM International. West Conshohocken, PA.

Bektas, F., Wang, K., & Cai, W. (2016). Aggregate freezing-thawing performance using the Iowa pore index. Final report. Center for Transportation Research and Education, Iowa State University. Ames, IA, USA.

Chen, F., & Qiao, P. (2015). Probabilistic damage modeling and service-life prediction of concrete under freeze–thaw action. Materials and Structures, 48(8), 2697-2711.

Chen, T. C., Yeung, M. R., & Mori, N. (2004). Effect of water saturation on deterioration of welded tuff due to freeze-thaw action. Cold Regions Science and Technology, 38(2-3), 127-136.

Crovetti, J. A., & Kevern, J. T. (2018). Joint sawing practices and effects on durability. Report No. WHRP 0092-16-01. Madison, WI: Wisconsin Department of Transportation WHRP. 152 pages.

Fagerlund, G. (1977). The international cooperative test of the critical degree of saturation method of assessing the freeze/thaw resistance of concrete. Matériaux et Construction, 10(4), 231-253.

Fagerlund, G. (1996). Predicting the service life of concrete exposed to frost action through a modelling of the water absorption process in the air-pore system. In The modelling of microstructure and its potential for studying transport properties and durability (pp. 503-537). Springer, Dordrecht.

Hamoush, S., Picornell-Darder, M., Abu-Lebdeh, T., & Mohamed, A. (2011). Freezing and thawing durability of very high strength concrete. American Journal of Engineering and Applied Sciences, 4(1), 42-51.

Koubaa, A., & Snyder, M. B. (1996). Evaluation of frost resistance tests for carbonate aggregates. Transportation Research Record, 1547(1), 35-45.

Koubaa, A., Snyder, M. B., & Peterson, K. R. (1997). Mitigating Concrete Aggregate Problems in Minnesota. Minnesota Department of Transportation, Research Services Section.

Kuosa, H., Ferreira, M., & Leivo, M. (2013). Freeze-Thaw Testing CSLA Projekct—Task 1: Literature Review. VTT Technical Research Centre of Finland, Finland.

Lane, D. S. (1993). Experience with ASTM P214 in testing Virginia aggregates for alkali-silica reactivity. Transportation research record, (1418).

Luo, S., Bai, T., Guo, M., Wei, Y., & Ma, W. (2022). Impact of Freeze–Thaw Cycles on the Long-Term Performance of Concrete Pavement and Related Improvement Measures: A Review. Materials, 15(13), 4568.

Marks, V. J., & Dubberke, W. (1982). Durability of concrete and the Iowa pore index test. Transportation Research Record: Journal of the Transportation Research Board, No. 853, pp. 25–30.

Obla, K. H., Kim, H., & Lobo, C. L. (2016). Criteria for freeze-thaw resistant concrete mixtures. Advances in Civil Engineering Materials, 5(2), 119-141.

Perron, S., & Beaudoin, J. J. (2002). Freezing of water in Portland cement paste–an ac impedance spectroscopy study. Cement and Concrete Composites, 24(5), 467-475.

Pospíchal, O., Kucharczyková, B., Misák, P., & Vymazal, T. (2010). Freeze-thaw resistance of concrete with porous aggregate. Procedia Engineering, 2(1), 521-529.

Powers, T. C. (1945, January). A working hypothesis for further studies of frost resistance of concrete. In Journal Proceedings (Vol. 41, No. 1, pp. 245-272).

Powers, T. C., & Willis, T. F. (1949). The air requirement of frost-resistant concrete. In Highway Research Board Proceedings; Highway Research Board. Washington D.C.

Powers, T. C., & Helmuth, R. A. (1953). Theory of volume changes in hardened Portland-cement paste during freezing. In Highway research board proceedings (Vol. 32).

Qiao, P., McLean, D. I., & Chen, F. (2012). Concrete performance using low-degradation aggregates (No. WA-RD 790.1). Washington (State) Department of Transportation. Office of Research and Library Services.

Rhoades, R., & Mielenz, R. C. (1946, June). Petrography of concrete aggregate. In Journal Proceedings of the American Concrete Institute. (Vol. 42, No. 6, pp. 581-600).

Scherer, G. W. (1999). Crystallization in pores. Cement and Concrete research, 29(8), 1347-1358.

Senior, S. A., & Rogers, C. A. (1991). Laboratory tests for predicting coarse aggregate performance in Ontario. Transportation Research Record, (1301).

Shakoor, A., & Scholer, C. F. (1985, July). Comparison of aggregate pore characteristics as measured by mercury intrusion porosimeter and Iowa pore index tests. In Journal Proceedings (Vol. 82, No. 4, pp. 453-458).

Stark, D. (1976). Characteristics and utilization of coarse aggregates associated with D-cracking (No. Rpt. No. RD047. 01P). ASTM International.

Stark, D., Morgan, B., & Okamoto, P. (1993). Eliminating or minimizing alkali-silica reactivity. Report No. SHRP-C-343. Strategic Highway Research Program, National Research Council. Washington, D.C.

Tabatabai, H., Titi, H., Lee, C.-W., Qamhia, I., & Puerta Fella, G. (2013). Investigation of testing methods to determine long-term durability of Wisconsin aggregates. Madison, WI: Wisconsin Department of Transportation WHRP, 90 pages.

Tang, L., & Petersson, P. E. (2004). Slab test: Freeze/thaw resistance of concrete—Internal deterioration. Materials and structures, 37(10), 754-759.

Thompson, S. R., Olsen, M. P., & Dempsey, B. J. (1980). D-Cracking in Portland Cement Concrete Pavements. US Department of Commerce, National Technical Information Service.

Touma, W. E., Fowler, D. W., Carrasquillo, R. L., Folliard, K. J., & Nelson, N. R. (2001). Characterizing alkali-silica reactivity of aggregates using ASTM C 1293, ASTM C 1260, and their modifications. Transportation research record, 1757(1), 157-165.

Verbeck, G. J., & Landgren, R. (1960). Influence of physical characteristics of aggregates on frost resistance of concrete. Proceedings of the American Society for Testing Materials, Vol. 60, pp. 1063–1079.

Weyers, R. E. (2005). Testing methods to determine long term durability of Wisconsin aggregate resources. Wisconsin Highway Research Program.

Williams, S. G., & Cunningham, J. B. (2012). Evaluation of aggregate durability performance test procedures. Final Report, TRC-0905, University of Arkansas, Arkansas, United States. Available online: https://www.ardot.gov/wp-content/uploads/2020/11/TRC0905_Evaluation_of_Aggregate_Durability_Performance_Test_Procedures.pdf (accessed on July 2022).

Wisconsin Department of Transportation. (2022, May 17). Wisconsin Department of Transportation Facilities Development Manual (FDM). Retrieved July 18, 2022, from https://wisconsindot.gov/pages/doing-bus/eng-consultants/cnslt-rsrces/rdwy/fdm.aspx

Geologic Overview of Wisconsin Bedrock Sources

Wisconsin aggregates are quarried from bedrock or mined from sand and gravel pits. The bedrock geologic record of Wisconsin consists of two major time divisions: the Precambrian (Archean Eon and Proterozoic Eon) and the Phanerozoic Eon (WGNHS, 2005). Precambrian bedrock is older than 600 million years and primarily consists of igneous and metamorphic basement rock. The Phanerozoic is above the Precambrian and younger than 600 million years, and predominantly consists of sedimentary rocks and recent surficial glacial deposits (WGNHS, 2005). Precambrian rocks are present in the northern and northwestern regions of Wisconsin, whereas Phanerozoic bedrock is present in the southern, central, and western parts of the state.

The Precambrian bedrock of Wisconsin consists of Archean and Proterozoic Eons. Precambrian rocks are at relatively shallow depths or at the surface across a majority of Northern Wisconsin, and are overlain by several hundred feet of Paleozoic bedrock in South and Central Wisconsin (LaBerge, 1984). Archean-aged bedrock is older than 2,500 million years and consists of gneiss in Central and Northern Wisconsin as well as granitic intrusions in volcanic rocks. Archean bedrock in Wisconsin has been highly deformed (WGNHS, 2005).

Proterozoic Eon bedrock consists of four major groups. The oldest rock consists of sedimentary slates, greywacke and iron formations, and volcanic and intrusive igneous rocks that are approximately 1,800 million to 2,000 million years old. The igneous and intrusive suites from this time are mostly basaltic pillow lavas with some rhyolitic deposits from 1,850 million years ago. These rocks were extensively deformed during the Penokean Orogeny (LaBerge, 1984). The “Penokean aged” granites formed during the orogeny can be readily observed where Wisconsin red granite has been quarried in the north-central regions of the state. Following the Penokean Orogeny, relatively thick deposits of sandstone were deposited, metamorphosed to quartzite, and

folded between 1,400 and 1,750 million years ago. Remnants of the Proterozoic quartzite are present at the Baraboo Quartzite syncline in Columbia and Sauk Counties, outcrops of the Barron Quartzite in the Blue Hills in Barron and Rusk Counties, and outcrops of the Rib Mountain Quartzite in Marathon County (WGNHS, 2005). Middle Proterozoic bedrock consist of granites in northeastern Wisconsin from the Wolf River complex from 1,400 to 1,500 million years ago (WisDOT, 2017). The final major Precambrian event in Wisconsin was the Keweenawan, which is characterized by basaltic lava flows associated with the mid-continental rift that extended from Lake Superior to Kansas. Keweenawan-aged rocks are present in northwestern Wisconsin and are from about 1,100 to 1,200 million years ago (LaBerge, 1984). Keweenawan bedrock consists of older basalt and gabbro associated with volcanic activity from the rift activity, and younger sandstone. Precambrian time in Wisconsin is characterized by cycles of volcanic activity, sedimentary deposition and subsequent metamorphism, and erosion.

The Phanerozoic Eon consists of three eras, the Paleozoic, the Mesozoic, and the Cenozoic Eras. The Paleozoic consists of sequences of sandstone, shale, calcareous limestone, and dolomitic limestone; the Mesozoic is only possibly represented by gravels as no Mesozoic bedrock is present in Wisconsin; and the Cenozoic by glacial deposits (WGNHS, 2005). Paleozoic aged bedrock is present in the southern half of the state. The focus of this study is primarily on Phanerozoic calcareous and dolomitic limestone beds.

The Paleozoic Era is marked by several sea level transgressions and regressions that covered Wisconsin. Beginning in the Cambrian (501 to 488 million years ago), near-shore sediments were deposited, leaving interbedded sandstone and shales. As shown on Figure 1, Cambrian aged deposits stretch across the northwest and central portions of the state. Cambrian aged rocks consist of the Elk Mound, Tunnel City and Trempealeau Groups, that mainly consist

of sandstone with interbedded shales. However, some dolomitic and calcitic limestone beds are present in Cambrian aged rocks.

Sea level changes continued throughout the Ordovician Period (488 to 444 million years ago) continuing sedimentary deposition. Ordovician aged rocks consist of: the Prairie du Chien Group, consisting of Oneota and Shakopee limestones with some sandstones; the Ancel Group, which contains the Glenwood shale and St. Peter Sandstone; the Sinnipee group, which includes the Platteville Limestone (which has interbedded shales), the Decorah formation of shaley limestone, the Galena formation of dolomitic and calcareous limestone, and the Maquoketa shale (which separates the upper Ordovician from the lower Silurian). Ordovician aged formations arch across the eastern and southern portions of Wisconsin and are quarried for dolomitic and calcareous limestone. Sea levels submerged Wisconsin at the end of the Ordovician into the Silurian, and relatively thick limestone (later altered to dolomite) was deposited (WGNHS, 2005). Silurian aged rock is present along the eastern edge of the state, as shown on Figure 1, along the "Silurian Ridge." Silurian dolomite is quarried extensively for use as road base and concrete aggregate in these regions and is generally thinly-bedded to massive with sub-vertical and sub-horizontal jointing where extensively exposed (USGS, 1978). The youngest bedrock deposits in Wisconsin are Devonian-aged dolomite and shale. However, Devonian-aged rock is only present along Lake Michigan in Ozaukee and northern Milwaukee Counties. Bedrock was uplifted during the end of the Paleozoic, which is apparent in the eastward dip of Ordovician and Silurian aged rocks.

Within the last million years, during the Pleistocene, Wisconsin underwent series of glaciations that deposited ridges and hills of sand and glacial till, and created lakes across the state,

except in the southwest. Sand and gravel pits are mined from former glacial kames or outwash deposits across the formerly glaciated portions of Wisconsin (LaBerge, 1984).

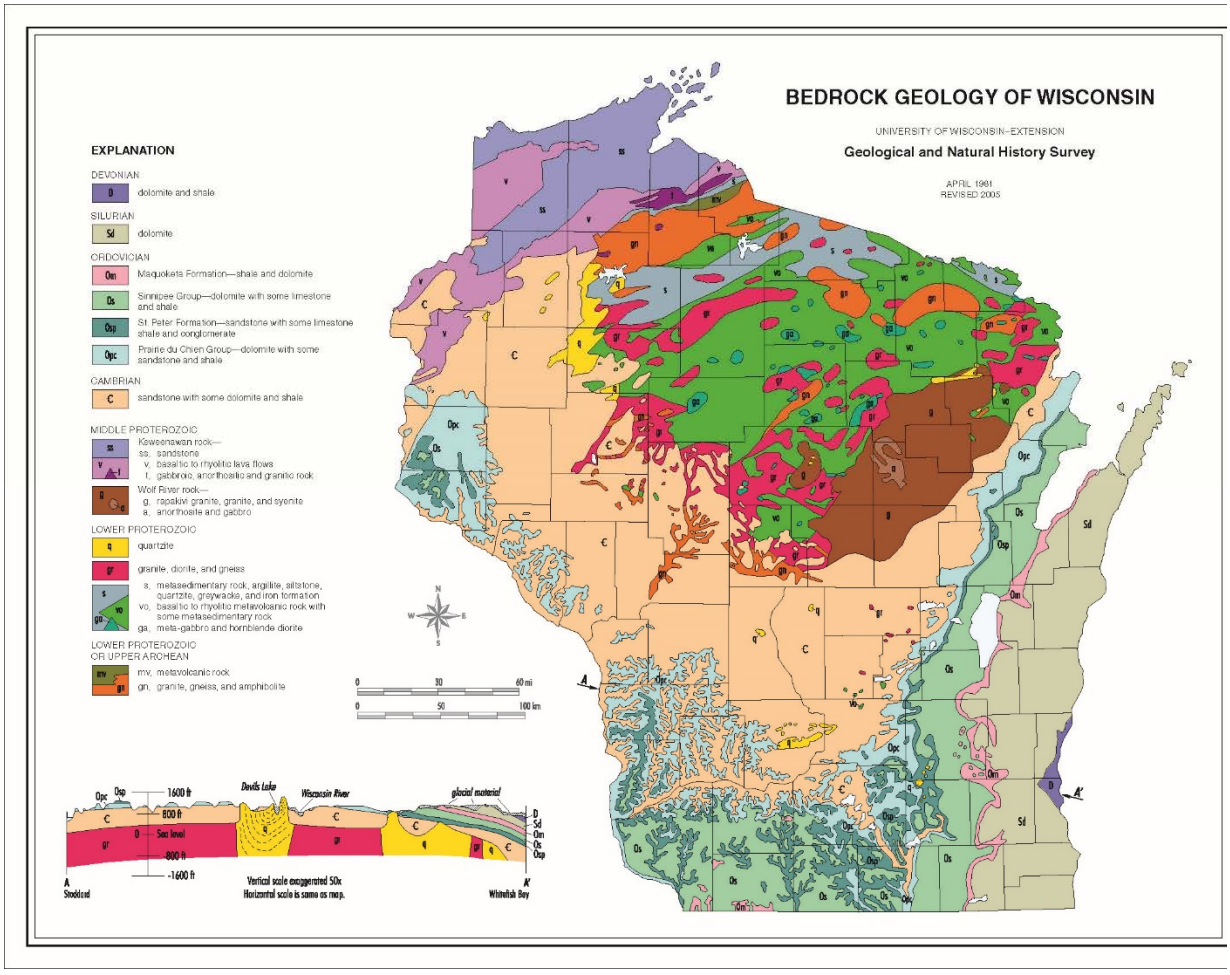

Figure 1: Bedrock geology map of Wisconsin (WGNHS, 2005)

Table 1: Portland cement concrete mixture proportions used to create concrete cylinders CLS-Q-11

Material	Source	Weight (lbs)	Actual R.D.	Volume
Cement	Alpena	395	3.15	2.01
Fly Ash	Portage	170	2.76	0.98
Slag		0	0.00	0.00
Coarse A		0	1.00	0.00
Fine	Sand	1258	2.68	7.53
Coarse B	CLS-Q-11	1887	2.65	11.42
Not Used		0	1.00	0.00
Not Used		0	1.00	0.00
Water	Well	215	1.00	3.44
Air %		6.0		1.62
TOTAL		3925		27.00

	AP	LQQ	AQ	GQ	MQ	WQ	WP
Sieve Size	F-T Aggregate #1 (AP) - 2.692 (OD)/1.36 [SSD Weight in lbs]	F-T Aggregate #2 AQ - 2.716 (OD)/1.56 [SSD Weight in lbs]	F-T Aggregate #3 LQQ - 2.564 (OD)/3.31 [SSD Weight in lbs]	F-T Aggregate #4 GQ - 2.608 (OD)/0.586 [SSD Weight in lbs]	F-T Aggregate #5 MQ - 2.774 (OD)/1.025 [SSD Weight in lbs]	F-T Aggregate #6 WQ - 2.621(OD)/0.477 [SSD Weight in lbs]	F-T Aggregate #7 WP - 2.726 (OD)/0.792 [SSD Weight in lbs]
1 1/2"	0	0	0	0	0	0	0
1"	20.8	20.9	20.4	20.3	21.1	20.4	20.9
3/4"	33.6	33.8	33.0	32.8	34.2	32.9	33.8
1/2"	33.6	33.8	33.0	32.8	34.2	32.9	33.8
3/8"	33.6	33.8	33.0	32.8	34.2	32.9	33.8
# 4	33.6	33.8	33.0	32.8	34.2	32.9	33.8
# 8	4.8	4.8	4.7	4.7	4.9	4.7	4.8
#16	0	0	0	0	0	0	0
Volume of Mixture (cu ft)	11.28	11.23	11.42	11.46	11.16	11.44	11.25
	4.5%	4.7%	5.7%	5.3%	4.6%	4.5%	5.6%
w/c ratio	0.38	0.39	0.40	0.40	0.39	0.39	0.38
Weights determined using 2.25 cu ft trial batch using a 60% coarse/40% fine split							

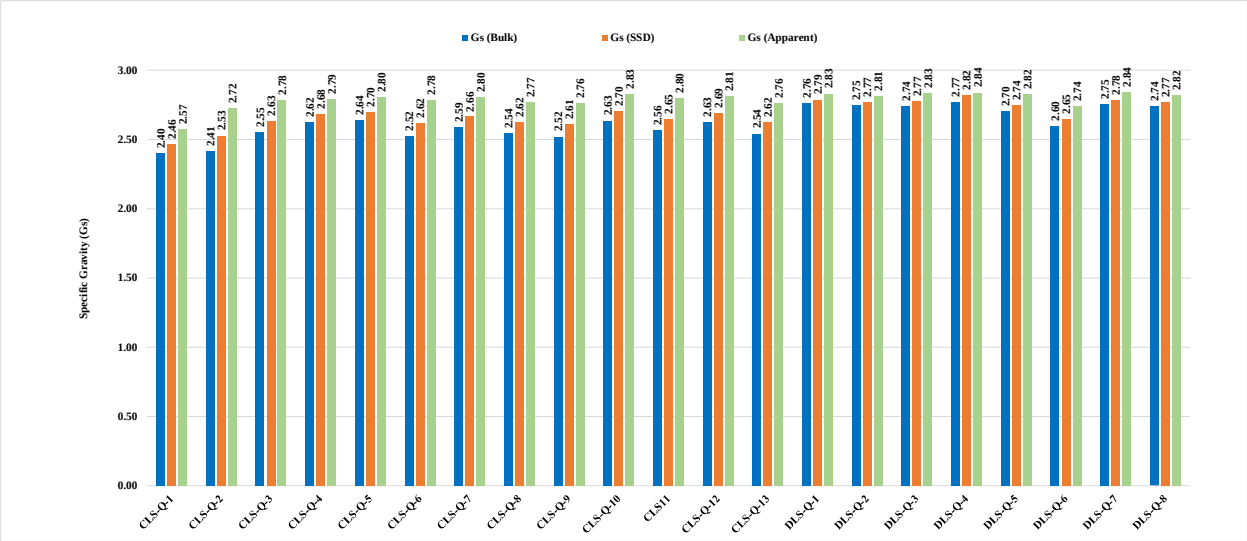

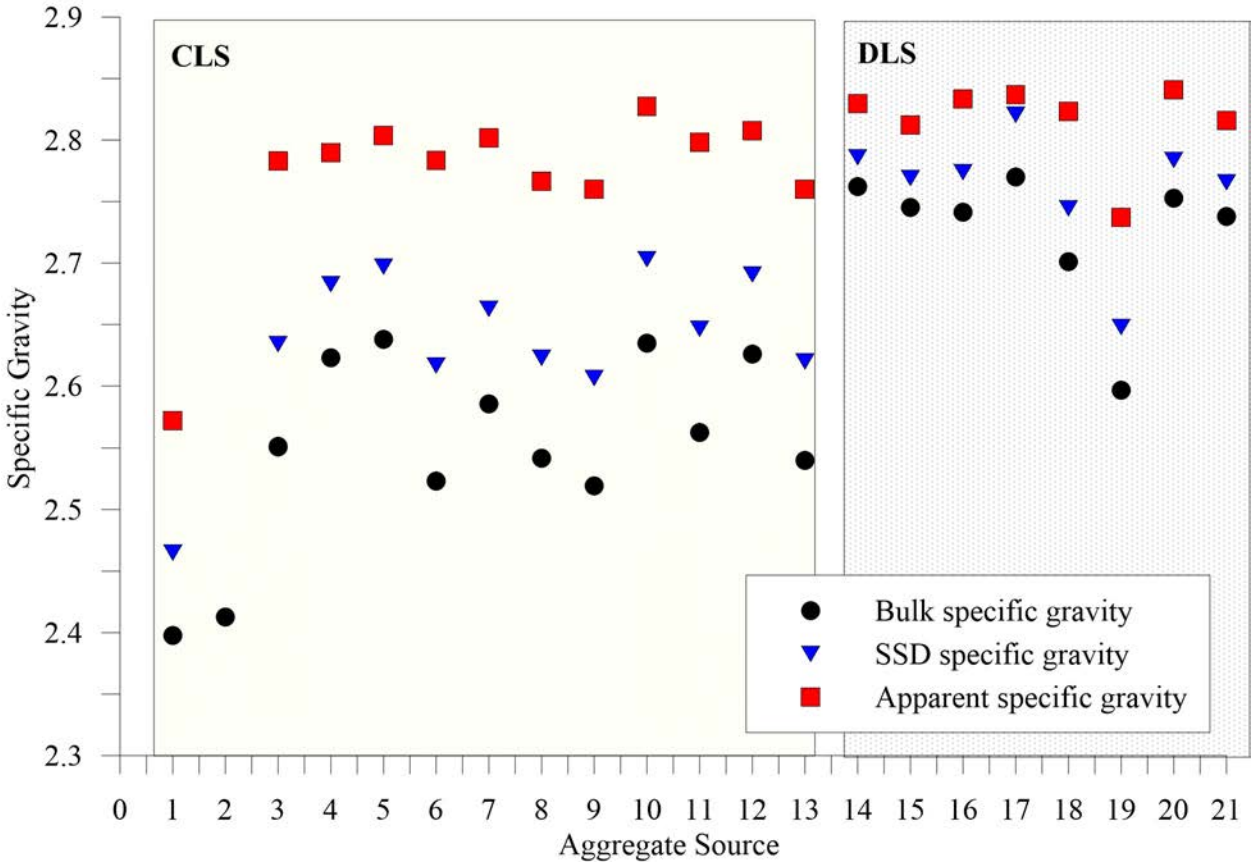

Figure 1: Specific gravity of the investigated coarse aggregates.

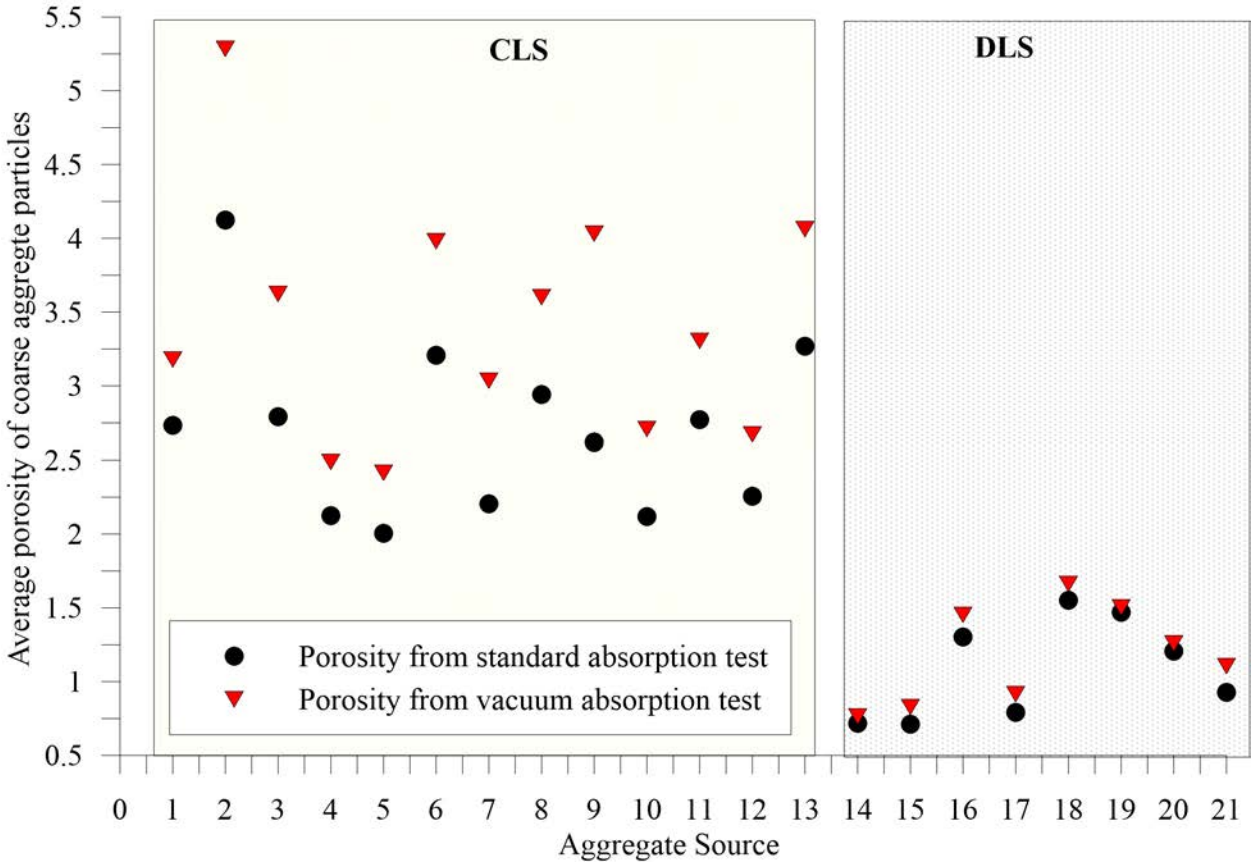

Figure 2: Average porosity of the investigated coarse aggregates.

Literature Review – Additional Materials

Aggregate Breakage/Disintegration Mechanisms in Freezing Conditions

The pore structure of an aggregate plays an important role for long-term resistance to freeze-thaw conditions. Aggregate pore systems consist of pore space accessible from the surface and pore space isolated from the surrounding, which forms the majority of pores in an aggregate (Alexander and Mindess 2005). The researchers suggested that the main mechanism of freeze-thaw damage in an aggregate's pore structure is either because of the increase in volume of water during freezing or because of the pressure increase due to the growth of ice. Alexander and Mindess (2005) state aggregates can be classified into three groups in respect to freeze thaw behavior: (1) aggregates having such a small pore volume (generally less than about 0.5%) that freezing expansion results in strains too small to cause cracking; (2) aggregates in which the hydraulic pressure generated by the flow of water ahead of a freezing front in a critically saturated pore system is able to crack the aggregate itself. Such aggregates must have a sufficiently low permeability and long enough flow path to generate high pressures; and (3) aggregates with a sufficiently high permeability to prevent hydraulic pressures being large enough to crack the aggregate. Smaller aggregates are considered less likely to suffer distress based on the suggested mechanism.

Luo et al. (2022) summarized the most agreed upon deterioration theories for concrete pavements due to freeze-thaw effects. These theories are: (1) the hydrostatic pressure hypothesis proposed by Powers in 1945 and 1949; (2) the osmotic pressure hypothesis proposed by Powers and Helmuth in 1953; (3) the theory of critical saturation by Fagerlund in 1977; and (4) the salt crystallization pressure hypothesis. These classical models were obtained from purely physical assumptions and/or from tests with net cement or mortar specimens.

The effects of freeze-thaw on concrete pavements include (1) mass loss of concrete due to surface spalling generated during freeze–thaw cycles and strength deterioration due to internal cracking; (2) the specific heat capacity of concrete can decrease; (3) the thermal conductivity and the coefficient of thermal expansion can increase; and (4) the porosity of the concrete will increase due to a coarsening effect due to the initiation and propagation of internal deterioration under freeze–thaw cycles (Luo et al. 2022).

The Hydrostatic pressure hypothesis **(Powers 1945; 1949)** suggests that when temperature drops to a certain level, some pore water in the concrete pore space will change into solid ice and expand by 9%. The remaining unfrozen pore water in the frozen zone will thus migrate to the unfrozen zone, which results in a hydrostatic pressure in the surrounding matrix. The hydrostatic pressure increases with the length of the pore water flow. When the flow is more significant than the limited flow length, the hydrostatic pressure exceeds the tensile strength of the cement matrix, and microcracks will initiate and propagate. With the repetition of freeze–thaw cycles, cracks will slowly accumulate, and the pores will become more connected, leading to macro-scale deterioration in concrete. Based on Powers' theory, the freeze–thaw damage only occur when the pore saturation is higher than 91.7%. However, freeze–thaw damage can be observed in concrete with a saturation rate of 70–80%.

Based on Powers' hydrostatic pressure hypothesis, Fagerlund (1996) further proposed a hydrostatic pressure model and a built theory model for calculating the maximum hydrostatic pressure. The maximum hydrostatic pressure (P_{max}) generated by icing is inversely proportional to the permeability

coefficient of the concrete matrix (k), directly proportional to the square of the air bubble spacing (d), the cooling rate ($\frac{d_\theta}{d_t}$), and the icing rate ($\frac{d_{wf}}{d_t}$). Therefore, it is considered that incorporating air-entraining agents into concrete can generate closed air bubbles and decrease the maximum expansion pressure by lowering the permeability coefficient and air bubble distance. The maximum hydrostatic pressure occurs at a distance x = d/2 in between the two air bubbles.

The Osmolarity hypothesis (Powers and Helmuth 1953) suggests that organic liquids which do not expand upon freezing still cause damage to concrete. Therefore, Powers and Helmuth (1953) further developed the osmotic pressure hypothesis. The hypothesis indicates that the concrete pore solution is weakly alkaline and contains ions of multiple elements. As a result, the salt in a concrete pore solution can lead to the formation of ice crystals at hostile temperatures and can increase the concentration of the unfrozen solution in the frozen zone. A concentration difference between the concrete pore solution in the frozen and unfrozen zones can thus be generated, resulting in osmotic pressure. When the osmotic pressure increases to a certain level, the formed tensile force will exceed the tensile strength of the concrete, causing cracks and creating frost damage.

The Theory of Critical Saturation was first proposed by Fagerlund (1977), which describes a substantial satiation value for porous materials. This theory is based on the hydrostatic pressure theory. It has been confirmed that freeze–thaw damage development in concrete depends on the saturation rate of the concrete. Once the threshold is exceeded, the concrete will crack upon one freeze–thaw cycle. Research suggests that critical satiation is a physical material property independent of other environmental factors (Chen et al. 2004). Thus, if external environmental effects of a concrete is converted to satiation, the difference between the satiation and the concrete's critical satiation could measure the concrete's resistance to freezing in a particular environment. The critical saturation degree has been proposed to depict the influence of internal saturation on freeze–thaw damage development. Meanwhile, the influence of pore solution salinity on freeze–thaw damage level has not been widely investigated. It is found that external loading can accelerate the development of freeze–thaw damage, and the acceleration becomes more evident under higher stress levels. Further, deicing salts can interact with concrete during freeze–thaw cycles, generating internal pores or leading to crystalline expansion pressure.

The Salt Crystallization Pressure Hypothesis originates from the growth of ice from large to small pores. Due to capillary effect, a hemispherical interface is formed between ice and water. The difference in the ice–water interface curvature and the cylindrical pore curvature cause pressure to generate, and the crystallization pressure acts to balance the pressure caused by the difference in curvature. The maximum driving force for crystallization are salt crystals growth, which is driven by supersaturation, and ice crystals volume increase, that are driven by supercooling (Scherer, 1999). The pressure generated on the walls of concrete pores subjected to frost damage is affected by the pore size and the interfacial energy between the pore wall and the crystals. Note that the freezing point of the pore solution decreases as the pore size increases. Water movement in the pore system will be restricted by ice formation in the large pores, which also results in buildup of hydraulic pressure. When the crystallization pressure exceeds the concrete tensile strength under a subcooling state, cracks are generated in the concrete.

In addition to the four hypotheses above, some essential components for the theoretical system of concrete freeze–thaw damage mechanisms include pore structure, stresses due to temperature change, ice prism, micro-ice-lens, and salt freeze (Luo et al. 2022). Typically, D-cracking in concrete pavements is primarily caused by the cracking of aggregates susceptible to freeze–thaw damage, due

to the moisture absorption of certain coarse aggregates. D-cracking is a progressive structural deterioration in concrete pavements. Further, deicing salts spread during snowy times can lead to severe freeze–thaw damage due to increased crystal expansion pressure.

The main factors influencing the frost durability of concrete include porosity (permeability), aggregate characteristics, moisture state, and climatic conditions. In particular, the aggregate properties that may influence the frost durability are aggregate pore size and its distribution, absorption capacity, degree of saturation of the aggregate, as well as the size and type of coarse aggregates (Qiao et al., 2012). Proper curing is also a requirement for durable concrete. Further, the mechanical properties of aggregates including strength, elastic modulus, abrasion resistance, and resistance to polishing have an essential impact on concrete durability (Qiao et al., 2012). According to Bektas et al. (2016), pore size of aggregates has a high correlation with aggregate freezing-thawing performance. Larger pore volumes and smaller pore sizes lead to poor freezing-thawing durability (Rhoades and Mielenz 1946; Verbeck and Landgren 1960). Marks and Dubberke (1982) found that aggregates associated with D-cracking have predominantly pore sizes ranging from 0.04 to 0.20 μm in diameter.

An exhaustive list of durability tests was summarized by Weyers et al. (2005). Most of these tests are simulative tests that expose the aggregates to freezing and thawing conditions:

- Resistance of concrete to rapid freezing and thawing (ASTM C666, AASHTO T 161)
- Frost resistance of coarse aggregate in concrete (ASTM C682/ASTM C671) - withdrawn
- Potential alkali reactivity of aggregates, mortar bar method (ASTM C1260)
- Determination of length change of concrete due to alkali-silica reaction (ASTM C1293)
- Soundness of aggregates by freezing and thawing (AASHTO T 103)
- Washington hydraulic fracture test. This test simulates freezing and thawing action on aggregates by creating internal forces in the aggregate using hydraulic pressures.
- Test method for the resistance of unconfined coarse aggregate to freezing and thawing (CSA A23.2-24A)
- Thermogravimetric analysis
- Lightweight pieces in aggregate (ASTM C123 or AASHTO T 113)

Kuosa et al. (2013) described several freezing and thawing test methods, both direct and indirect, for aggregates in loose states or in mortar/concrete. Freeze thaw testing methods were divided into direct (subjecting samples to alternating freezing and thawing) and indirect methods (property measurement for a property that affects frost resistance or deterioration). If there is a valid theoretical background behind the indirect methods, they are normally faster and have acceptable accuracy. Freeze-thaw test methodologies include volume change, mass change or change in dynamic modulus of elasticity. These characteristics are of significant practical value but they do not provide direct evidence for a particular mechanism of freeze-thaw action. The authors concluded that no single laboratory test method can fully reproduce the conditions in the field. The researchers reported that recently, electrical methods have also been used to study the freezing-thawing process. Perron and Beaudoin (2002) suggested that these methods have promise for development of new rapid methods of durability testing. Dielectric spectroscopy (or electrochemical impedance spectroscopy) measures the dielectric properties of a medium as a function of frequency. This method was found to be sensitive to nucleation and growth of ice crystals.

Senior and Rogers (1991) summarized major findings on testing methods that correlate with aggregates freeze-thaw resistance in granular bases and in asphalt and concrete layers. According to their findings, the expected freeze-thaw performance of aggregates in granular base is best measured by the micro-Deval test and water absorption. The physical quality of Portland cement concrete aggregates is best measured by the micro-Deval test, water absorption, and unconfined freezing and thawing. The quality of asphaltic concrete aggregates is best measured by the micro-Deval test, polished-stone value test, and unconfined freezing and thawing test. Petrographic examination was also reported as an essential tool for evaluating aggregate quality. For concrete, the researchers concluded that no test procedure by itself is totally reliable for separating good, fair, and poor aggregate performance. If two tests are chosen, then micro-Deval combined with unconfined freeze-thaw seem to be the most reliable.

Koubaa et al. (1997) divided freeze-thaw tests for aggregates and concrete mixes into two categories: correlative tests, and simulative tests. Correlative Tests (quick screening tests) - require relatively little time to perform, and are less expensive and easier to perform. They include the absorption and specific gravity tests (ASTM C127), absorption-adsorption test (PCA Method), acid-insoluble residue test (ASTM D3024), Iowa pore index test, Washington hydraulic fracture test, petrographic examination, X-ray diffraction, X-ray fluorescence, thermogravimetric analysis, and determination of pore size and volume by mercury porosimeter (ASTM D4044). Simulative tests, on the other hand, simulate environmental freeze-thaw exposure conditions. These tests better correlated with the field freeze-thaw performance of the coarse aggregates, but are time-consuming and require expensive equipment. Tests include the rapid freezing and thawing test (ASTM C666), the aggregate particle freeze-thaw test (ASTM C131), the Powers' slow cool test (ASTM C671), the sulfate soundness test (ASTM C88), and the Virginia Polytechnic Institute (VPI) single-cycle slow freeze test.

Following is a detailed description of some of the common durability tests and/or tests that correlated well with field data. These are the common tests reported in literature and ASTM/AASHTO standards:

Resistance of Concrete to Rapid Freezing and Thawing (ASTM C666/C666M, AASHTO T 161)

The test method covers the determination of the resistance of concrete specimens to rapidly repeated cycles of freezing and thawing by two different procedures: Procedure A, rapid freezing and thawing in water, and procedure B, rapid freezing in air and thawing in water. The test is intended to determine the effects of variations in both properties and conditioning of concrete in the resistance to freezing and thawing. Specific applications include specified use in ASTM C494/C494M, ASTM C233, and ranking of coarse aggregates for effect on concrete freeze-thaw durability, especially where soundness of the aggregate is questionable. Samples that pass this test are assumed either not critically saturated, made with sound aggregates, have a proper air-void system, and/or were allowed to mature properly. Procedure A is generally considered more aggressive to better reveal defective materials, although some consider the constant saturation of the test specimens to be unrealistic. Some users prefer Procedure B as a more representative procedure for the saturation patterns in field applications.

The nominal freezing-and-thawing cycle for both procedures consist of alternately lowering the temperature of the specimens from 40 to 0°F (4 to -18°C) and raising it from 0 to 40°F (-18 to 4°C) in two to five hours. For Procedures A and B, more than 25% and 20% of the cycle time shall be used for thawing, respectively. The test specimens shall be prisms or cylinders made and cured in

accordance with the applicable requirements of Practice ASTM C192/C192M and ASTM C490. Molded beam specimens shall be cured for 14 days prior to testing. Specimens may also be cores or prisms cut from hardened concrete. Field specimens should not be allowed to dry to a moisture condition below that of the structure from which it was taken, which can be accomplished by wrapping in plastic.

The test procedure entails the following: start the freezing-and-thawing tests by placing the specimens in the thawing water at the beginning of the thawing phase of the cycle. Then, remove the specimens from the apparatus, in a thawed condition, at intervals not exceeding 36 cycles of exposure to the freezing-and-thawing cycles, then test for fundamental transverse frequency and measure length change (optional). Afterwards, continue each specimen in the test until it has been subjected to 300 cycles or until its relative dynamic modulus of elasticity reaches 60% of the initial modulus, whichever occurs first. For the optional length change test, 0.10% expansion may be used as the end of test. Calculations for this test procedure include

(1) The relative dynamic modulus of elasticity using the following equation: $P_c = \left(\frac{n_1^2}{n^2}\right) x100\%$, where P_c is the relative dynamic modulus of elasticity after 'c' cycles of freezing and thawing (%), n is the fundamental transverse frequency at zero cycles, and n_1 is the fundamental transverse frequency after c cycles.

(2) The durability factor, which is calculated using the following equation: $DF = \frac{PN}{M}$, where: P is relative dynamic modulus of elasticity at N cycles (%), N is the number of cycles at which P reaches the specified minimum value for discontinuing the test or the specified number of cycles at which the exposure is to be terminated, whichever is less, and M is the specified number of cycles at which the exposure is to be terminated.

(3) Length change in percent (optional), which is calculated using the following equation: $L_c = \left(\frac{l_2 - l_1}{L_g}\right) x100\%$, where L_c is the length change of the test specimen after C cycles of freezing and thawing (%), l_1 is the length comparator reading at zero cycles, l_2 is the length comparator reading after C cycles, and L_g is the effective gage length between the innermost ends of the gage studs in Specification ASTM C490.

One issue in implementing the ASTM C666 method is the amount of time required to complete the test. It may take over two months to complete one test depending on the length of the freeze-thaw cycle. More recently, a third procedure was developed by Janssen and Snyder (1994) to better simulate field conditions and is referred to as Procedure C (freezing and thawing while wrapped in terry cloth); to create a more representative testing environment. By wrapping concrete beams in terry cloth, the use of the rigid containers is eliminated while allowing for the beam to retain its moisture; thus providing more realistic conditions than Procedures A and B (Weyers et al. 2005).

Qiao et al. (2012) indicted ASTM C666 is the most commonly used test method for determining the freezing and thawing resistance of concrete. Since the degree of saturation is considered important for the performance of concrete in a frost test, absorption during the test is sometimes measured. Tang and Petersson (2004) used the ultrasonic pulse transmission time (UPTT) measurement for measurement of internal damage. Pospichal et al. (2010) employed the UPTT and resonance method to determine the degradation of specimens.

Note that the WisDOT (2022) uses a modified version of the standard AASHTO T 103 in which the Methanol/water solution is used to prepare samples following procedure B, and requires 16 freeze-thaw cycles be performed on coarse aggregates for durability evaluation. After the cycles are complete, samples are dried, sieved, and weighted to determine the weight loss.

Sodium/magnesium sulphate soundness test (ASTM C88/C88M, AASHTO T 104)

The sodium sulfate soundness test is conducted to evaluate freeze-thaw resistance of aggregates by the mechanism of expansive force due to sodium sulfate or magnesium sulfate salt rehydration during the test (i.e., via wetting and drying cycles). AASHTO T 104 standard test procedure is comprised of five cycles. Each cycle consists of two phases: 1) immersing the aggregate specimen in the sodium sulfate or magnesium sulfate solution for 16 to 18 hours; 2) oven-drying the specimen to a constant mass. Rehydration and growth of the salt crystals within aggregate pores during immersion generates an internal expansive force that simulates the expansion of water during freezing conditions. Sieve analysis of the aggregate material to determine mass loss is performed after completion of the five wetting/drying cycles. ASTM C88/C88M is another similar standard test used for the same purpose.

Sodium sulfate soundness is used by WisDOT as a main quality indicator of coarse aggregates for durable long-term performance. WisDOT requires that the maximum coarse aggregate mass loss using the sodium sulfate soundness test is 12% (WisDOT, 2022). The sodium sulfate soundness test is imprecise and has been shown to have relatively variable single operator coefficients of variation (Weyers et al., 2005). Williams and Cunningham (2012) evaluated the sodium sulfate soundness test method and found that the results variability decreased the reliability of the test. Previous research has shown that the sodium sulfate soundness test can be unreliable and is possibly a poor indicator of freeze-thaw durability.

Frost resistance of coarse aggregate in concrete (ASTM C682/ASTM C671)

As explained by Weyers et al. (2005), this method uses 75mm (3 in) diameter and 150mm (6 in) long specimens. Specimens are cooled from 1.7°C (35°F) to –17.8°C (0°F) at 3°C/h (5°F/h) in water-saturated kerosene every two weeks. In between test cycles, the specimens are stored in water at 1.7°C (35°C). Frost resistance criterion is a sharp increase in dilation by a factor of two or more between the cycles. The Frost resistance period is taken as 12 cycles (24 weeks or one winter period). Note that moisture states other than saturated or dry are difficult to achieve and maintain during this test procedure. Thus, the variability of results is affected by the moisture state, which has to be representative of field conditions for reliable performance predictions. Note that the equipment is relatively extensive for test procedures, and includes a freezing chamber, strain frames, length and temperature measuring apparatus, and a conditioning cabinet. However, several specimens can be tested in the 24-week test period because 20 sets of specimens can be tested in each two-week cycle period. Despite the good correlations, this testing method was withdrawn by ACI Committee C09 in 2003.

Potential Alkali Reactivity of Aggregates, Mortar Bar Method (ASTM C1260)

As explained by Weyers et al. (2005), ASTM C1260 can be used as a rapid indicator of alkali aggregate reactivity, taking only 16 days. The test consists of casting specimens and then placing

them in a moist room for 24 hours. After initial curing, specimens are removed from the molds and comparative readings are taken. The specimens are then stored in tap water at 80°C for 24 hours. After the 24-hour period, the zero readings are taken, and the specimens are then placed in a 1N NaOH solution at 80°C. Readings are taken at 14 days and at three additional intermediate readings, as a minimum. Expansions of less than 0.10% indicate innocuous aggregates. Expansions greater than 0.20% indicate potentially deleterious aggregates. Expansions between 0.10% and 0.20% indicate the aggregates/concretes should be subjected to additional testing. The AASHTO counterpart to ASTM C1260 (AASHTO T 303), was recommended by NCHRP Project 4-30 (2002) for use as an indicator for aggregate reactivity. However, some deleteriously reactive coarse aggregates do not expand excessively in this test (Stark et al. 1993; Lane 1993).

Determination of Length Change of Concrete Due to Alkali-Silica Reaction (ASTM C1293)

As explained by Weyers et al. (2005), the purpose of ASTM C1293 is to evaluate the potential of an aggregate to expand deleteriously due to any form of alkali-silica reactivity. Concrete prisms are cast with an alkali content of 1.25% by mass of cement. The alkali content is obtained by adding NaOH to the concrete mixing water. The concrete prisms are then stored over water having a temperature of 38°C for one year. An expansion limit of 0.04% is used as the acceptance criterion. Touma et al (2001) reported that if the storage temperature is increased to 60°C, the required testing time can be reduced to three months. ASTM C1293 is generally accepted as the most reliable test method for identifying reactive aggregates. Thus, the standard form of ASTM C1293 shall be used in lieu of other test methods if time permits. The test method may also be used to evaluate the potential for Alkali-carbonate reactivity (ACR).

Unconfined Aggregate Particle Freeze-thaw Test (ASTM C131)

As explained by Koubaa et al. (1997), this method consists of freezing and thawing aggregates in water, an alcohol-water mixture (typically 5% concentration), a water-salt mixture (typically 3 to 5% concentration), or in air (freezing) and water (thawing). The aggregate samples are placed in plastic bags and completely covered with the test solution. Fifty cycles of freezing and thawing are used when testing in water or water-salt mixtures, and 16 cycles when testing in water-alcohol mixtures. Mass loss is measured in terms of the percent mass of sample that will pass a sieve smaller than the size upon which it was originally retained, which is an indicator of the deterioration of each size fraction. A 10% mass loss is often used as the borderline. This test method has been **criticized** because of poor correlation with field freeze-thaw performance for carbonate aggregates, the required testing time, failure to simulate the effects of aggregate confinement by mortar in concretes, and the poor repeatability of the test results.

Powers' Slow Cool Test (ASTM C671)

As explained by Koubaa et al. (1997), this test method consists of placing concrete specimens in a water bath at a temperature of 2°C, and then submerging them in a water-saturated kerosene bath during a temperature change from 2°C to -9.5°C at a rate of -15°C/hr. The temperature and length change are measured during the cooling cycle, after which the samples are placed back in the constant temperature water bath. The procedure is repeated every other week. Two durability indicators are assessed in this test: the critical dilation and the period of frost immunity. The critical dilation is the dilation at the last cycle before dilation begins to increase sharply (i.e., when the expansion rate increases by a factor of two or greater). The test is terminated when the critical

dilation is reached. The period of frost immunity is the number of cycles for which the dilation has remained almost constant. Note that frost-resistant aggregates may never produce critical dilations in this test. Further, there is some controversy in literature on whether this test correlates better with field performance; compared to ASTM C666.

Virginia Polytechnic Institute Single-Cycle Slow Freeze Test

As explained by Koubaa et al. (1997), this test consists of subjecting 75 x 100 x 400mm concrete beams to a single cycle of freezing while measuring the dilation. After 14 days of moist curing at 23°C, the transverse fundamental frequency, mass, and length are measured. The specimens are then cooled in a conventional freezer for three hours. Length measurements are taken every 15 minutes as the specimens' temperature drops from 21°C to 4.5°C, and every 5 minutes while the specimens' temperature is between 4.5°C and - 9.5°C. The test relies on measuring a time slope (bt) and a temperature slope (bl) to determine the durability of aggregate sources in two to three weeks. Accelerated curing of the specimens can significantly reduce the testing time. The cumulative change in length and the temperature change between 4°C and -6°C are used to determine the minimum temperature slope, (bl), which occurs when hydraulic pressures cause expansion due to ice formation. A temperature slope of zero or less implies that the aggregate used is susceptible to D-cracking, while a temperature slope above zero is considered inconclusive. The time slope (bt) is the minimum slope that occurs in a time interval of 20 to 60 minutes and has units of mm/hour. When the time slope is less than -10.2, the freeze-thaw durability of the aggregate is questionable. When it is higher than 2.5, no further testing is required, and the aggregate is durable. When the time slope is between 10.2 and 2.5, further testing may be needed. Although no agency reports regular use of this test, results reported in the literature correlate very well with rapid freezing and thawing tests and field performance.

Comparison of available test procedures

Weyers et al. (2005) concluded that length change or dilation measurements (e.g., the optional measurements by ASTM C666) are recommended to assess D-cracking. Stark (1976) proposed a failure criterion of 0.035% expansion after 350 cycles. With this proposed method, only two freezing and thawing cycles are specified per day, to be more simulative of actual field performance. Further, the calculation of a durability factor using the dynamic modulus measurements as per ASTM C666/AASHTO T 161 I recommended, but may not be as indicative of field performance as length change measurements (Weyers et al. 2005). Pre-soaking carbonate aggregates in chloride solution before casting and testing concrete in AASHTO T 161 was found to be a good method for assessing the salt susceptibility of aggregates upon freezing and thawing (Weyers et al. (2005).

Weyers et al. (2005) also investigated the predictive capabilities of a wide range of aggregate durability tests for Wisconsin coarse aggregates to develop an efficient testing protocol. The authors concluded that the testing protocol should not only cover the durability of individual aggregate particles, but also the durability of the inclusion materials (i.e., Portland cement concrete or bituminous concrete), to understand the adverse effects that unsound aggregates will have on the structure. From their research efforts, aggregates with vacuum saturated absorptions (VSAs) of 2% or less met the acceptance criteria for LA abrasion, Micro-Deval, unconfined and confined freezing and thawing tests. This resulted in a large reduction in the required testing for WisDOT.

Tube suction test is another test used to predict the freezing and thawing durability of unbound aggregate base layers. The test monitors the capillary rise of moisture in a cylinder of compacted aggregate and measures the dielectric constant at the surface with a probe. The dielectric constant is a measure of the unbound water in the aggregate sample, which correlates with the freezing and thawing performance of the aggregates (Weyers et al. 2005). The researchers concluded that the scope of research on the tube suction test is too limited, and there are no set limits for the acceptance or rejection of aggregates tested using this procedure. Thus, it was not recommended for inclusion as a standard test (Weyers et al. 2005).

Koubaa et al. (1997) conducted a study to identify the mechanisms causing premature failure in concrete pavements in Southern Minnesota. The study also identified aggregate sources responsible for the premature failure of concrete pavement by D-cracking, documented the accuracy of existing aggregate freeze-thaw durability tests, and developed a new methodology for quickly and reliably assessing freeze-thaw durability. A single quick, simple, economical and reliable method for identifying frost-susceptible aggregate particles was not identified, although quick tests that can determine the frost resistance of one aggregate relative to others were identified. The selection of tests for use is based on aggregate minerology, as well as the results of some of the quick screening tests. The most widely used tests to identify the susceptibility of coarse aggregate to D-cracking are the rapid freezing and thawing test (ASTM C666) and the Powers single-cycle slow freeze test (ASTM C 671, withdrawn). More rapid tests are often considered incapable of accurately determining the acceptability of a coarse aggregate with respect to frost susceptibility.

Bektas et al. (2016) indicated that Iowa DOT developed the Iowa pore index test in the 1970s to identify the D-cracking potential of coarse aggregates, particularly limestones. For the test, water is pushed into 0.5 to 0.75 in. sized aggregates under a pressure of 35 psi, in a sealed system, for 15 minutes. The amount of water entering the aggregate in the first minute is termed the primary load, and the amount of water entering the aggregate in the following 14 minutes is termed the secondary load, or pore index. The primary load is an indicator of the quantity of macropores, while the secondary load is an indicator of the quantity of small voids (micropores). The quantity of micropores is closely associated with the aggregate's freezing-thawing durability. A secondary load of 27 or greater is believed to indicate a poor freezing-thawing durability. The test procedure is relatively quick and simple, and States other than Iowa have also evaluated the test and found a strong correlation between the Iowa pore index and the field performance of aggregates for freeze-thaw durability (Thompson et al. 1980, Shakoor and Scholer 1985, Koubaa and Snyder 1996). Generally, it is acknowledged that the aggregates that contribute the most to freeze-thaw durability are the coarse aggregates having high porosities and medium-sized pores (0.1 to 5 μm). These aggregates can get easily saturated and cause concrete deterioration and popouts.

Qiao et al. (2012) investigated the long-term performance of concrete batches with low-degradation (LD) or normal degradation (NM) aggregates subjected to freezing and thawing. The researchers measured the dynamic modulus and fracture energy for both groups after different numbers of freeze-thaw cycles through nondestructive modal and cohesive fracture tests, respectively. Due to the higher air content (4.8%) in the concrete samples made with the LD aggregates, the surface scaling following freeze-thaw conditioning was found to be less severe than concretes with NM aggregates, which had an air content of 3.0%. The cement paste near the specimen surface seemed to degrade faster than the inner parts of the specimen. Thus, surface scaling and loss of mass due to frost action significantly influences the measured dynamic modulus, and this type of frost damage is not able to

characterize the degradation of aggregates. Since local defects are caused by frost damage, including intergranular debonding in the interfacial transition zone (ITZ) between the cement paste and aggregates/quartz sands and intragranular defects (microcracks) in both the cement paste and aggregates, the surface mass loss is not representative to the whole sample performance.

For this purpose, Qiao et al. (2012) compared to the dynamic modulus of elasticity and the fracture energy tests, and found that the latter is a more sensitive parameter for evaluating concrete degradation caused by frost action; particularly for examining degradation of aggregate and ITZs in the concrete. The study also concluded that the dynamic modulus test is significantly influenced by surface scaling in the specimens, reflecting degradation at the specimen surface and a loss in mass, which may overshadow the effect of internal damage and aggregate degradation due to the freeze-thaw. Thus, the dynamic modulus test (ASTM C666) may not be effective in characterizing the degradation of concrete with different aggregates. In conclusion, the measured decrease in the dynamic modulus of elasticity test in ASTM C666 demonstrates for concrete degradation through freeze-thaw conditioning but is sensitive to the surface scaling, which may not represent the degradation of concrete samples as a whole. In contrast, the cohesive fracture test is effective for evaluating the concrete material degradation through the freeze-thaw conditioning cycles.

Further, Koubaa et al. (1997) tested field specimens retrieved from pavement sections that exhibited D-cracking using ASTM C666. Specimens from sections that exhibited D-cracking showed low durability factors (<60), high dilations (>0.1%), or both. On the other hand, pavement sections that exhibited no D-cracking exhibited high durability factors (>70) and low dilations (<0.065), which is consistent with their field performances. ASTM C666 procedure C provided better correlation with field performance than procedure B. The researchers also concluded that petrographic examination should be the first step in evaluating frost resistance because identification of aggregate composition and origin seems to provide a basis for better selection of subsequent durability tests. The durability tests they proposed included the Washington hydraulic fracture test, VPI single-cycle slow-freeze test and the rapid freezing and thawing test using ASTM C666 procedure B (or C) and salt-treated aggregates.

For Wisconsin, Tabatabai et al. (2013) investigated the performance of Wisconsin coarse aggregates for durability evaluation. Aggregate test results from WisDOT test database as well as data from tests performed on 69 aggregates by Weyers et al. (2005) were analyzed. A multi-parameter regression analysis was performed on the data from the WisDOT database. Results of the multi-parameter regression analysis indicated that the lowest correlation exists between the unconfined freeze-thaw test and other tests. Tabatabai et al. (2013) noted that the sodium sulfate soundness and unconfined freeze-thaw had the lowest correlation (R=0.12991), even though the sodium sulfate soundness test has been regarded as a test to rapidly measure freeze-thaw resistance. The researchers concluded that the unconfined freeze-thaw test is measuring an aggregate characteristic that is different from other tests and recommended the test to be an individual requirement for any aggregate test protocol. The tests compared are presented in Table 1. These tests include Micro-Deval test, vacuum-absorption test (ABS), LA abrasion and impact (LAA), sodium sulfate soundness (SSS), and unconfined freeze/thaw (UFT).

Table 1. Correlation between different freeze-thaw durability tests (Tabatabai et al. 2013)

Variables	Micro-Deval	ABS	LAA	SSS	UFT
Micro-Deval	1	0.9271	0.7529	0.7487	0.3933
ABS	0.9271	1	0.7570	0.6485	0.3383
LAA	0.7529	0.7570	1	0.4931	0.3238
SSS	0.7487	0.6485	0.4931	1	0.1299
UFT	0.9399	0.3383	0.3238	0.1299	1

Crovetti and Kevern (2018) performed freeze-thaw durability tests in accordance with ASTM C666, Procedure A - fully saturated rapid testing procedure. The freeze-thaw testing was performed on concrete prisms that were 3 in. by 4 in. by 12 in. The prisms were saw-cut from pavement test strips with two mix designs: one using southern Wisconsin limestone aggregates, and the other using northern Wisconsin igneous gravel aggregates. During the testing, the dynamic modulus and mass of the concrete prisms were measured every 30 freeze-thaw cycles. Freeze-thaw testing on specimens from each concrete mix was performed to 300 cycles, and to 600 cycles for select specimens. The researchers reported that the concrete specimens made with limestone aggregates and granite gravel maintained high durability levels after 600 cycles. Only one concrete specimen made with limestone (specimen L01) exhibited a low relative dynamic modulus that decreased below 90% after about 330 through 600 freeze-thaw cycles, decreasing below 75% at cycle 600.

Hamoush et al. (2011) studied the freeze-thaw durability of high strength concrete prisms (3 in. by 4 in. by 16 in.). For the study, ASTM C666 procedures were followed for freeze-thaw conditioning and the dynamic modulus was measured before starting freeze-thaw cycles, and at 40, 70 and 100 cycles. They reported that the measured dynamic modulus increased from 0 to 40 cycles and then decreased from 40 to 100 cycles.

A study conducted by Chen and Qiao (2014) measured the dynamic modulus of concrete prisms (3 in. by 4 in. by 16 in.). Samples were freeze-thaw conditioned in accordance with ASTM C666 procedure A. The mix design was kept constant for all the concrete specimens, and the dynamic modulus of the prims were measured. Chen and Qiao (2014) reported that the larger variance of dynamic modulus between specimens was more apparent after 600 freeze-thaw cycles. Additionally, all the samples relative dynamic modulus had dropped below 60% for all samples after 1,200 freeze-thaw cycles, which is considered the failing threshold.

The effect of rapid freeze-thaw cycles on concrete durability, beyond 300 cycles, was studied by Olba et al. (2016) using ASTM C666 procedure A. In the study, the mass loss and dynamic modulus of concrete beam specimens (3 in. by 4 in. by 15.5 in.) were measured throughout the test up to 3,200 freeze-thaw cycles. After 3,200 freeze-thaw cycles, a majority of the tested samples showed an excellent freeze-thaw performance and possessed relative dynamic modulus values above 80%. The relationship between freeze-thaw cycles and sample degree of saturation was studied using sealed concrete samples with various degrees of saturation. The researchers concluded that there is a critical degree of saturation that the concrete must possess in order for freeze-thaw related failure to occur. Results of the freeze-thaw testing on the investigated concrete specimens indicated that the critical degree of saturation is around 88%.

Midwest State DOTs Aggregate Acceptance Specifications

A search for the practice of the DOTs in the Midwest was conducted to understand their practice and requirements regarding freeze-thaw testing for aggregates in the U.S. The available specifications were collected for the eleven Midwestern states and is summarized below and in Table 1:

- **Michigan DOT** has developed its own procedures regarding freeze-thaw testing of loose aggregates and aggregates in concrete (MTM 124 and MTM 115, respectively). MTM 124 “Michigan test method for determining aggregate durability by unconfined freezing and thawing” follows the AASHTO T 103 method for unconfined freeze thaw, but the sieves used for regrading after freeze-thaw testing are slightly smaller than those specified by AASHTO T 103. The freezing and thawing apparatus is as described in ASTM C 666 for testing by Procedure B. Samples are immersed in water for 24 hours without vacuum treatment prior to the start of freezing and thawing. Alternate freezing and thawing cycles are repeated for a total of 300 cycles. For aggregates in concrete, Michigan DOT uses MTM 115 “Michigan test method for testing concrete for durability by rapid freezing in air and thawing in water.” The same apparatus used for ASTM C666 Procedure B is utilized and follows the ASTM C666 procedure except for few modifications outlined in the standard. Length change calculations are performed for the tested beams. The beams are made and cured according to MTM 114 “Michigan test method for making concrete specimens for freeze-thaw testing of concrete coarse aggregate.” The coarse aggregates are first vacuum saturated then 24-hour soaked prior to sample preparations. Note that for investigative screening purposes only, Michigan DOT utilizes Iowa Pore Index testing as per MTM 128 “Test method for determination of Iowa pore index of coarse aggregates.”
- **Indiana DOT** also has its own procedures for freeze-thaw testing of aggregates. ITM 209 “Soundness of aggregates by freezing and thawing in brine solution.” Rapid freezing and thawing cycles in a 3% sodium chloride solution are performed. One cycle consists of lowering the temperature form 70-75 F to below -15 F for at least 15 minutes then heating to 70-75 F for at least 15 minutes. A total of 25 cycles are performed, and weight loss for each fraction is determined at the end of the testing. This procedure is also followed closely for aggregates used in concrete, except for concrete mixes with coarse aggregates of Class AP, a premium aggregate class for Indiana DOT. If the coarse aggregates are rated Class A and to classify the aggregates as Class AP for use in concrete mixes, procedure ITM 210 “Class AP coarse aggregate” is utilized. Test beams are casted and tested according to ASTM C666 procedure B for a 3-hours cycle or 8 cycles per day. Test is continued for 350 cycles or until the beams break. The length change is calculated and reported.
- **Iowa DOT** utilizes the Iowa pore index test as per IM 219 “Secondary Pore Index” test procedure to test aggregates for freezing and thawing susceptibility for aggregate classes 2, 3 and 3i for aggregates used in concrete mixes. The limit is 20-30 for aggregate

acceptance in concrete depending on the aggregate class. Procedure IM 211 “” is utilized to test the freeze thaw susceptibility of coarse aggregates for revetments. Procedure A is used for Classes A, B, C and E revetment, while procedure A is utilized for Class D revetment aggregates. The detailed procedures for these test methods are not publicly available online. Lastly, there some special provisions for Iowa DOT projects were found to request running ASTM C666 for aggregates in concrete. An example is a special provision for Scott County, contract No. IMN-074-1(180)5-0E-82, for lightweight concrete. In this special provision, ASTM C666 procedure A was specified, with a durability factor of 85 or higher after 300 cycles.

- **Kansas DOT** utilizes method KTMR-21 “Soundness of aggregates by freezing and thawing.” This test procedure follows the AASHTO T103 procedure closely, except for some changes marked in the procedure, and applies 25 cycles of freezing and thawing to the tested aggregates. The soundness (freeze-thaw less ratio) is calculated and reported. For aggregates in concrete mixes, KTMR-22 “Resistance of concrete to rapid freezing and thawing” procedure is utilized. This is a modified ASTM C666 Procedure B testing method for freezing and thawing durability. The KTMR-22 follows ASTM C666 closely except for some changes to sections 6 – 8 in the original procedure that are detailed in the test procedure. One of the changes is that the test is terminated after 660 cycles of freezing and thawing are applied, relative modulus drops below 60%, or expansion exceeds 0.10%; whichever occurs first. Measurements are taken and recorded in intervals not exceeding 56 cycles.
- **Illinois DOT** conducts an Illinois modified procedure of the AASHTO T 104 for testing the freeze-thaw susceptibility of aggregates. The Illinois modified procedure requires conducting a sodium sulphate soundness test, with five freeze-thaw cycles. For aggregates in concrete mixes, an Illinois modified AASHTO T 161 Procedure B is utilized. The Department has applied some modifications to the original sections of the AASHTO T 161 procedure, including revising sections 2.1, 4.6, 8.1, 8.3, adding three new sections (3.5, 4.7, and 7.1.1), and deleting a multitude of the existing sections (e.g., sections 7.3, 7.4, 8.2, Note 6, 9.1 – 9.3, 10.2.1 – 10.2.7, 10.4, and others). A total of 300 cycles are conducted, and failed beams are replaced with dummy beams for the completion of 300 cycles.
- **Minnesota DOT** uses a modified AASHTO T 104 soundness test for testing aggregates for freeze-thaw durability. Only the magnesium sulfate solution is allowed, and the test is conducted for five cycles. The modifications to the standard AASHTO T 104 procedure are published in a dedicated document (No. 1209 – lab manual). For concrete beams, Minnesota DOT likely does not have a dedicated test procedure, even though multiple published research projects conducted for MnDOT have tested concrete beams for freeze-thaw durability according to ASTM C666 procedure.
- **Missouri DOT** conducts a Soundness freeze-thaw test utilizing the water-alcohol freeze method in accordance with procedure TM-14 “Soundness test of coarse aggregate - water-alcohol freeze method.” The water-alcohol solution concentration is 0.5% by volume, Methyl Alcohol to ordinary tap water. The total number of cycles to completion is 16 cycles as a minimum. The freezing cycles are 15.25 hrs. during the day and 6.25

hrs. during night. The percentage loss at the end of the 16 cycles is measured and recorded. For aggregates used in concrete, ASTM C666 Procedure B is utilized.

- **Nebraska DOT** utilizes procedure NDOT T-103 “Soundness of Aggregates by Freezing and Thawing.” For fine aggregates and aggregates used in concrete mixes, the freeze-thaw durability is determined by AASHTO T 104 procedure, sodium sulfate soundness. For coarse aggregates, the tested material shall consist of representative material coarser than the No. 4 sieve. A modified AASHTO T 103, procedure B, with vacuum absorption treatments and a total of 16 cycles is utilized. For aggregates in concrete, ASTM C666 Procedure A with 300 cycles of testing is utilized.
- **North Dakota DOT** uses AASHTO T 104 (sodium sulfate soundness) test procedure for testing aggregates for freezing and thawing. There seems to be no dedicated or enforced procedure for testing aggregate confined in concretes.
- **Ohio DOT** adopts the AASHTO T 103 and T 104 procedures for testing aggregates for freeze-thaw durability. AASHTO T 104 is predominantly used for most applications. For aggregates in concrete, a modified ASTM C666, Procedure B according to supplement 1024 is utilized. Supplement 1024 is entitled “Method of testing coarse aggregates to determine susceptibility to D-cracking,” and summarized the changes to the standard procedure. For example, 350 cycles are performed for all samples, and measuring length change is mandatory for all tested samples (i.e., not optional) unless the samples deteriorate badly.
- **South Dakota DOT** utilized procedure SD 220 for testing the freeze-thaw durability of coarse and fine aggregates. This method follows AASHTO T 104 test procedure entirely for sodium sulfate soundness for 5 cycles of testing. There seem to be no dedicated or enforced test procedure for aggregates in concrete.

Table 1: Midwest State DOTs Aggregate Acceptance Specifications

State	Test for virgin aggregates	Test for aggregates in Concrete
Michigan	**MTM 124 with no vacuum treatment** (AASHTO T 103 but smaller sieves, ASTM C666 apparatus, 300 cycles total)	**MTM 115 with vacuum treatment** (ASTM C666 equivalent, 300 cycles) **MTM 128** Iowa Pore Index (not enforced, for investigative screening)
Indiana	**ITM 209** (25 cycles of unconfined aggregates freeze-thaw in a 3% NaCl solution) **Also use AAHTO T 103 and AASHTO T 104** Choosing between ITM 209 or AASHTO T 104 for acceptance is left to the discretion of the engineer	**ITM 209** – if coarse aggregates are NOT class AP **ITM 210** - to classify aggregates as Class AP (AASHTO T 161/ ASTM C666 Procedure B are followed closely, 350 cycles or until beams break)
Iowa	**IM 219** (Secondary Pore Index, Maximum limit of 20-30 depending on aggregate class) **Test Method 211 (freeze-thaw, Methods A-C)**	**IM 219** (Secondary Pore Index, Maximum limit of 20-30 depending on aggregate class) **ASTM C666, Procedure A** (in select special provisions, 300 cycles)
Kansas	**KTMR-21** (follows AASHTO T 103 method except as specified, 25 cycles) KTMR-21 also used for aggregates in HMA	**KTMR-22** (modified ASTM C666 procedure B, test terminated after 660 cycles or if relative modulus drops below 60% or if expansion exceeds 0.10%; whichever occurs first.)
Illinois	**AASHTO T 104** (Na_2SO_4 Soundness 5 Cycle, Illinois Modified)	**Illinois Modified AASHTO T 161** (Procedure B for polymer concrete, 300 cycles)
Minnesota	**MN-1219** (AASHTO T 104, but only magnesium sulfate solution allowed, 5 cycles)	
Missouri	**TM-14** (Soundness - water-alcohol freeze method, 16 cycles) AASHTO T 104 (Sodium Sulphate, only for coarse aggregates in ultra-thin bonded asphalt wearing surfaces)	**ASTM C666**, Procedure B (300 cycles)

Nebraska	**NDOT T-103** (For some coarse aggregates: Modified AASHTO T 103, procedure B – Vacuum absorption, 16 cycles; For fine aggregates, and aggregates in concrete AASHTO T 104 procedure is closely followed, sodium sulphate)	**ASTM C666 Procedure A** (300 cycles)
North Dakota	**AASHTO T 104** (sodium sulfate)	No dedicated test
Ohio	**AASHTO T 104** *(primarily)* **AASHTO T 103** *(limited applications)*	**Modified ASTM C666 (**Procedure B, Supplement 1024 shows all modifications, 350 cycles**)**
South Dakota	**SD 220 – *Follows AASHTO T 104 entirely*** (Sodium Sulfate Soundness; 5 cycles)	

State / Agency	**Procedure**	**Limit**
Indiana DOT	AASHTO T 103, Procedure A	• Classes AP, AS, A, and B: 12% max • Classes C and D: 16% max • Class E: 20 % • Class F: 25%
Indiana DOT	Sodium Sulphate Soundness (AASHTO T 104)	• Classes AP, AS, A, and B: 12% max • Classes C and D: 16% max • Class E: 20 % • Class F: 25%
Indiana DOT	ITM 209 (3% Brine solution)	• Classes AP, AS, A, and B: 30% max • Classes C and D: 40% max • Class E: 50% max. • Class F: 60% max.
Kansas DOT	KTMR-21 (Modified AASHTO T 103)	• Aggregates in concrete: 10% max. • Aggregates in polymer concrete: 8% max. • Aggregates in HMA and micro surfacing: 10% max • Aggregates for base, cement treated bases, backfills, subgrade modifications, shoulders, ditches, and miscellaneous construction: 15% • Aggregates for MSE walls, underdrains, cover materials: 10% max.

State / Agency	Procedure	Limit
Missouri DOT	TM-14 (Modified AASHTO T 103) AASHTO T 104 (Sodium Sulphate)	• Aggregates for concrete: 18% max. • Ultrathin bonded asphalt wearing surface: 12% max.
Nebraska DOT	NDOT T-103 (Modified AASHTO T 103, Procedure B) AASHTO T 104 (sodium sulfate, used only for aggregates for concrete)	• Aggregates for microsurfacing: 12% max. • Aggregates for Armor coat: 5% max • Aggregates for Chip seal: 7% max. • Riprap: 14% max. • Aggregates for HMA: 12% max. • Aggregates for concrete: 10% max. (AASHTO T 104 procedure)
Ohio DOT	AASHTO T 104 (sodium sulfate) AASHTO T 103 *(only for aggregates in quick setting concrete mortar and for slope protection and filter aggregates for dump rock fill)*	• Aggregates for porous backfill, underdrains: 15% • Aggregates for concrete: 10% max. for fine aggregates; 12% max. coarse aggregate • Aggregates for HMA: 15% max. for fine aggregates; 12% max. coarse aggregate • Aggregates for asphalt concrete base, structural backfills, and embankments: 15% max. • Aggregates for slope protection and filter aggregate for dump rock fill: both 15% max. (AASHTO T 104), 20% max. (AASHTO T 103) • Screenings: 15% max. • Aggregates for quick setting concrete mortar: 2% max. (AASHTO T 103)